2
2009

This is to certify that the
thesis entitled

CHARACTERISTICS AND ORIGIN OF SILTY KETTLE BOTTOM DEPOSITS IN A SANDY NORTHERN LOWER MICHIGAN LANDSCAPE

presented by

TREVOR C. HOBBS

has been accepted towards fulfillment
of the requirements for the

M.S. degree in Geography

Major Professor's Signature

4-1-09

Date

CHARACTERISTICS AND ORIGIN OF SILTY KETTLE BOTTOM DEPOSITS IN A SANDY NORTHERN LOWER MICHIGAN LANDSCAPE

By

Trevor C. Hobbs

A THESIS

Submitted to
Michigan State University
in partial fulfillment of the requirements
for the degree of

MASTER OF SCIENCE

Geography

2009

ABSTRACT

CHARACTERISTICS AND ORIGIN OF SILTY KETTLE BOTTOM DEPOSITS IN A SANDY NORTHERN LOWER MICHIGAN LANDSCAPE

By

Trevor C. Hobbs

Many dry, topographically closed basins (i.e. kettles) in the sandy interlobate uplands of Osceola county contain a ~1m thick sequence of silty sediment in the bottom-center of the depression. These deposits are anomalous, when compared to the preponderance of sand in this area. The purpose of this research was to determine the most likely origin(s) of these silty deposits, and assess their paleoenvironmental importance. Two possible hypotheses explaining the origin of the silt were examined: (1) it was winnowed out of the surrounding upslope sediments via slopewash, or (2) it is loess. Sediments from 53 kettle bottoms and adjacent backslopes were sampled to characterize and compare their particle size distributions. Eight of these kettle bottoms were also depth-sampled to reconstruct their depositional histories. Silt mineralogy data from four kettle bottoms and adjacent backslopes were later compared to determine the likely source of the silt. Two samples of charcoal fragments found in buried soils in silty kettle bottom sediments yielded radiocarbon ages of 6840 ± 30 and 920 ± 20 cal. years BP. The combined evidence suggests that the kettle bottom silt is locally redistributed loess that was deflated from surfaces destabilized by fire during the Holocene and preferentially deposited in kettle bottoms. These data provide a new and potentially important paleoenvironmental proxy for recently glaciated landscapes, and highlight the point that episodic periods of dryness and landscape instability have permeated the post-glacial period in Michigan.

Dedicated to my loving Grandmother, Lucille, who exemplified perseverance

ACKNOWLEDGEMENTS

I'm fortunate to have learned from those whom I consider to be the best workers and teachers in the field of geomorphology. First and foremost, this thesis would not have been possible without the inspiration, guidance, and support of my advisor, Randy Schaetzl- thank you for everything you've given me. Also, my other committee members, Alan Arbogast and Grahame Larson, deserve special thanks for being role models and excellent teachers. I'd also like to thank Dave Lusch and Kevin Kincare for lending their brilliant ideas and time in the field. Finally, I'd like to thank Brandon Curry and Catherine Yansa for contributing their input.

This thesis would not have been possible without the camaraderie and support of my fellow graduate students. Thank you Steve for your relationship with Endnote. Special thanks goes out to Bilal (Yoda) and Meleia for bagels and honest conversation. Blumer- I could always count on you to have coffee ready every morning. Kristy- thanks for feeding me various snacks when I was starving. Joel- thanks for showing me new music. Zukas- thanks for *really* showing me new music (no offense Joel), and upping the homebrew quality. Bigsby- thanks for your workspace and setting an example of how to run far. To all other grad students in the department of Geography- thanks for setting the bar high.

I am forever indebted to my network of friends in the Lansing community who have lent unconditional support over the past two years. To Corie Peirce, Chris Dorman, little H-man, Tomm Becker, and the community of folks at the MSU Student Organic Farm- thank you for what you do. Your food has nourished my intellect and continually

fuels healthy bodies and conscious minds everywhere. Also, to all those folks in the Eastside neighborhoods (there are too many of you to list)- thanks for the potlucks, laughs, and being great neighbors and citizens. To all the amazing housemates I've been fortunate enough to live with and learn from over the past two years- you've shaped me; thank you. Finally, the Waffle house (222 Horton) deserves special thanks for always keeping an open door.

I am infinitely grateful to the network of musicians and people in the Earthwork community for balancing out my graduate life. Micah and Andrea- thank you for maintaining the creative spirit in me, and believing that there would be a day when I finish my thesis. Chris and Brandon- thank you for opening up to me, both musically and emotionally. And to all others that I've been fortunate enough to play, record, and associate with over the years- you've enriched my graduate experience with your music.

Other people graciously contributed their time and/or resources in the field: to my best friend Jonny B, and students Kelly Anderson, Erin Dixon, Daniel Star, and Aaron Walker- thank you for your time in the field. To Steph, thanks for letting me drive your Subaru, and sorry that I destroyed the undercarriage.

Finally, and most importantly, thank you to my parents and family for being my rock- you've always tolerated and believed in my pursuits, and for that I am forever grateful.

TABLE OF CONTENTS

CHAPTER 1 - Introduction 1

CHAPTER 2 - Study Area 7

2.1 Geographic Setting 7
2.2 Study Area Extent 7
2.3 Hydrography 9
2.4 Geomorphology 13
2.5 Soils 27
2.6 Vegetation 31
2.7 Climate 38

CHAPTER 3 - Methods 40

3.1 Preliminary Work 40
3.2 Field Methods 41
3.3 Laboratory Methods 49

CHAPTER 4 - Results and Discussion 56

4.1 Extent of Silt in Kettle Bottoms 57
4.2 Texture of Kettle Bottom Deposits and Surrounding Backslopes 61
4.3 Comparing Silt Content in Kettle Bottom and Backslope Pairs 67
4.4 Silt Contents with Depth - Geomorphically Stable Sites 82
4.5 Spatial Patterns of Silt Content - Backslopes vs. Kettle Bottoms 92
4.6 Depth Characteristics of Kettle Bottom Deposits 95
4.7 Timing of Silt Deposition 119
4.8 Source of Kettle Bottom Silt - Local vs. Extra Regional? 126
4.9 Origin of Kettle Bottom Deposits - Summary of Evidence 134

CHAPTER 5 - Paleoenvironmental Significance 136

5.1 Soil Charcoal as an Indicator of Fire 136
5.2 Fire on Sandy Substrates 138
5.3 A Warmer and Dryer Climate During the Mid-Holocene 139
5.4 Evidence for Climate Fluctuation from Nearby Studies 140
5.5 The Possible Role of Climate and Fire in Destabilizing Sandy Surfaces 145
5.6 Paleoenvironmental Significance - Summary 146

CHAPTER 6 - Conclusions 148

6.1 Geomorphology of the Evart Upland 148

6.2 Characteristics and Origin of Silty Kettle Bottom Deposits 148
6.3 Silt Deposition Contemporaneous with Holocene Fires 151
6.4 Kettle Bottom Silt is Local 151
6.5 Paleoenvironmental Significance 152

APPENDIX 153

BIBLIOGRAPHY 158

LIST OF TABLES

Table 2.1- Morphometric characteristics of kettles. 17

Table 2.2- Characterization data for the five most common soil series mapped on the Evart Upland , listed in order of abundance from most (top) to least (bottom)..... 28

Table 2.3- Average monthly climate data for 30-year period (1971-2000)..... 39

Table 4.1- Average textural components of backslope and kettle bottom deposit samples. 62

Table 4.2- Downslope, point-to-point comparisons of mode sand grain size. 77

Table 4.3- Summary of evidence regarding the origin of kettle bottom deposits..... 135

Table A.1- Textural data for backslope samples. Numbers expressed as percent of sample. MWPS = mean weighted particle size..... 154

Table A.2- Textural data for kettle bottom deposit samples. Numbers expressed as percent of sample. MWPS = mean weighted particle size..... 156

LIST OF FIGURES

Figure 1.1- The Evart Upland is a complex assemblage of outwash with many kettles, situated between the Lake Michigan and Saginaw lobes of the former Laurentide ice sheet. The Evart Upland is in central Osceola County, MI (highlighted red). Images in this thesis are presented in color. 2

Figure 2.1- Color, hill-shaded, digital elevation model (DEM) of Osceola County, MI. The extent of the Evart Upland is shaded gray. The dashed line represents the Pere-Marquette State Forest boundary. The black lines are major highways. 8

Figure 2.2- Combined topographic map (3-meter contour interval) and color-shaded DEM of the western portion of the Evart Upland. The black line separates dry kettles on the upland from bogs, wetlands, and lakes in the lowlands, and is the approximate boundary of the study area. 10

Figure 2.3- Combined topographic map (3-meter contour interval) and color-shaded DEM of the northeastern portion of the Evart Upland. Lower relief, wet, hummocky terrain characterizes the surrounding lowlands to the northeast. 11

Figure 2.4- Grayscale DEM of the Evart Upland and surrounding areas, showing hydrologic features. Blue lines represent perennial streams and rivers (data source: Osceola County Hydrography shapefiles from the Michigan Geographic Data Library (Michigan Department of Information Technology, 2007)). The Muskegon River, located south of the upland, flows to the southwest. The Hersey River, flowing south, joins the Muskegon River at the bottom of the map. 12

Figure 2.5- A) Grayscale DEM of the Evart Upland showing the location of transect line A-B (red) that was used to construct the topographic profile shown in part B. The NNE trending ridge extending from the eastern portion of the study area is not considered part of the Evart Upland. B) Topographic profile of transect line A-B. Kettles on the upland have much greater local relief than kettles in the surrounding lowlands near the Muskegon River. 16

Figure 2.6- Grayscale DEM of the study area with major kettles highlighted in red. A total of 535 kettles were mapped within the boundary of the Evart Upland. 18

Figure 2.7- Grayscale DEM showing two areas on the Evart Upland with distinct kettle morphology (below); one from the western portion (upper left), the other from the southeastern portion (upper right). The two topographic maps above (3-meter contour interval) are the same scale. 19

Figure 2.8- USGS topographic map (3-meter contour interval) showing examples of ridges (ridge tops shaded tan) next to kettles (shaded red) in the study area. The

ridges in the left map are relatively flat topped and have steep sides. The ridge in the right map is massive with deeply gullied sides. 21

Figure 2.9- Combined USGS topographic map (3-meter contour interval) and color-shaded DEM showing low areas (yellow shading) between ridges (brown shading). In these low areas kettles are grouped. Major ridge crests are traced with black lines. Kettles are shaded red 22

Figure 2.10- Combined hillshade and color-shaded DEM presented in a three-dimensional view looking northwest, at the Evart Upland. The boundary of the upland is outlined in black. The red lines trace weakly integrated stream valleys that are headed by kettle chains upslope 24

Figure 2.11- A) Topographic map (3-meter contour interval) of a portion of the Evart Upland. The red polygons outline kettles. The blue line outlines the drainage basin of kettles that subtly transition to Twin Creek, south of the map. Note that the long axis orientation of the kettles that occupy the central portion of the valley is more or less parallel to the valley. Kettles in the northern most portion of the drainage basin are not well integrated. B) Inset map of a grayscale DEM showing the location of the drainage basin (shaded blue) on topographic map in (A). The Evart Upland is outlined in black. Blue lines on the inset map are perennial streams. 25

Figure 2.12- Color shaded DEM showing examples of a composite kettle (A) and lake (B) that have contrasting long axis trends as described in the text. Kettles are shaded red. Lakes are not shaded 27

Figure 2.13- Map of the five most common soil series on the Evart Upland (SSURGO digital soils data (Soil Survey Staff, 2007)). All other mapped series are left blank (gray areas on the upland). Grayling and Rubicon soils are mapped in narrow valleys, deep, dry kettles, and low areas between ridges. McBride soils increases in abundance on the east side of the upland, while Rubicon soils are generally absent there 30

Figure 2.14 Combined hillshade and presettlement vegetation map showing the Evart Upland and surrounding areas. The study area boundary is outlined black. Presettlement vegetation data from (Comer et al., 1998). 33

Figure 2.15- The Evart Upland is primarily used for timber production. Clear cutting is common. Photo by R. Schaetzl. 34

Figure 2.16- Some kettles lack canopy cover. In the photograph above, the surrounding forested summits open up to sweet fern and grasses (visible in the foreground) in the kettle bottom. Photo by R. Schaetzl 34

Figure 2.17- Topographic map (3-meter contour interval) of the northwestern portion of the study area. Non-forested kettles are shaded white on this topographic map.

Black arrows point to examples of kettles that are non-forested. Other larger areas with white shading were clear-cut at the time the topographic map was made (1983). 35

Figure 2.18- A) Bracken fern is common on steep slopes (above photo looking up a kettle backslope with a 35% gradient) where soils tend to be quite dry and sandy (i.e. favorable conditions for brackenfern). B) Rice grass commonly grows in the understory of flat landscape positions. Photos by T. Hobbs. 36

Figure 2.19- This kettle was plowed for tree planting. Rows of raised soil are still visible on the ground (shown by black arrows). Only trees occupying backslope, shoulder, and summit positions successfully grew. Photo by R. Schaetzl. 37

Figure 3.1- Schematic representation of a typical kettle in the study area (not to scale) showing the locations of samples gathered within each kettle. 44

Figure 3.2- Location of sampled kettles on the Evart Upland. Kettles are outlined red. A total of 53 kettles were sampled. Two samples were gathered at each site, resulting in a total of 106 samples. 45

Figure 3.3- Particle size distribution curves for selection of backslope samples used in the X-ray diffraction analysis. The range of grain sizes extracted from the samples is 20-53 μm. The lower limit of 20 μm was chosen because backslope samples have very little silt below that size. 53

Figure 4.1- Aerial extent of silty sediments in the bottom of kettle site 17 (above). The kettle area is shaded gray. The extent of silt is shaded brown. The red arrow gives the perspective of the photograph at left. 59

Figure 4.2- Aerial extent of silty sediments in kettle bottom at kettle site 31 (above). The area of the kettle is shaded gray. The extent of silt is shaded brown. The red arrow gives the perspective of the photograph at left. 60

Figure 4.3- Particle size distribution curves of all 53 backslope samples. The average particle size distribution is highlighted red. Blue and green curves represent the coarsest and finest textured sample, respectively. 63

Figure 4.4- Particle size distribution curves of all 53 kettle bottom deposit samples. The average particle size distribution is highlighted red. Blue and green curves represent the coarsest and finest textured sample, respectively. 64

Figure 4.5- Lower half of the USDA textural triangle, showing the texture of kettle bottom samples (blue star) vs. kettle backslope samples (green x). Kettle bottom deposit samples generally have loam and silt loam textures. Kettle backslope samples are dominantly sand and loamy sand in texture. The main area of textural overlap of kettle bottoms and backslopes is circled and shaded gray. 65

Figure 4.6- Average particle size distribution curves for all kettle bottom (red) and backslope (blue) samples. Both populations have a bimodal particle size distribution with peaks in the sand and silt range. The silt peak is different for each population (18 μm and 45 μm for bottoms and backslopes, respectively), while the sand peak is the same (315 μm). 68

Figure 4.7- Particle size distribution curves for three kettle bottom/backslope pairs that have the greatest textural difference (i.e. have the greatest difference in silt content) of the population of sample pairs. The kettle bottom/backslope pairs are color-coded; solid lines represent kettle bottom samples, while the dashed lines represent corresponding backslope samples. The colored bars at the top of the graph indicate the difference in silt peak location between bottom/backslope pairs. 70

Figure 4.8- Particle size distribution curves for three kettle bottom/backslope pairs representative of the average difference in silt content among the whole population. The kettle bottom/backslope pairs are color-coded; solid lines represent kettle bottom samples, while the dashed lines represent corresponding backslope samples. The colored bars at the top of the graph indicate the difference in silt peak location between bottom/backslope pairs. 71

Figure 4.9- Particle size distribution curves for three kettle bottom/backslope pairs that are the most texturally similar. The kettle bottom/backslope pairs are color-coded; solid lines represent kettle bottom samples, while the dashed lines represent corresponding backslope samples. The colored bars at the top of the graph indicate the difference in silt peak location between bottom/backslope pair. 73

Figure 4.10- Vectors showing the amount of downslope coarsening (blue) and fining (red) with respect to mode sand grain size between backslopes and kettle bottoms. Each vector contains two sets of x-y coordinates. The starting position of the arrow is the sand peak in backslope samples. The end position of each arrow represents the sand peak in the adjacent kettle bottom. Large changes in the x-coordinate denote significant coarsening or fining downslope. Large changes in the y-coordinate denote significant differences with respect to the amount of sand between the two landscape positions. 78

Figure 4.11- Photograph looking downslope from the rim of kettle site 33. A gully is visible in the foreground and leads to a fan-like deposit downslope in the kettle bottom. Photo by T. Hobbs. 80

Figure 4.12- Photograph showing the top of the kettle bottom deposit profile at site 33. The fan deposit shown in Fig. 4.11 is preserved as a sandy layer from 0-5 cm in this photo. This erosional event buried the charcoal rich soil from 5-15 cm. Photo by R. Schaetzl. 81

Figure 4.13- Location of stable site-1 relative to the other stable site locations. B) Topographic map showing surface characteristics of stable site-1. C) Photograph of surface vegetation at this site. 84

Figure 4.14- Depth plot showing distribution of four silt components with depth at stable site-1 85

Figure 4.15- A) location of stable site-2 relative to the other stable site locations. B) Topographic map showing surface characteristics of stable site-2. C) Photograph of surface vegetation at this site. 86

Figure 4.16- Depthplot showing distribution of four silt components with depth at stable site-2 87

Figure 4.17 A) location of stable site-3 relative to the other stable site locations. B) Topographic map showing surface characteristics of stable site-3. C) Photograph of surface vegetation at this site. 88

Figure 4.18- Depthplot showing distribution of four silt components with depth at stable site-3 89

Figure 4.19- Ordinary kriged grids of three silt components: coarse silt (left), medium silt (middle), and fine silt (right) between backslope samples (top row) and kettle bottom samples (bottom row). North is up in all of the grids. Black dots represent sample locations across the study area. Greater silt content is represented by increasingly darker color in both sample types. However, the values of percent silt are different for each sample type because kettle bottoms have far more silt than backslopes. 94

Figure 4.20- A) Location of site 17 in relation to other depth sampled kettles on the Evart Upland. B) Topographic map showing kettle site 17 with additional basin characteristics (right). 98

Figure 4.21- Depositional sequence of kettle bottom sediments at site 17. The dashed line marks the top of the coarse, sandy substrate sediments. The solid line marks the top of a buried soil. 99

Figure 4.22- A) Location of site 24 in relation to other depth sampled kettles on the Evart Upland. B) Topographic map showing kettle site 24 with additional basin characteristics (right). 100

Figure 4.23- Depositional sequence of kettle bottom sediments at site 24. The dashed line marks the top of the coarse, sandy substrate sediments. The solid line marks the top of a buried soil. 101

Figure 4.24- A) Location of site 33 with in relation to other depth sampled kettles on the Evart Upland. B) Topographic map showing kettle site 33 with additional basin characteristics (right). 102

Figure 4.25- Depositional sequence of kettle bottom sediments at site 33. The dashed line marks the top of the coarse, sandy substrate sediments. The solid lines mark the top of buried soils..... 103

Figure 4.26- A) Location of site 42 with in relation to other depth sampled kettles on the Evart Upland. B) Topographic map showing kettle site 42 with additional basin characteristics (right). 104

Figure 4.27- Depositional sequence of kettle bottom sediments at site 42. The dashed line marks the top of the coarse, sandy substrate sediments. The solid line marks the top of a buried soil. 105

Figure 4.28- A) Location of site 45 with in relation to other depth sampled kettles on the Evart Upland. B) Topographic map showing kettle site 45 with additional basin characteristics (right). 106

Figure 4.29- Depositional sequence of kettle bottom sediments at site 45. The dashed line marks the top of the coarse, sandy substrate sediments. The solid line marks the top of a buried soil. 107

Figure 4.30- A) Location of site 49 with in relation to other depth sampled kettles on the Evart Upland. B) Topographic map showing kettle site 49 with additional basin characteristics (right). 108

Figure 4.31- Depositional sequence of kettle bottom sediments at site 49. The dashed line marks the top of the coarse, sandy substrate sediments. The solid lines mark the top of buried soils..... 109

Figure 4.32- A) Location of site 52 with in relation to other depth sampled kettles on the Evart Upland. B) Topographic map showing kettle site 52 with additional basin characteristics (right). 110

Figure 4.33- Depositional sequence of kettle bottom sediments at site 52. The dashed line marks the top of the coarse, sandy substrate sediments. The solid line marks the top of a buried soil. 111

Figure 4.34- A) Location of site 53 with in relation to other depth sampled kettles on the Evart Upland. B) Topographic map showing kettle site 53 with additional basin characteristics (right). 112

Figure 4.35- Depositional sequence of kettle bottom sediments at site 53. The dashed line marks the top of the coarse, sandy substrate sediments. The solid lines mark the top of buried soils..... 113

Figure 4.36- Simplified versions of the depthplots in figures 4.20 - 4.35, ranked in order of increasing susceptibility to slopewash deposition from the surrounding backslopes: steepest backslopes and smallest area-to-drainage basin ratio (left) to shallowest backslopes and largest area-to-drainage basin ratio (right). These profile representations are not drawn to scale relative to each other..... 116

Figure 4.37- This photograph shows a trough containing the sequence of kettle bottom sediments at site 53. The pale tan sediments at the bottom of the photo are the sandy substrate sediments (lowermost C-horizon). Overlying the buried soil is the first interval of silty, aeolian sediment (brown colored). Photo by R. Schaetzl..... 120

Figure 4.38- A) Photo and data from the soil profile excavated at site 33. This site contains four buried soils, with charcoal randomly spread throughout the profile, but mostly concentrated within the soils. B) Depth plot showing the down profile textural variation at site 33. Black lines indicate the top of buried soils. C) Close up of the lowermost buried soil from which charcoal was extracted at ~ 120 cm. Note: the one-meter mark on the tape measure is above the extent of the picture, therefore, the 20 cm mark in this frame is actually 120 cm. Photos by R. Schaetzl..... 121

Figure 4.39- A) and B) Woody charcoal pieces commonly found in buried soil at site 33. C) Seeds were also found in the buried soil. D) Many small fragments of charcoal sticks (~0.25-0.5 mm) within the matrix of sand grains..... 122

Figure 4.40- Pieces of amorphous, black-colored silica found interspersed within the lowermost buried soil at Site 33..... 123

Figure 4.41- Particle size distribution curves for two of the most texturally different kettle bottom-backslope pairs. The range of silt-sized particles extracted from both is outlined (20-53 microns)..... 129

Figure 4.42- Bottom: sites 24 and 42 both have distinct intervals of aeolian deposition in the kettle bottom as indicated in the depthplots (intervals circled). Above: Particle size distribution curves of the two aeolian intervals and their adjacent backslopes. The 20-53 μm fraction of these samples and their adjacent kettle backslope samples were extracted for X-ray diffraction analysis..... 130

Figure 4.43- Results of the X-ray diffraction analysis for the two most texturally different kettle bottom-backslope pairs. Each kettle bottom-backslope pair is color-coded. Dashed lines represent backslope samples, while solid lines represent kettle bottom samples. Each diffraction pattern is offset 500 counts above the underlying pattern for ease of visual comparison. As such, the Y-axis should not be read as an absolute

count. Three significant minerals are present in the samples: Quartz, K-feldspar, and plagioclase feldspar. 131

Figure 4.44- Results of the X-ray diffraction analysis for the two kettle bottoms containing distinct aeolian units. Each kettle bottom-backslope pair is color-coded. Dashed lines represent backslope samples, while solid lines represent kettle bottom samples. Each diffraction pattern is offset 500 counts above the underlying pattern for ease of visual comparison. As such, the Y-axis should not be read as an absolute count. Three significant minerals are present in the samples: Quartz, K-feldspar, and plagioclase feldspar. 132

Figure 5.1- A Holocene record of aeolian activity from Elk Lake, MN. Black shading represents % Na (higher values indicate increased dryness). Line pattern shading indicates mass accumulation rate. The red bracket highlights a cycle of increased aeolian activity that corresponds with the oldest radiocarbon date obtained in this study. Diagram after Dean (1997). 142

Figure 5.2- Diagram showing the comparison of hydroclimate histories reconstructed from Hole Bog, MN (Blue) and Minden Bog, MI (red) for the past 2500 yrs after (Booth et al., 2006). Both records show a prominent dry interval around 1000 cal. years BP (highlighted yellow). This time period corresponds to the radiocarbon date of 920 cal. years BP obtained in this research. 144

CHAPTER 1 - Introduction

In many glaciated landscapes there are areas of hummocky topography containing numerous internally drained depressions, called kettles (Bennett and Glasser, 1996). Kettles are enclosed, bowl-like hollows in the landscape, marking the spot where former detached masses of glacial ice melted in place. As topographically closed and internally-draining depressions, kettles collect and retain sediment over time, thereby preserving a record of sediment inputs in the bottom of the basin (Walker and Ruhe, 1968). The sediments in kettles can, therefore, be studied to reconstruct the geomorphic history of the basin. To that end, areas with many adjacent kettles may provide opportunities to study the geomorphic history of the landscape they occupy.

This study focuses on a densely kettled upland (herein referred to as the Evart Upland) in the northwestern Lower Peninsula of Michigan, near the town of Evart. The Evart Upland lies within the southern portion of the North-Central interlobate drift realm of Michigan, between the former Lake Michigan and Saginaw lobes of the Laurentide ice sheet (Rieck and Winters, 1993) (Fig. 1.1). The landforms and drift in this part of Michigan are largely composed of sandy sediments associated with deposition via glaciofluvial processes (Rieck and Winters, 1993; Schaetzl and Weisenborn, 2004; Schaetzl and Forman, 2008). Situated in an interlobate reentrant, the Evart Upland likely formed as glaciofluvial sediments buried a complex arrangement of stagnant ice. As such, this landscape is characteristically sandy, and upon melting of the buried ice, became topographically complex with many kettles.

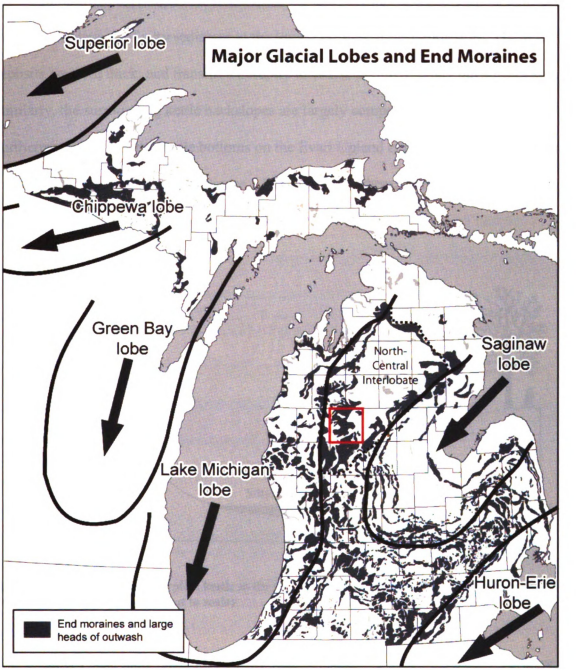

Figure 1.1- The Evart Upland is a complex assemblage of outwash with many kettles, situated between the Lake Michigan and Saginaw lobes of the former Laurentide ice sheet. The Evart Upland is in central Osceola County, MI (highlighted red). Images in this thesis are presented in color.

Initial field investigations of the Evart Upland revealed that many of the kettles there have a deposit of silty sediment in the lowest portion of the depression. These silty deposits are ~1m thick, and transition abruptly to coarse textured, sandy outwash below. Similarly, the surrounding kettle backslopes are largely composed of sandy drift. Furthermore, some of the kettle bottoms on the Evart Upland contain buried soils within the sequence of silty sediments. Figure 1.2 (below) is a schematic representation of a typical kettle in the study area.

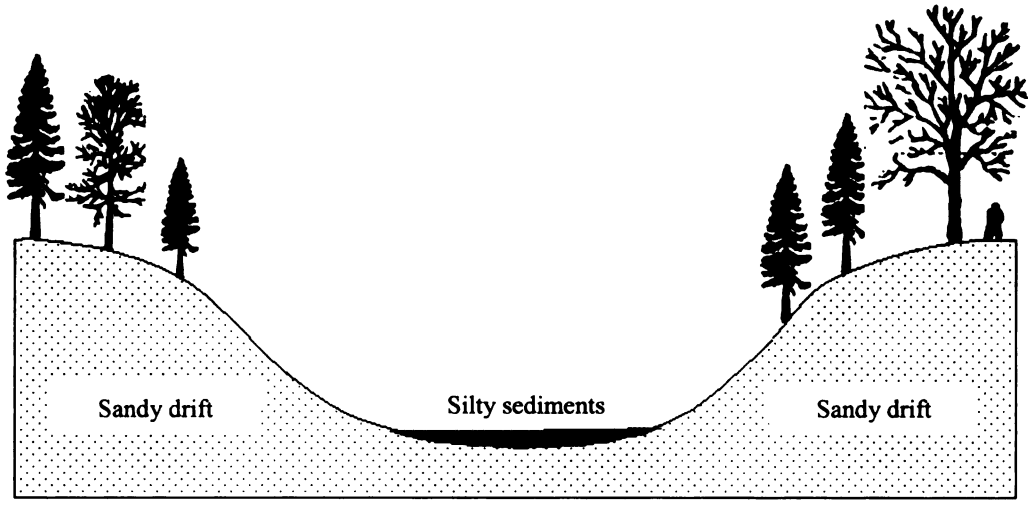

Figure 1.2- Cross section of a typical kettle in the Evart Upland, containing silty sediments in the lowest part of the depression. (not to scale)

Other researchers have documented similar deposits in kettle bottoms elsewhere, specifically in the Grayling Fingers region of Michigan (Schaetzl and Weisenborn, 2004; Schaetzl, 2008). Because deposits of silt in the kettle bottoms on the Evart Upland appear to be anomalous with respect to the preponderance of sandy sediments that

dominate this region, the purpose of this research is to determine the likely geomorphic origin(s) for the silt, and assess its paleoenvironmental importance.

There are two possible geomorphic scenarios by which silty sediments could be deposited in the kettles on the Evart Upland. Both of these scenarios are outlined below in the form of research hypotheses:

Hypothesis 1- the silt was winnowed from the surrounding upslope sediments

This hypothesis suggests that the surrounding backslopes were the source of silt in kettle bottoms. A textural difference between the bottomlands and surrounding backslopes is not uncommon in internally drained hillslopes, such as kettles. In fact, on most steep, internally drained hillslopes, normal erosion and downslope sorting processes result in a gradual sequence of progressively finer textured soils in the downslope direction because smaller particles are often preferentially entrained, and more easily transported further downslope (Milne, 1936; Walker and Ruhe, 1968; Malo et al., 1974).

Hypothesis 2- the silt is loess (aeolian silt)

This hypothesis suggests that the silt in kettle bottoms was brought into the kettles by wind. Schaetzl and Weisenborn (2004) and Schaetzl (2008) concluded that the silty deposits in the Grayling Fingers region of Michigan, which overlie sandy drift on stable, flat uplands there (and in kettle bottoms on those same uplands) most likely have an aeolian origin (i.e. loess). Given that the Grayling Fingers region is less than 150 km northeast of the Evart Upland, it is possible that the silty sediments in kettle bottoms on the Evart Upland have a similar origin.

The two hypotheses outlined above suggest drastically different paleoenvironmental interpretations for the post-glacial period in this part of Michigan. A slopewash origin for the kettle bottom silt suggests that precipitation in the past has been significant and consistent enough to generate runoff, continually transporting sediments downslope. This hypothesis also presumes a type of uniformitarianism- that the same geomorphic processes (slopewash) observable on many hillslopes today, have been operating in the Evart Upland since the landscape stabilized after deglaciation. In contrast, an aeolian origin for the kettle bottom silt suggests that there were exposed/unstable surfaces nearby with sufficient silt content, and at some time in the past, there existed ample winds to transport that silt to the Evart Upland. Moreover, this hypothesis suggests that different processes (other than what are observable today) were operative in this landscape in the post-glacial period. These two hypotheses are tested in, and form the core of, this thesis.

The Evart Upland is primarily state forest land, allowing for full, unrestricted access to sample sites. The great abundance of kettles in the study area provided multiple field sites to sample, thereby facilitating the creation of a robust and spatially extensive data set. The primary field methods used here included extensive sampling of soils from different landscape positions, (such as kettle bottoms, backslopes, and other geomorphically stable sites), in order to characterize their texture and compare their particle size distributions, both with depth at specific sites, and across the study area. The primary lab method used here involved analyzing the textural properties of these samples by laser particle size analysis. Other lab methods, such as radiocarbon analysis and X-ray diffraction, were used to answer additional research questions (listed below). In addition,

publicly available geospatial data (such as, topography, soils, etc.) were used in conjunction with textural data in a geographic information system to 1) support/refute the two aforementioned hypotheses regarding the origin of the kettle bottom silt, and 2) characterize the geomorphology of the Evart Upland.

A number of additional questions, prompted by preliminary analysis of the data, were generated throughout the course of this research. These questions did not easily fit into a hypothesis-testing framework, and were answered by gathering additional data from the field. Data obtained via additional field sampling provided supplementary evidence to support/refute hypotheses regarding the origin of the kettle bottom silt. These questions are listed below:

1. How do kettle bottom sediments change (texturally) with depth?
2. When was silt deposited in kettle bottoms in the study area?
3. If the silt in kettle bottom is aeolian, is it local or from an extra regional source, or both?

Details of the methods used to address these questions, and the two aforementioned hypotheses (as well as their results), are presented in the following chapters, in the order they are listed here.

The Evart Upland was chosen as a study area because relatively little is known about the geomorphology of this part of the Lower Peninsula of Michigan. Therefore, the abundance of kettles provided an opportunity to establish a base of knowledge about the geomorphology of an area previously undocumented. The results of this research will hopefully draw attention to the importance of dry kettles as repositories of geomorphic information in formerly glaciated areas.

CHAPTER 2 - Study Area

2.1 Geographic Setting

The study area (the Evart Upland) is a 68 km^2 area of sandy, rolling hills located in Osceola County, MI. The upland is centered on, and encompassed by several USPLS townships: Township 18N, Range 8W; Township 19N, Range 8W; Township 18 N, Range 9W; and Township 19N, Range 9W, of Osceola County, MI. South of the upland is the Muskegon River and the city of Evart. The Evart Upland is primarily forested, and is largely owned and managed by the state of Michigan as part of the Pere-Marquette State Forest. U.S. Highways 131, 10, and 115 pass to the west, south and northeast of the study area, respectively (Fig. 2.1). Access to the Evart upland is possible via county and seasonal roads, and various two-track paths.

2.2 Study Area Extent

The extent of the Evart Upland is herein defined by a combination of topographic and hydrologic characteristics. The Upland proper is characterized by highly undulating and hummocky terrain, containing numerous dry kettles. The lowlands that surround the Evart Upland are characterized by low relief, wet, hummocky terrain (i.e. most of the kettles are bogs and wetlands, often containing ponded water). Indeed, I define the boundary between the Evart Upland and the surrounding lowlands as the elevation where dry upland kettles transition to wet lowland depressions. This *boundary*, however, is

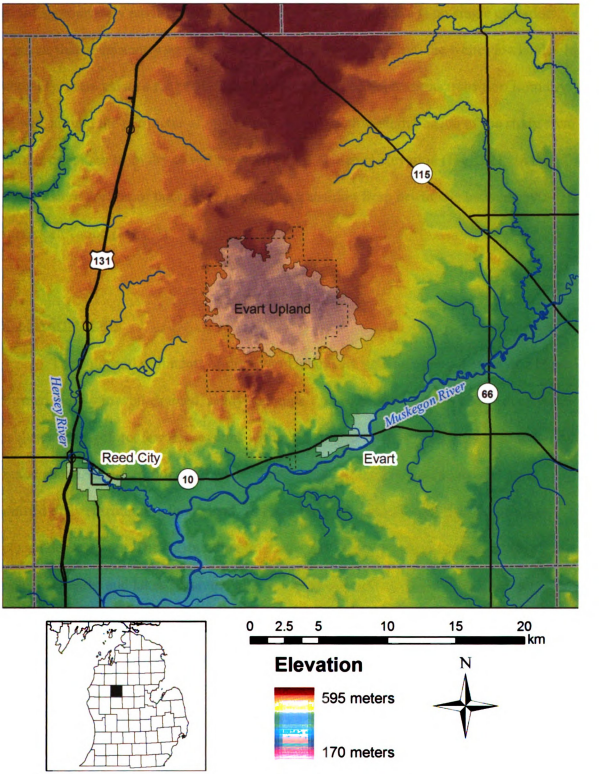

Figure 2.1- Color, hill-shaded, digital elevation model (DEM) of Osceola County, MI. The extent of the Evart Upland is shaded gray. The dashed line represents the Pere-Marquette State Forest boundary. The black lines are major highways.

more appropriately envisioned as a transitional *zone*, since there is no single elevation contour that consistently separates the dry upland landscape from the wetter lowlands. In actuality, there exists a range of elevations where closed depressions transition from dry to wet, around the perimeter of the upland. In the southwestern portion of the study area, kettles transition from dry to wet between 370-390 meters elevation (Fig. 2.2). In the northeastern portion of the study area, kettles transition from dry to wet between 390-410 meters elevation (Fig 2.3).

2.3 Hydrography

The soils and sediments of the Evart Upland are generally very dry, having been formed mainly in well-drained, sandy sediment. As such, the sediments have deep water tables, and therefore, few depressions within the upland contain permanent wetlands. As noted above, however, bogs and wetlands are very common in the transitional zone immediately surrounding the upland, where groundwater discharges into hummocky closed depressions. The surrounding lowlands are, therefore, characterized by numerous bogs, wetlands, and lakes separated by low relief (3-6m) hummocks (Fig. 2.3). Some significant lakes in the surrounding lowlands include Silver Lake, Strawberry Lake, and Hicks Lake. Most of the lakes in the surrounding lowlands are kettle lakes. However, Little Long Lake and Big Long Lake occupy narrow curving valleys, suggesting that they could be of subglacial (meltwater erosional channel) origin (Fig. 2.4).

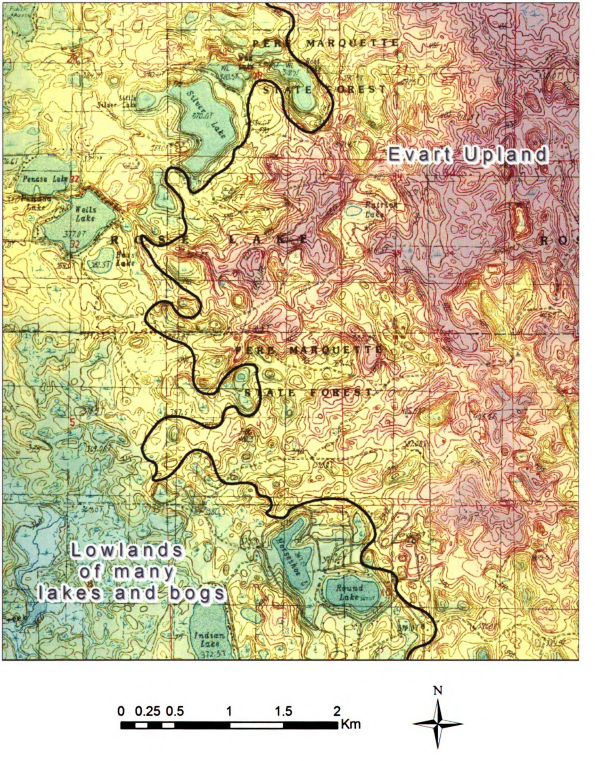

Figure 2.2- Combined topographic map (3-meter contour interval) and color-shaded DEM of the western portion of the Evart Upland. The black line separates dry kettles on the upland from bogs, wetlands, and lakes in the lowlands, and is the approximate boundary of the study area.

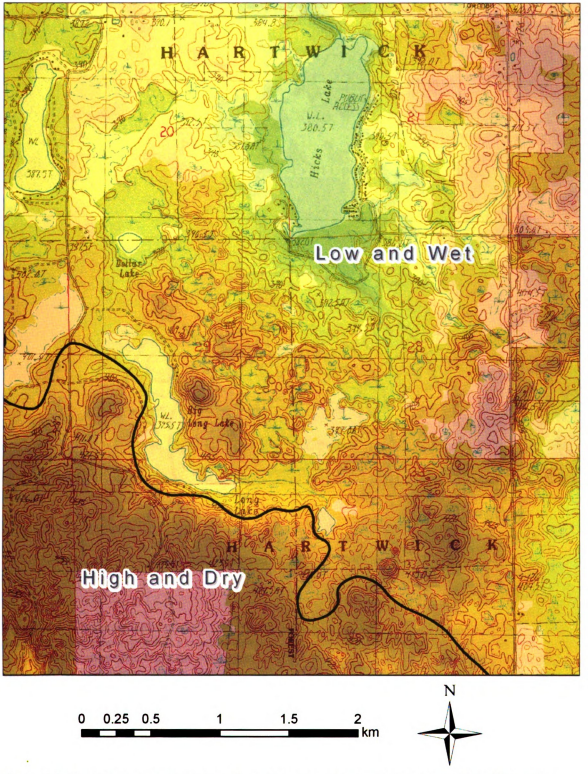

Figure 2.3- Combined topographic map (3-meter contour interval) and color-shaded DEM of the northeastern portion of the Evart Upland. Lower relief, wet, hummocky terrain characterizes the surrounding lowlands to the northeast.

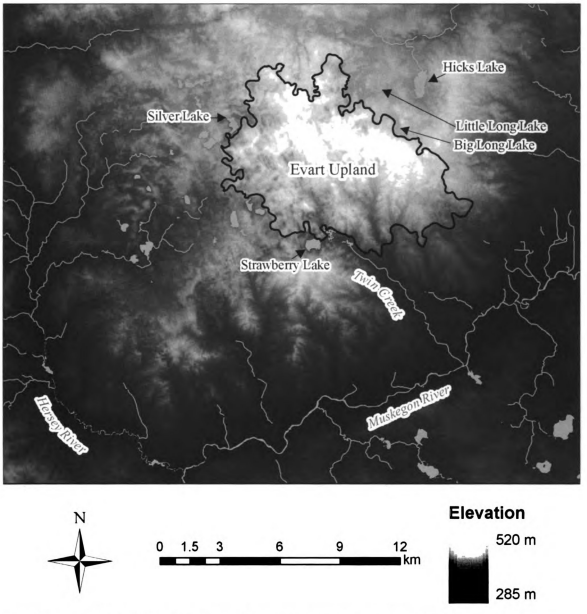

Figure 2.4- Grayscale DEM of the Evart Upland and surrounding areas, showing hydrologic features. Blue lines represent perennial streams and rivers (data source: Osceola County Hydrography shapefiles from the Michigan Geographic Data Library (Michigan Department of Information Technology, 2007)). The Muskegon River, located south of the upland, flows to the southwest. The Hersey River, flowing south, joins the Muskegon River at the bottom of the map.

In general, most perennial streams in and around the study area flow radially away from the Evart Upland, eventually making their way to larger rivers. Major rivers in the area include the Muskegon and the Hersey, which border the Evart Upland to the south and west, respectively. A network of weakly integrated stream valleys extends up the central portion of the upland from the south and southeast. These stream valleys subtly transition upslope to dry valleys containing kettle chains (discussed below). Twin Creek and its ephemeral tributaries are the most notable of such features.

2.4 Geomorphology

The Evart Upland is situated between the former Lake Michigan and Saginaw lobes of the Laurentide ice sheet (see Fig. 1.1, Introduction chapter). As is typical of interlobate terrain (Rieck, 1976), the topographic expression of the upland is undulating and complex. This complexity can likely be attributed to the wastage of detached stagnant ice masses, which resulted in a number of localized closed depressions (kettles). Because this study emphasizes kettles as repositories of geomorphic and sedimentologic information, the majority of the geomorphic characterization below focuses on the distribution and morphology of the kettles themselves.

2.4.1 Methods Used to Characterize the Geomorphology of the Study Area

The geomorphic interpretations made herein are largely based on the analysis of digital USGS topographic maps for the study area. As such, most of the interpretations are not verified by analysis of the landforms in the field. Where applicable, references to

supporting literature are made regarding the formation of similar landforms in nearby regions. This characterization was done to assist in analysis of the field data and discussion of the landscape.

The primary method of characterizing this landscape involved mapping the locations of closed depressions (kettles). The purpose of mapping kettles was to better understand the surface morphology of the upland and to aid in selecting sample sites. Major kettles within the boundary of the Evart Upland were digitally mapped in a GIS, using ArcMap 9.2 (ESRI, Redlands, CA). Kettles too small to be identified on USGS 7.5 minute topographic quadrangles (i.e. shallower than the three meter contour interval) were not mapped.

A Digital Raster Graphic (DRG) of USGS topographic quadrangles for Osceola County was used as the data base for the kettle mapping exercise. The rims of kettles (i.e., their perimeters), defined as the highest closed contour line of each depression, were individually traced on the DRG in ArcMap. The editing was done at a scale of 1:3,500 to ensure that the perimeters of kettles were accurately traced. Kettle depth was recorded during the mapping exercise by determining the elevation difference between the deepest part of the depression (as best estimated) and the kettle rim. The mapped kettles were projected in Michigan Georef (meters) so that the plan geometry (perimeter and area) of each kettle could be calculated. All other spatial data depicted in the maps in this chapter were gathered from the Michigan Geographic Data Library (Michigan Department of Information Technology, 2007).

2.4.2 Topographic Characteristics

The surface expression of the Evart Upland is undulating, very hummocky, and complex, with little or no external drainage. Four observations are noteworthy, with regard to the topography of the upland: 1) kettles are very common, 2) massive sandy ridges, devoid of kettles, are also common, 3) in the low areas between the ridges, many kettles (often linked in chains) exist, and 4) the ridges and kettle chains exhibit a conspicuous linearity, dominantly trending NW-SE. Each of these topographic traits is discussed individually in the sections that follow, along with some possible interpretations of their origin.

The irregular and dome-like Evart Upland rises up to 150 m higher than the surrounding lowlands (Fig. 2.5). Local relief on the upland (between kettle bottoms and adjacent summits) can be up to 24 m, but is typically about six meters. The highest hilltops in the central portion of the Evart Upland peak at about 460-470m above sea level (asl). Relief between the Upland and the Muskegon River floodplain to the south is about 170 m (Fig. 2.5).

The distinct ridge that trends north/northeast, radiating out, away from the east side of the Evart Upland (Fig. 2.5), has a subdued surface expression relative to the higher, central portion of the upland. Topographically, this ridge is similar to the southeastern portion of the upland, where relief between closed depressions and adjacent summits is generally about 3-6 m (i.e. the kettles there are generally small). Auger shavings from road cuts through the ridge suggest that it is comprised of sandy loam drift, making it texturally different than the rest of the Evart Upland, which is dominated by

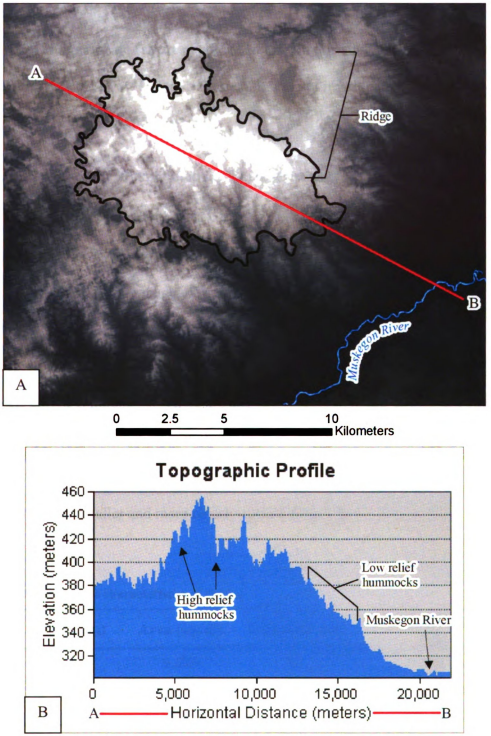

Figure 2.5- A) Grayscale DEM of the Evart Upland showing the location of transect line A-B (red) that was used to construct the topographic profile shown in part B. The NNE trending ridge extending from the eastern portion of the study area is not considered part of the Evart Upland. B) Topographic profile of transect line A-B. Kettles on the upland have much greater local relief than kettles in the surrounding lowlands near the Muskegon River.

sand-textured outwash. It is likely that this ridge is an end moraine of the Saginaw lobe, and thus, not an interlobate feature at all. Therefore, in this study, the ridge is not considered part of the Evart Upland. As such, it was not investigated with the same level of detail as the remainder of the upland.

2.4.3 Kettles: Range of Morphometric Characteristics

A total of 535 major kettles were identified and mapped within the extent of the study area, for a density of nearly eight major kettles per km^{2*} (Fig. 2.6). Kettles on the Evart Upland exhibit a wide range of morphometric characteristics such as, depth, area, perimeter, and perimeter to area ratio (plan view shape) (Table 2.1). Some kettles are a single depression; others are composite, having more than one depression encircled by the highest closed contour line. There are also differences in kettle density and size with respect to location on the upland. On the northwestern and central portions of the upland, larger, more widely spaced kettles are common. On the southeastern portion of the upland, kettles are smaller and more closely spaced (Fig. 2.7).

Table 2.1- Morphometric characteristics of kettles.

	Depth (m)	Area (sq. m)	Perimeter (m)	Area to perimeter ratio
Mean	6	9,670	337	0.08
Max	24	160,000	2,455	0.23
Min	<3	260	62	0.01

* There are many small kettles on the ridge that extends to the north/northeast that were not mapped.

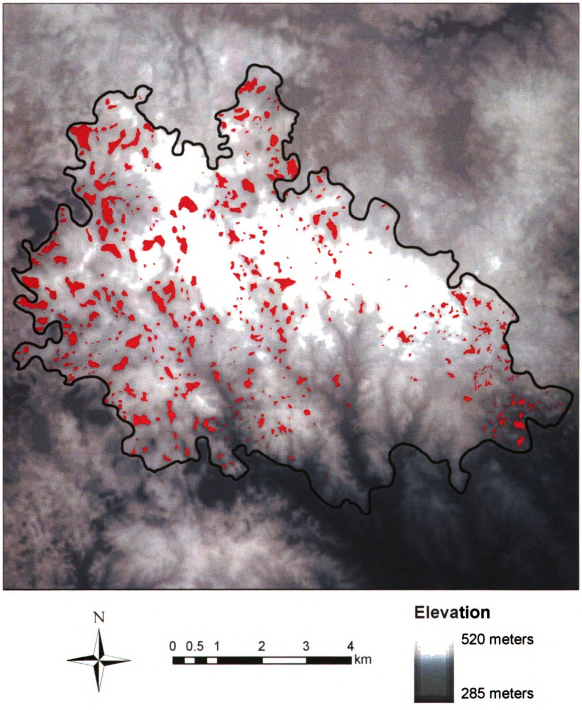

Figure 2.6- Grayscale DEM of the study area with major kettles highlighted in red. A total of 535 kettles were mapped within the boundary of the Evart Upland.

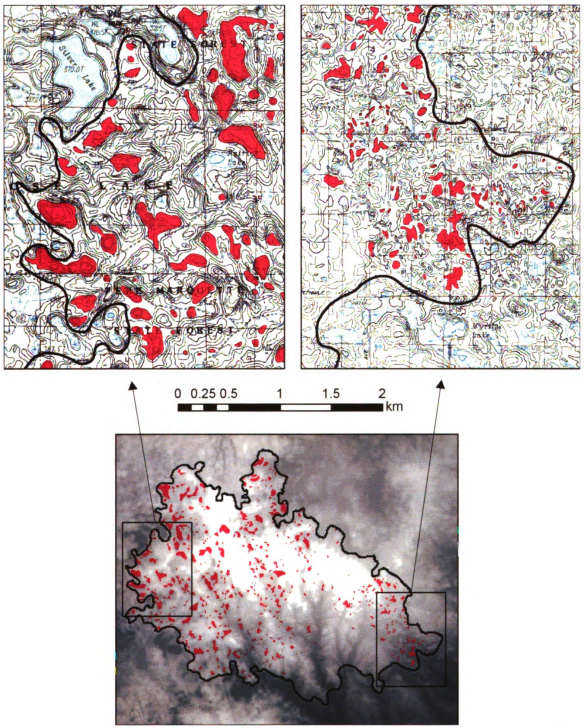

Figure 2.7- Grayscale DEM showing two areas on the Evart Upland with distinct kettle morphology (below); one from the western portion (upper left), the other from the southeastern portion (upper right). The two topographic maps above (3-meter contour interval) are the same scale.

2.4.4 Ridges

There are many distinct, elongate and round, conical (convex upward), mound-like landforms on the Evart Upland. For descriptive purposes, these landforms will herein be referred to as *ridges* (implying no genetic origin) because their sedimentology and internal structure were not explored in the field. Some of the ridges in the study area are broad and roughly linear. The most conspicuous of the ridges are massive and semi-conical, containing a number of localized peaks and gullied sides. The highest ridges peak at about 470 m in elevation. Some ridges are small and linear, while others are steep-sided and relatively flat-topped (2.8). Kettles are absent on nearly all of the ridges, but almost always surround them on the sides. Local relief between the ridge tops and surrounding kettles can be up to 70 meters.

In plan view, these ridges somewhat resemble the *hummocks* and *hummock tracts* described by Ham and Attig (1996) and Johnson et al. (1995) for stagnant ice landscapes in Wisconsin. However, unlike the hummocks they described, the ridges in the Evart Upland are interspersed with dry kettles (both kettle chains and groups of kettles), rather than ice-walled lake plains and wetlands, and therefore, likely have a different geomorphic origin. The abundance of dry kettles and ubiquity of well-sorted, sandy sediments across the study area suggest that the ridges are the result of glaciofluvial deposition, either within large crevasses in the former stagnant ice, or around isolated masses of stagnant ice. Upon full meltout of the stagnant ice and stabilization of the landscape, these sandy infillings then became positive topographic features. Similar interpretations were made for the formation of kettled portions of the Lake Michigan/ Saginaw interlobate terrain further south near Hastings, MI (Folsom, 1971; Rieck, 1979).

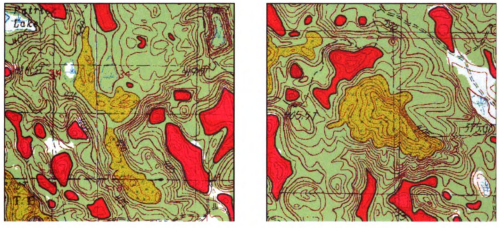

Figure 2.8- USGS topographic map (3-meter contour interval) showing examples of ridges (ridge tops shaded tan) next to kettles (shaded red) in the study area. The ridges in the left map are relatively flat topped and have steep sides. The ridge in the right map is massive with deeply gullied sides.

2.4.5 Low Areas Between Ridges

Between the largest ridges on the Evart Upland, there are low areas with many kettles (Fig. 2.9). These areas range in size, but are generally about 0.5 to 1.0 km^2 in area. Kettles within these low areas are sometimes linked in chains or are elongated parallel to each other; in other areas they are more randomly oriented. Some of the low areas contain groups of many adjacent kettles, and are surrounded by ridges that have multiple small peaks. The ridges surrounding low areas sometimes have steep sides, indicating that they were abutted by ice during their formation, i.e., they are ice-contact landforms. As such, it may be that the low areas containing many kettles were once filled to at least the elevation of the surrounding steep ridges with stagnant ice, and not until later did the much larger ice mass disintegrate into individual ice masses, eventually forming groups of kettles in topographically lower areas.

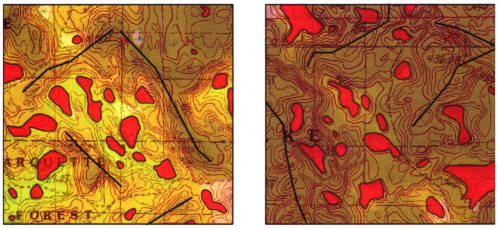

Figure 2.9- Combined USGS topographic map (3-meter contour interval) and color-shaded DEM showing low areas (yellow shading) between ridges (brown shading). In these low areas kettles are grouped. Major ridge crests are traced with black lines. Kettles are shaded red.

2.4.6 Kettle Chains

Some of the low areas between ridges on the Evart Upland contain kettle chains. The individual kettles comprising these kettle chains gradually become more integrated in the downstream direction, eventually transitioning to intermittent, and then perennial, stream valleys downslope (Fig 2.10). For example, the low area between the ridges in sections 1, 2, 11, and 12 of T8N, R9W contains a network of kettles that subtly transition into a series of ponds (i.e., Whitmore pond on the topographic map) that are then drained by Twin Creek further downstream (Fig. 2.11). Kettles that lie just beyond the highest reach of this drainage network are topographically isolated (not integrated by stream incision). The long axis of these non-integrated kettles is usually oriented parallel to the encroaching stream valley. Within the middle reaches of the valley, kettles are somewhat integrated; the highest closed contour line of adjacent kettles is usually the same elevation. However, in the lower valley reaches there are no dry kettles. Instead, ground water emerges to form a series of deranged shallow ponds and wetlands, which are drained by Twin Creek.

Schaetzl and Weisenborn (2004) have interpreted kettle chains in the Grayling Fingers region of Michigan (150 km northeast of the study area) as palimpsest features that inherited their orientation as ice overrode, and was preferentially preserved in, preexisting fluvial valleys. Their interpretation is supported by topographic evidence showing that 1) the kettle chains are sometimes arranged in a meandering pattern, yet 2) there are ridges that separate individual kettles within the chains. Therefore, it was suggested that their arrangement could not be the result of post-glacial stream incision (Schaetzl and Weisenborn, 2004). In the Evart Upland, however, the rims of adjacent

kettles in the middle and lower valley reaches are usually similar in elevation (not separated by significant ridges). Furthermore, the long-axis orientation of the kettles is usually parallel with both the valley they occupy and the perennial streams that drain the upland, neither of which meander significantly. Therefore, the stagnant ice masses that eventually formed the kettles may have been sources of meltwater in the late phases of deglaciation, facilitating development of the low valleys they occupied. This interpretation suggests that the perennial streams that drain the upland inherited their drainage pattern from the distribution of former ice masses, probably in linear chains, that occupied low areas between ridges on the Evart Upland.

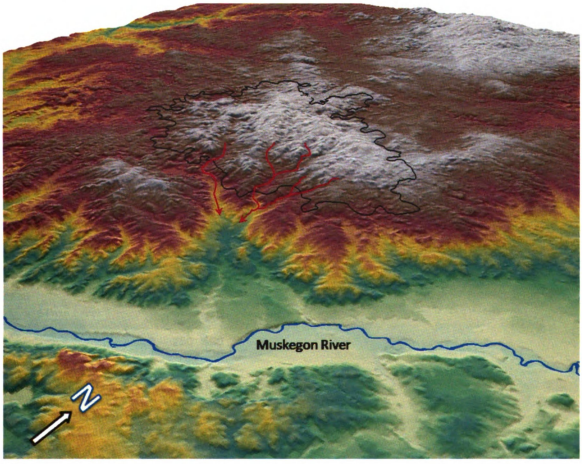

Figure 2.10- Combined hillshade and color-shaded DEM presented in a three-dimensional view looking northwest, at the Evart Upland. The boundary of the upland is outlined in black. The red lines trace weakly integrated stream valleys that are headed by kettle chains upslope.

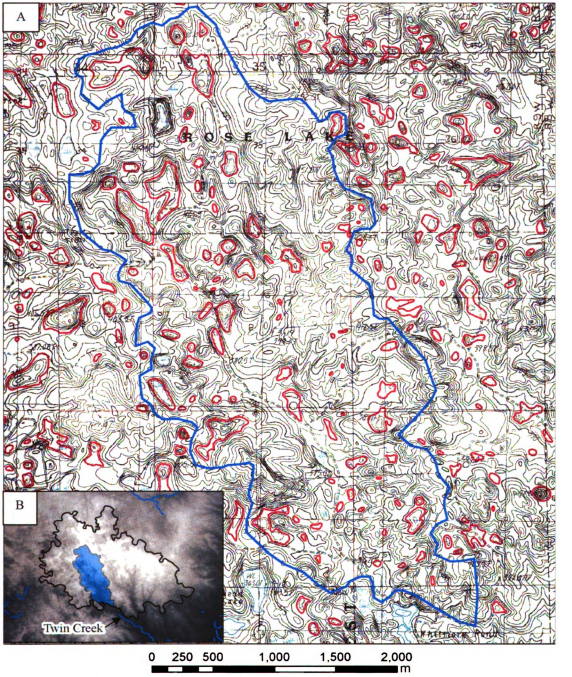

Figure 2.11- A) Topographic map (3-meter contour interval) of a portion of the Evart Upland. The red polygons outline kettles. The blue line outlines the drainage basin of kettles that subtly transition to Twin Creek, south of the map. Note that the long axis orientation of the kettles that occupy the central portion of the valley is more or less parallel to the valley. Kettles in the northern most portion of the drainage basin are not well integrated. B) Inset map of a grayscale DEM showing the location of the drainage basin (shaded blue) on topographic map in (A). The Evart Upland is outlined in black. Blue lines on the inset map are perennial streams.

2.4.7 Linearity of Kettles and Ridges

Both the kettles and ridges described above exhibit a consistent linearity across the study area, generally trending northwest-southeast. Superimposed on this trend is a secondary, less consistent northeast-southwest trend, evident in some ridges and depressions. Sometimes a single ridge or kettle possesses both trends. Even some of the surrounding lakes, such as Silver and Horseshoe lakes, which lie just west of the upland, possess both trends. This linearity manifests itself on multiple scales, from small kettles on the upland to large lakes in the surrounding lowlands (Fig. 2.12). The full geomorphic relevance of these observations is still unknown. However, it may be that the orientation of these landforms was controlled by the structure of the former stagnant ice, which, in this region was ultimately the product of two conjoining ice margins: the Lake Michigan ice from the west and northwest, and the Saginaw lobe ice from the east and northeast. Perhaps, upon meltout, the complex structural arrangement of stagnant ice then influenced the path of glaciofluvial meltwater, thereby playing an important role in the orientation of subsequent landforms.

In summary, the sandy sediments that make up ridges on the Evart Upland were likely areas of ice-contact glaciofluvial deposition, either within fractures in the stagnant ice, or as topographic lows on the former, ablating ice sheet surface. Evidence for this interpretation includes the frequent occurrence of high ridges that usually surround low areas containing many kettles. Some of these ridges have steep slopes, suggesting that they are ice-contact landforms (Bennett and Glasser, 1996). Most of these landforms have consistent long axis trends (NW-SE, and to a lesser extent, NE-SW), the orientation

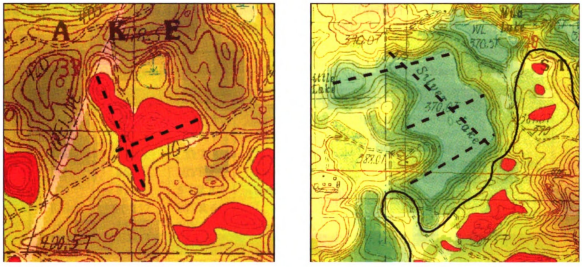

Figure 2.12- Color shaded DEM showing examples of a composite kettle (A) and lake (B) that have contrasting long axis trends as described in the text. Kettles are shaded red. Lakes are not shaded.

of which may have been inherited from the structure of the former stagnant ice, or its margins. Although the length of time that stagnant ice persisted in the study area is unclear, the presence of kettle chains within stream valleys suggests that ice masses persisted within the valleys throughout a later phase of landscape erosion, perhaps even until subaerial streams (still present today) became established.

2.5 Soils

Pedologic diversity across the Evart Upland is low. A total of five distinct, sandy soil series together make up more than 97% of the study area*. Table 2.1 lists these series in order of abundance within the study area. The five most common soil series mapped in the study area (in order of abundance) are Montcalm (coarse-loamy, mixed,

* This calculation was made by dividing the cumulative area of the five most common soil series by the area of the Evart Upland boundary.

Table 2.2- Characterization data for the five most common soil series mapped on the Evart Upland [1], listed in order of abundance from most (top) to least (bottom).

Horizons[2]	Depth (cm)	Color	Texture	Other Characteristics
Ap	0-18	10YR 4/2	loamy sand	-Drainage class: well -Runoff potential: low -Comprises 39.7% of study area -Most common series, generally more common along the lower portions of the upland
E	18-23	10YR 7/2	loamy sand	
Bhs	23-66	7.5YR 4/4	loamy sand	
E'	66-81	10YR 6/2	loamy sand	
Bt	81-91	5 YR 4/4	sandy loam	
E/Bt	91-152	10YR 6/2	sand	
C	152 +	10YR 6/3	loamy sand	
Ap	0-25	10YR 3/2	sand	-Drainage class: somewhat excessively -Runoff potential: low -Comprises 25.1% of study area -Common on the highest, central portion of the Evart Upland and occasionally upslope of Rubicon series
Bs	25-71	10YR 4/4	sand	
E	71-114	10YR 6/4	sand	
E/Bt	114-178	10YR 6/4	sand	
C	178 +	10YR 6/3	sand	
O	0-3	-	-	-Drainage class: excessively -Runoff potential: N/A -Comprises 18.4% of study area -Common in lower landscape positions such as deep kettles, valleys, and low areas between ridges.
A	3-8	10YR 2/1	sand	
E	8-18	10YR 6/2	sand	
Bhs	18-38	7.5YR 4/4	sand	
Bs	38-69	7.5YR 5/6	sand	
BC	69-79	10YR 6/3	sand	
C	79-153	10YR 6/3	sand	
Ap	0-15	10YR 3/2	sandy loam	-Drainage class: moderately well -Runoff potential: high -Comprises 12.4% of study area -Common on the east/southeast side of the study area
Bs	15-51	10YR 4/4	sandy loam	
Em	51-71	10YR 5/2	loamy sand	
E/Bt	71-91	10YR 6/3	loamy sand	
Bw	91-132	7.5YR 4/4	sandy clay loam	
C	132-152	7.5YR 4/4	sandy loam	
O	0-3	-	-	-Drainage class: excessively -Runoff potential: very low -Comprises 1.5% of study area -Least common series, typically found in deeper kettles in the northwestern portion of the study area
A	3-8	10YR 3/2	sand	
Bs1	8-22	10YR 5/4	sand	
Bs2	22-48	10YR 5/6	sand	
BC	48-61	10YR 6/8	sand	
C	61-152	10YR 6/3	sand	

[1] These data were compiled from a combination of SSURGO digital soils data (Soil Survey Staff, 2007) and the Soil Survey for Osceola County, MI (Mettert, 1969).
[2] Horizon designations used in Mettert (1969) were converted to current horizon nomenclature.

semiactive, frigid Alfic Haplorthods), Chelsea (sandy, mixed, mesic Lamellic Udipsamments), Rubicon (sandy, mixed, frigid Entic Haplorthods), McBride (coarse-loamy, mixed, semiactive, frigid Alfic Fragiorthods) and Grayling (sandy, isotic, frigid Typic Udipsamments). Most of the soils on the Evart Upland formed in sandy parent materials. Rubicon and Grayling soils are the sandiest of the five most common series on the Evart Upland. Chelsea soils are slightly finer textured than Rubicon and Grayling. Montcalm and McBride soils are the loamiest of the five most common series on the upland, with McBride slightly finer textured overall than Montcalm. Therefore, in order from coarsest to finest texture overall, the five most abundant series on the upland are: Grayling → Rubicon → Chelsea → Montcalm→ McBride (Table 2.1).

Grayling and Rubicon soils are often mapped in lower landscape positions, such as narrow valleys, deep, dry kettles, and low areas between ridges (Fig. 2.13). Rubicon soils are abundant in the northwestern portion of the study area, and decrease in abundance toward the southeast (Fig. 2.13). Chelsea soils are mostly mapped on the highest, central portion of the Evart Upland and occasionally upslope of Rubicon series. Like Rubicon soils, Chelsea soils decrease in abundance toward the east side of the study area. Montcalm soils are the most abundantly mapped series and, in general, are evenly distributed throughout the study area. Finally, McBride soils are common on the east and southeastern side of the study area (Fig. 2.13).

The ubiquity of sandy parent materials on the Evart Upland is the greatest factor (i.e. of the five soil forming factors outlined by Jenny (1941)) influencing the pedogenic development of these soil series. In that context, precipitation (specifically, snowmelt) is

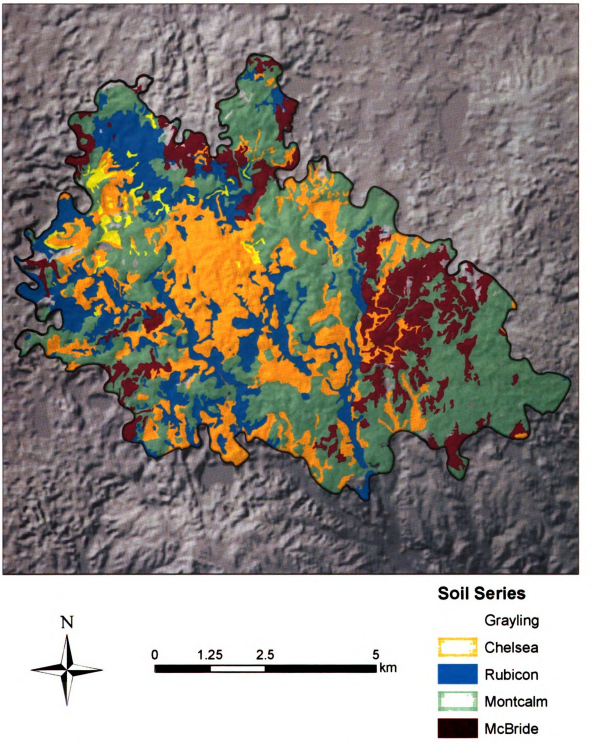

Figure 2.13- Map of the five most common soil series on the Evart Upland (SSURGO digital soils data (Soil Survey Staff, 2007)). All other mapped series are left blank (gray areas on the upland). Grayling and Rubicon soils are mapped in narrow valleys, deep, dry kettles, and low areas between ridges. McBride soils increases in abundance on the east side of the upland, while Rubicon soils are generally absent there.

also important. Soils here likely do not freeze deeply due to a combination of their location (just south of the mesic-frigid soil temperature boundary (Schaetzl et al., 2005)), and the insulating effect of thick snowpacks that exist here (Isard and Schaetzl, 1998). Consequently, these soils may receive more infiltration from snowmelt in the winter than soils further north or west. As such, the combination of a cool climate, sandy parent materials, and reasonably large amounts of snowmelt infiltration has led these soils to develop many pedogenic characteristics of Spodosols (Schaetzl, 1996).

In summary, the five most abundant soil series on the Evart Upland exhibit a range of pedogenic characteristics (Table 2.2), the development of which is mostly influenced by the texture of their respective parent materials. In general, Grayling, Chelsea, and Rubicon soils are sandy and excessively to somewhat excessively drained, whereas Montcalm and McBride soils are loamier. Furthermore, the sandier soils are usually mapped in lower landscape positions on the upland such as narrow valleys, deep, dry kettles, and the low areas occupied by weakly integrated kettle chains described above. In contrast, loamier soils are usually mapped on more stable landscape positions such as the central high portion and the southeastern portion of the upland (Fig. 2.13).

2.6 Vegetation

2.6.1 Past and Present

According to the regional landscape ecosystem classification of Albert et al. (1995), the Evart Upland lies within the Cadillac sub-subsection VII.2.1. Vegetation cover in this sub-subsection is characterized by northern hardwood forest species. At the time of European settlement, the excessively drained sandy ridges in this area were most

likely covered by oak-pine forests containing Red pine (*Pinus resinosa*), White pine (*Pinus strobus*), Red oak (*Quercus rubra*) White oak (*Quercus alba*), Black oak (*Quercus vilutina*), Red maple (*Acer rubrum*), and Bigtooth aspen (*Populus grandidentata*) (Albert, 1995).

Presettlement vegetation cover on the Evart Upland was much different than in the surrounding, wetter lowlands. According to Comer's (1998) presettlement vegetation map, the Evart Upland was primarily occupied by white pine-mixed hardwood forest prior to European settlement. In contrast, beech-sugar maple-hemlock forests dominated the surrounding lowlands. In general, the boundary of the upland coincides with the presettlement vegetation boundary between white pine-mixed hardwood forest and beech-sugar maple-hemlock forest (Fig. 2.14), as would be expected given that the upland soils are xeric and the surrounding lowlands contain permanent lakes and wetlands, set amidst generally loamier soils.

Today, forests in and around the Evart Upland are primarily reserved for timber production. Significant portions of the study area lack canopy cover due to recent clear cutting (Fig. 2.15). As such, forest cover on the upland is sometimes patchy, resembling a mosaic of mixed hardwood forest in various stages of regrowth. Common species on the upland are white pine, red pine, red maple, and bigtooth aspen. Other common trees include: beech (*Fagus grandifolia*), birch (*Betula papyrifera*), and oak (*Quercus spp.*).

2.6.2 Vegetation in Kettles

Some kettles on the Evart Upland are non-forested, allowing other vegetation types, (mostly grasses and ferns) to emerge (Fig. 2.16). This pattern is easily identifiable on the topographic maps of the study area (where kettles are shaded white), and on aerial

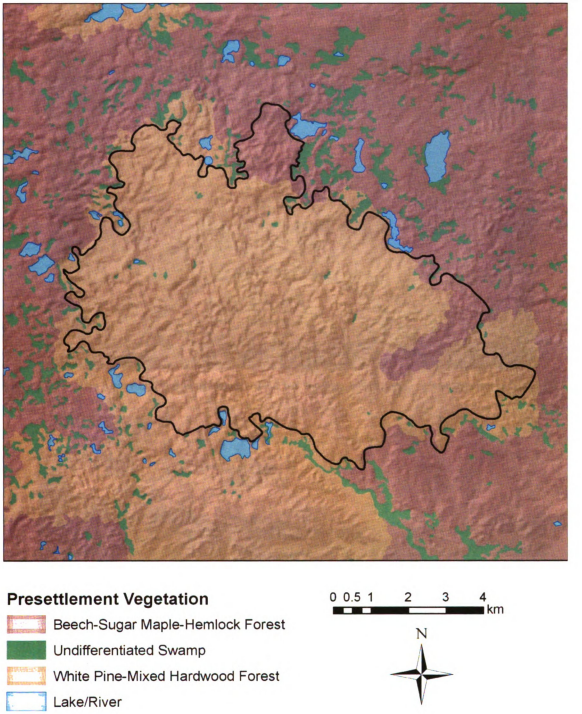

Figure 2.14 Combined hillshade and presettlement vegetation map showing the Evart Upland and surrounding areas. The study area boundary is outlined black. Presettlement vegetation data from (Comer et al., 1998).

Figure 2.15- The Evart Upland is primarily used for timber production. Clear cutting is common. Photo by R. Schaetzl.

Figure 2.16- Some kettles lack canopy cover. In the photograph above, the surrounding forested summits open up to sweet fern and grasses (visible in the foreground) in the kettle bottom. Photo by R. Schaetzl.

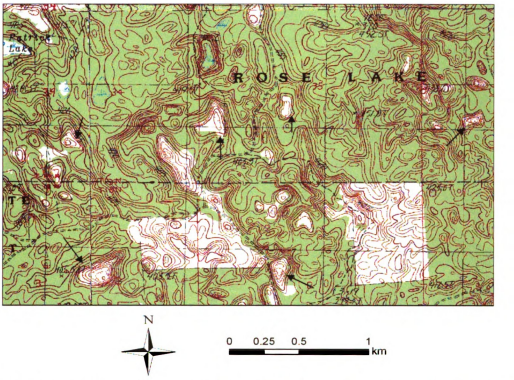

Figure 2.17- Topographic map (3-meter contour interval) of the northwestern portion of the study area. Non-forested kettles are shaded white on this topographic map. Black arrows point to examples of kettles that are non-forested. Other larger areas with white shading were clear-cut at the time the topographic map was made (1983).

photographs (Fig. 2.17). Typically, the vegetation across a kettle changes gradationally from summit to toeslope: forested summits gradually transition to toeslopes of grasses and ferns. The most common fern in the study area is bracken fern (*Pteridium aquilinum*). In Michigan, bracken fern mainly grows on dry, sandy soils (Schaetzl, personal communication). Bracken fern is common on the steepest slopes on the Evart Upland. Another common fern in the study area is sweet fern (*Comptonia peregrina*). Commonly found growing next to bracken fern on the upland, sweet fern also favors dry, sandy soils (NRCS, 2002). Finally, rice grass (*Oryzopsis asperifolia*) commonly grows in the understory of some of the flatter landscape positions on the upland (Fig. 2.18).

Figure 2.18- A) Bracken fern is common on steep slopes (above photo looking up a kettle backslope with a 35% gradient) where soils tend to be quite dry and sandy (i.e. favorable conditions for brackenfern). B) Rice grass commonly grows in the understory of flat landscape positions. Photos by T. Hobbs.

Figure 2.19- This kettle was plowed for tree planting. Rows of raised soil are still visible on the ground (shown by black arrows). Only trees occupying backslope, shoulder, and summit positions successfully grew. Photo by R. Schaetzl.

In some kettle bottoms, the subtle linear microtopography left behind by moldboard plows (evidence that the site was prepared for tree planting, probably in the 1930's and 1940's) is still visible along the ground (Fig. 2.19). Interestingly, only the trees occupying backslope, shoulder, and summit positions have survived in some of these kettles. The failure of re-growth in some kettle bottoms suggests that the gradational change in vegetation cover from summit to kettle bottom is natural and may depend on kettle shape and slope. The GLO (Government Land Office) survey reports of the sections in the study area, compiled when this part of Michigan was first surveyed in the late 1840's, do not make reference to an absence of trees in kettle depressions. However, in counties further northeast (sub-subsection VII.2.2, Grayling Outwash Plain),

it appears that GLO surveyors did note "large frost pockets" in depressions on the outwash plain often containing dry prairie openings (Albert, 1995), suggesting that the absence of forest vegetation in kettles here may be due to abnormally abundant frost events, leading to overall shorter growing seasons.

2.7 Climate

In general, the climate in the study area is typical of humid continental-mild summer locations. The climate station nearest the Evart Upland is about five km southeast of the upland, in Evart. Table 2.3 lists monthly average maximum and minimum temperatures, precipitation, and snowfall for station 202671 (Evart, MI) from 1971-2000. Given that the central portion of the Evart Upland is about 150 m higher and five km north of the nearest weather station, average temperature and precipitation values there may be slightly different from the weather station. The growing season length for Evart, MI is about 114 days (starts 5/25, ends 9/15). Climate data presented in this paragraph and in Table 2.3 were gathered from the NOAA Midwestern Regional Climate Center (NOAA, 2008).

Table 2.3- Average monthly climate data for 30-year period (1971-2000).

Station: (202671) EVART, MI*

Month	Max Temp. (°F)	Min Temp. (°F)	Precipitation (in)	Snowfall (in)
Jan	26.8	8.3	1.9	16.3
Feb	30	8.8	1.5	11.4
Mar	40.3	19.2	2.4	7.9
Apr	54.6	31.3	2.8	1.5
May	68.6	41.3	2.9	0.0
Jun	76.5	49.8	3.2	0.0
Jul	81.8	55	2.5	0.0
Aug	79	53.2	4.1	0.0
Sep	70	45.2	4.6	0.0
Oct	57.6	34.3	3.0	0.2
Nov	43.9	26.7	2.3	5.0
Dec	31.4	15.7	2.1	12.3
Average	**55**	**32.4**	**33.2**	**54.6**

* Data provided by the NOAA Midwestern Regional Climate Center, a part of the Illinois State Water Survey at the University of Illinois at Urbana-Champaign under the Institute of Natural Resource Sustainability, and located on the web at http://mrcc.isws.illinois.edu.

CHAPTER 3 - Methods

3.1 Preliminary Work

3.1.1 Data Sources

An important prerequisite to the field component of this research involved gathering the appropriate spatial data related to the physical features of the Evart Upland and surrounding areas (i.e. topography, soils, hydrography, etc.). These data were gathered to gain an understanding of the processes responsible for the formation of the landscape, and to aid in hypothesis generation about the origin of the silty deposits in kettle bottoms. To that end, topographic quadrangles (7.5 minute series) of the study area were obtained from the United States Geological Survey (USGS). These paper maps were pieced together and laminated for use in the field, both for keeping track of which kettle sites were visited and occasionally to navigate the terrain on foot. Also, the appropriate GIS shapefiles of Osceola County, MI were downloaded from the Michigan Geographic Data Library (Michigan Department of Information Technology, 2007). These files included: public land units, roads, a digital elevation model (DEM), a digital raster graphic (DRG) of the topographic quadrangles, NRCS-SSURGO soils data, and hydrography. These shapefiles were added to an Argonaut TFlex laptop equipped with ArcMap software (Redlands, CA) to aid in field navigation and analysis of the data.

3.1.2 Selection of Sample Sites

Initial, reconnaissance field investigations revealed that, more often than not, non-forested kettles tended to have silty bottom sediments, whereas forested kettles tended to

have sandier bottom sediments. The details of the relationship between presence/absence of forest cover and sediment texture in kettle bottoms is not fully understood, and remains untested in this thesis. Nevertheless, non-forested kettles were preferentially chosen as target sample sites because initial field investigation suggested (albeit anecdotally) that they tended to have siltier kettle bottom sediments than forested kettles. From the 535 major kettles mapped within the study area, a total of 159 target kettle sites were identified and marked as a "target kettle" on a new point shapefile in a GIS. Then, this file was loaded onto the laptop, and used as a guide to navigate to target sample sites.

3.2 Field Methods

3.2.1 Navigation

A 4-wheel drive vehicle, GPS unit, and laptop computer equipped with ArcMap software, were used in combination to navigate to target kettle sites throughout the study area. The following shapefiles were added to ArcMap for navigation and sampling purposes: the DEM of Osceola County, the DRG of Osceola County, roads, kettles, and target kettle sites. The GPS unit (Garmin GPSmap 76C) was linked to an Argonaut TFlex laptop for live position tracking, using software created by the Minnesota Department of Natural Resources (DNR Garmin software). For efficiency, target kettles near road corridors were given preference for sampling. However, because road conditions through the study area are poor (deeply incised two-tracks are common), some of the key, target kettles that are far from roads needed to be navigated to on foot, using the laminated topographic maps.

3.2.2 Addressing Hypothesis 1- Slopewash Origin

If the source of kettle bottom silt is the surrounding backslopes, brought in by slopewash, then there should be a gradual increase in silt content from the kettle backslope soils (the presumed source) to the kettle bottom deposits (site of deposition) due to downslope particle size sorting (Kleiss, 1970; Malo et al., 1974; Chen et al., 2002). A number of downslope sorting mechanisms, such as rainsplash, slopewash, and sediment rafting (Paton et al., 1995), tend to preferentially transport finer sediments further, and result in a predictable pattern of progressively finer soils downslope (Milne, 1936).

To determine whether or not slopewash was/is responsible for the silty deposits in kettle bottoms, two field tasks were completed: 1) I measured the aerial extent of silty deposits in kettle bottoms and 2) I collected two samples from each kettle- one from the kettle bottom deposit and the other from about halfway up the steepest, closest concave backslope position. The first task was completed to better understand the nature of the boundary between the kettle bottom soils and the backslope soils; a gradual, diffuse boundary would support a slopewash origin for the silt, whereas an abrupt boundary would suggest that slopewash is unlikely. The second task was completed to better understand the textural difference between kettle bottom deposits and kettle backslopes across the study area. If the kettle backslopes contain silt that is of comparative amount and texture to that deposited in kettle bottoms, then a slopewash origin is feasible. If the silt content between the two landscape positions is drastically different, then it is likely that slopewash is not responsible for the kettle bottom deposits.

3.2.2a Extent of silt in kettle bottoms

The aerial extent of kettle bottom silt was measured at two sites; these sites were chosen because they represent a range of kettle shapes within the study area. One of them was the largest kettle sampled (site 31), and the other was slightly smaller than average size (site 17). Starting from the bottom center portion of the kettle bottom, the top 20-25 cm of the soil was removed with a push probe, and hand textured. Hand texturing continued at 1 m intervals along the kettle bottom, working outward (upslope). When the sediment texture at this depth changed from silty to sandy, a stake was placed in the ground. Then, the hand-texturing procedure started again from the bottom-center of the depression. Eventually, an oval of 10-12 stakes outlined the boundary between the silty kettle bottom deposits and the surrounding sandy backslope soils. This boundary was easy to identify while push probing because the sandy soils in the backslopes tended to fall out of the probe upon pulling it out of the ground, due to their low moisture holding capacity. In contrast, the moister silty kettle bottom deposits tended to remain in the push probe when pulled out of the ground. As such, the stakes were placed where the soils became sandy and dry enough to easily fall out of the push probe. Finally, the long and short axes of the ovals were measured, and their area was computed using the formula for a simple ellipse. The ratio of the oval area (extent of silty deposits) to the kettle area (automatically calculated during the kettle mapping effort) was then determined for the two kettles.

3.2.2b Comparing texture of kettle bottom and backslope soils across the study area

Two samples were acquired from each kettle, using a bucket auger- one from the kettle bottom and the other from the kettle backslope (Fig 3.1). The kettle bottom sample was acquired from the bottom-center portion of the depression, at a depth where the sediments were (as determined by hand texturing) the siltiest. The sample depth differed in each kettle bottom, but ranged between 40-70 cm. The kettle backslope sample was gathered from the closest, steepest, convergent backslope position (often about halfway up the slope), given that this is where slopewash processes would be most concentrated (Pennock and De Jong, 1987), and from which, potential sources of backslope silt would be winnowed via slopewash. Kettle backslopes were consistently sampled from 15-30 cm depth in order to capture a representative sample that has not been stripped of its silt content (if backslopes are indeed the source of kettle bottom silt). Of the 159 target sites identified, 53 kettles were sampled, resulting in 106 kettle bottom and backslope samples combined (Fig. 3.2).

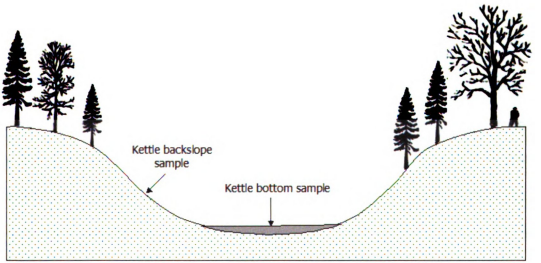

Figure 3.1- Schematic representation of a typical kettle in the study area (not to scale) showing the locations of samples gathered within each kettle.

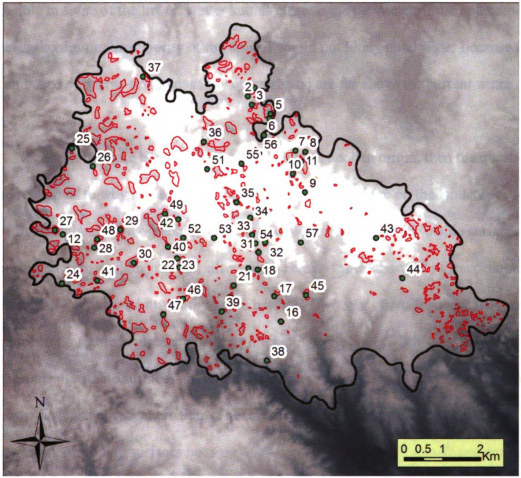

Figure 3.2- Location of sampled kettles on the Evart Upland. Kettles are outlined red. A total of 53 kettles were sampled. Two samples were gathered at each site, resulting in a total of 106 samples.

3.2.3 Addressing Hypothesis 2- Aeolian Origin

The textural data from each kettle bottom deposit and adjacent backslope was analyzed to address the feasibility of an aeolian origin for the kettle bottom silts at each kettle site. If the textural data indicate that slopewash is not likely responsible for the deposits of kettle bottom silt, then invoking an aeolian origin for the silt is reasonable. The only other scenario that could explain the presence of silt in kettle bottoms is if the kettles on the Evart Upland once contained ponded water, offering a low energy environment in which near-surface silty sediment could be deposited. This scenario may

be feasible in some of the lower, wetter kettles close to the perimeter of the upland. However, kettles on the majority of the upland would not likely pond water because they are composed of coarse-textured, sandy outwash and are far above the current water table.

If the silt in kettle bottoms does indeed have an aeolian origin, then the question would remain as to why it was preserved there and not elsewhere on the landscape. Most of the Evart Upland is topographically steep and sloping, offering few stable surfaces for the preservation of aeolian silt (i.e., silt would be easily transported off of steep slopes and eventually deposited into nearby kettle basins). However, there are some flat, geomorphically stable landscape positions on the Evart Upland (albeit very few). Geomorphically stable surfaces are defined herein as low-lying, flat landscape positions that show no signs of recent erosion. These sites are more likely to collect and retain aeolian silt than sloping surfaces because of the greater potential for runoff and erosion inherent with increasing slope. Therefore, I chose three geomorphically stable surfaces to sample to analyze their silt distribution with depth. Soils at these three sites were depth sampled with a bucket auger at 10-20 cm intervals. Depth sampling continued down into the C-horizon, ranging between 75-105 cm depth. An aeolian origin for the kettle bottom silt would be supported by evidence indicating that geomorphically stable, flat landscape positions contain an increase in silt in their upper profiles, since silt is more likely to be preserved here than on sloping surfaces, and because aeolian silt would have been the last sediments deposited, and thus would be retained in the upper profile. This scenario assumes that a silt increase in the upper soil profile is not due to physical

weathering, which is reasonable for the Evart Upland, given that soils there are young and relatively poorly developed.

3.2.4 Addressing Additional Research Questions

After the aforementioned field data were collected and analyzed, a number of other research questions arose. These questions are outlined below with an explanation of how additional field data were gathered to answer them. In all cases, the additional data contributed supporting evidence for the origin of the kettle bottom silt.

3.2.4a - How do kettle bottom sediments change (texturally) with depth?

While sampling kettles across the study area, I encountered a number of kettle bottoms containing buried soils. The presence of buried soils in kettle bottom deposits revealed that this landscape has experienced alternating periods of stability and instability through time. Clearly, the sequence of sedimentation in kettles would reveal more about the nature of silt deposition in this landscape. Therefore, I chose eight kettle sites, each containing buried soils, to sample with depth. I chose sites with buried soils because they more clearly show signs of former landscape stability and instability than kettles without buried soils. Using a bucket auger, samples were gathered at ~10-20 cm intervals. The depth and thickness of buried soils, along with pedogenic horizon sequences, were noted in the field. Depth sampling continued into the lowermost coarse sandy outwash (substrate) sediments underlying the silt. The depth to these substrate sediments ranged between 110 and 220 cm, depending on the site.

3.2.4b - When was silt deposited in kettle bottoms in the study area?

The opportunity to answer this question arose upon discovery of charcoal fragments lodged in buried soils at two kettle bottom sites. In one kettle bottom containing a particularly strong sequence of buried soils (site 33), a soil pit was excavated. After cleaning the profile face, images of the soil were taken (see Fig. 4.38, Chapter 4). The horizon sequence, depth and thickness of buried soils, and presence of charcoal, were all noted. The lowermost buried soil contained a number of small charcoal fragments (Fig 4.38, Chapter 4). A large volume (~25 liters) of this soil-with-charcoal mixture was gathered and transported back to the soils lab at the Michigan State University Geography building, to extract charcoal for radiocarbon dating (extraction methods explained in next section). At another site (site 17), macroscopic pieces of charcoal (about 0.5 to 3 cm in length) were discovered while depth sampling. These charcoal pieces were carefully removed from the bucket auger shavings and placed in a sample bag. The depth that the charcoal was recovered from was noted.

3.2.4c - What is the source of silt in kettle bottoms?

If the silt in kettle bottoms is aeolian, then it follows that perhaps it could be from some extra-regional source, and therefore, possess recognizable differences in silt mineralogy, as compared to the silt within adjacent backslopes (local silt). On the other hand, a similar mineralogical composition of silt in kettle bottoms and adjacent backslopes would suggest a more local source for the kettle bottom silts. To answer this question, the silt mineralogy of four kettle bottom and adjacent backslope pairs were analyzed and compared using X-ray diffraction. Because the methods used to answer this

question are primarily lab-based, they are described in more detail below, in the section titled "X-ray diffraction analysis."

3.3 Laboratory Methods

3.3.1 Sample Preparation

The soil samples were brought back to the soils lab in the Geography building and allowed to air dry for several days. Samples that still contained moisture after several days were heated in an oven at about 65 ^{o}C overnight to remove excess water. Each sample was lightly ground with a mortar and pestle, and passed through a 2-mm sieve to remove coarse fragments. The remaining fine-earth samples were then homogenized in a sample splitter to ensure that a representative sub-sample for particle size analysis was obtained.

3.3.2 Particle Size Analysis

3.3.2a Background

In recent years, laser diffractometry has generally replaced the more traditional sieve-pipette method for particle size analysis (Sperazza et al., 2004; Arriaga et al., 2006). Laser diffraction analysis is faster, more accurate, and provides a near-continuous distribution of particle size data, whereas data generated by the sieve-pipette method generally are output as discrete particle size fractions, e.g., 50-125 microns, 2-50 microns, etc. Although the data produced by the two methods are comparable and highly correlated (Arriaga et al., 2006), some differences do exist, mainly in the clay fraction (Buurman et al., 1997).

Laser diffractometry commonly underestimates the amount of clay (< 2 microns), when compared to the pipette method (Loizeau et al., 1994; Beuselinck et al., 1998) probably because of its platy shape, which slows the rate at which it settles within a traditional pipette analysis cylinder. For this reason, Konert and Vandenberghe (1997) suggested that a clay-silt break of 8 microns be utilized for laser diffractometry data, in order to facilitate any comparisons between laser diffractometry and traditional pipette particle size analysis data. Similarly, in-house data from the soils lab at Michigan State University suggested that correlations between clay contents by pipette (from former studies) vs. laser diffractometry are highest when the clay-silt break for the latter is set at 6 microns. Thus, in this study, the clay/fine silt boundary was set to 6 μm to offset the slight over-estimation of clay by the laser hardware.

3.3.2b Data output

Particle size distributions for each sample were measured with a Malvern Mastersizer 2000 laser particle size analyzer. This particular model measures the distribution of grain sizes from 0-1000 μm in near continuous detail, while the 1000-2000 μm fraction is expressed as a single value. The user defines what data are included in the output file, depending on the intent of the research. For this study, two output templates were used: the first includes the necessary fields to create a particle size distribution curve, the second includes many grain size ranges, including clayfree calculations and ratios of certain silt fractions. These data tables are listed in the Appendix.

3.3.2c Obtaining a representative sub-sample

Before the particle size analysis was run, a representative sub sample from each sample bag was placed into a small vial. The quantity placed in each vial varied depending on the texture of the sample (very sandy samples require more sediment, where clay or silt rich samples require less sediment), but, in general, the weights ranged between 0.25 to 1.0 g. A mixture of distilled water and 5 mL of dispersing solution ($(NaPO_3)_6$ and Na_2CO_3) was added to each vile. The vials were then agitated on an orbital shaker for two hours to fully disperse the individual grains in the sample.

3.3.3 Radiocarbon Analysis

3.3.3a Sample Preparation

The charcoal removed from kettle bottoms at site 17 and site 33 required different preparation techniques for radiocarbon analysis because the fragments were much different in size. The larger charcoal pieces gathered from site 17 required very little further preparation; they were removed from the sample bag with tweezers, rinsed with distilled water, and placed in a beaker to dry in an oven at ~25 °C overnight. The smaller charcoal pieces within the bulk-sampled buried soil from site 33 were extracted as follows: aliquots of soil were rinsed through a 250 μm sieve to separate the mineral component from the larger fragments of charcoal. The charcoal fragments (and other sediment larger than 250 μm, which included plant fragments and sand grains) were then rinsed with distilled water and carefully flushed onto a petri dish. The petri dish was then placed under a Leica MZ6 binocular microscope and pieces of the charcoal were removed with tweezers and placed in distilled water and dried in an oven at 65 °C until

all the water evaporated. This process- sieving, extracting, and drying- was repeated until the desired dry weight of 0.2 grams total charcoal was obtained. The samples were repackaged in new sample bags, labeled, and sent to the Center for Applied Isotope Studies (CAIS) at the University of Georgia. There, the Graphite $^{14}C/^{13}C$ ratios of the charcoal samples were analyzed using an accelerator mass spectrometer. The $^{13}C/^{12}C$ ratios were measured separately using a stable isotope ratio mass spectrometer and expressed as $\delta^{13}C$ with an error of less than 0.1‰.

3.3.4 X-Ray Diffraction Analysis

3.3.4a Silt separation

The goal of the silt separation procedure that I employed in this research was to isolate a range of grain sizes shared by adjacent kettle bottom/backslope sample site pairs. The four sites chosen, from among 53 total pairs, included those that showed the greatest evidence for an aeolian origin for the kettle bottom silt samples*- sites 24, 28, 31, and 42. At sites 28 and 31, the kettle bottom silt appeared least likely to be derived via slopewash (i.e. these sites had the greatest difference in silt content between the kettle bottom and adjacent backslope). Sites 24 and 42 were kettles included in the depth sampling procedure. These two sites contained intervals of well-sorted, nearly pure silt in the sequence of kettle bottom sediments. It is assumed that these intervals most clearly show evidence of an aeolian depositional unit in the kettle bottoms, and therefore, mineralogical differences (if evident) between them and adjacent backslope silts would be most pronounced in such samples.

* This procedure was carried out after examining the results of particle size analysis.

The 20-53 μm grain size range was chosen for the silt separation analysis. The lower limit (20 μm) was chosen because the four backslope samples show an increase in silt at 20μm, and contain very few particles below that size (Fig. 3.3). The upper limit chosen for silt separation was 53 μm, given that this size is the closest sieve size available to the upper range of silt (50 μm). The 20-53 μm size fraction was separated from kettle bottom and backslope samples as follows: approximately 10 grams of each sample were placed in a bottle containing a mixture of distilled water and 5 mL of dispersing solution ($(NaPO_3)_6$ and Na_2CO_3). The bottles were agitated on an orbital shaker for two hours to fully disperse the sediments. The dispersed samples were passed through a 53 μm sieve with distilled water, into a 1000 mL graduated cylinder, to separate any sediments larger than 53 μm. Sediments smaller than 20 μm were isolated using a calculation of Stokes' law that determines the time it takes for grains to settle to a given depth. Using this law, I

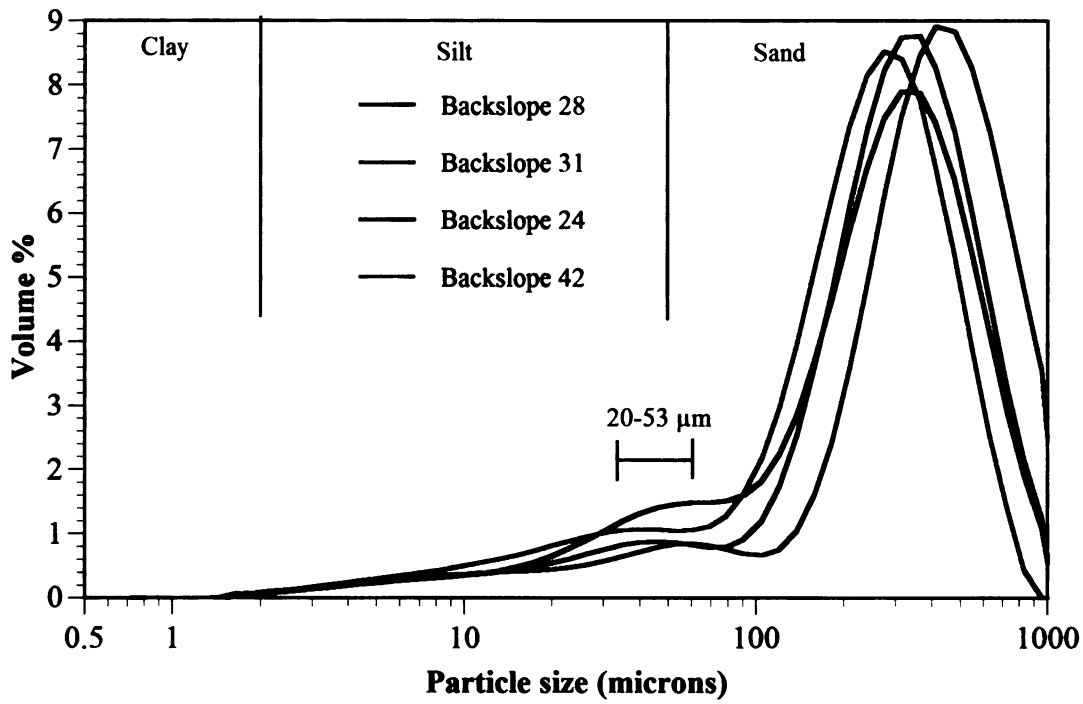

Figure 3.3- Particle size distribution curves for selection of backslope samples used in the X-ray diffraction analysis. The range of grain sizes extracted from the samples is 20-53 μm. The lower limit of 20 μm was chosen because backslope samples have very little silt below that size.

determined that sediments larger than 20 μm should settle at or below 20 cm after three minutes, 48 seconds. To facilitate this separation procedure, I then mixed the samples in the cylinder by tipping them back and forth multiple times to fully suspend the sediments. Then, the sediments were allowed to settle in the graduated cylinder for 3 minutes, 48 seconds, after which time a suction hose was used to remove the sediment-rich supernatant to a depth of 20 cm. This process was repeated 4-7 times, depending on the clay content of the samples, until the supernatant was clear.

The 20-53 μm sub-samples were then dried in an oven overnight at 65 °C and then pulverized with a Fritsch Analysette 3 Spartan Pulverisette for about three minutes until the silt was uniformly crushed to < 5 μm. The crushed silt powder was then stored in vials for transport to the X-Ray diffraction lab in the department of Geological and Environmental Sciences at Hope College, in Holland, Michigan.

3.3.4b Lab analysis

A total of eight samples were analyzed (four kettle bottom/backslope pairs). A random powder mount technique was used for the X-ray diffraction analysis. This technique involved carefully tapping the powder into the container, using the edge of a glass slide in order to optimize random orientation of the crushed silt particles (Zhang et al., 2003). The randomly oriented silt powder was then X-rayed in a MiniFlex+ X-ray Diffractometer (Rigaku Corporation, The Woodlands, TX) using Cu-Kα radiation. The first three samples were X-rayed in the 21°-33° 2θ range for a two second count time and a 0.02° step size, as an exploratory method to determine what minerals were present. It was later concluded that the primary peaks for any significant minerals present in the

samples were captured within the 25°-29° 2θ range, and therefore, the remaining samples were X-rayed within this range. Quartz, K-feldspar, and plagioclase were the only three clearly identifiable, commonly occurring minerals present in the samples. The three minerals were assigned to 26.5 2θ, 27.4 2θ, and 27.8 2θ values, respectively. The diffraction patterns of the four kettle bottom-backslope pairs were plotted, stacked, and qualitatively compared to look for significant differences in silt mineralogy.

CHAPTER 4 - Results and Discussion

Fieldwork and sampling confirmed that 53 of the 59 kettles visited in the field contain lenticularly-shaped, silty deposits in the center-bottom portion (i.e., the deepest part) of the depression. The recurring pattern of silt deposition in kettle bottoms throughout the Evart Upland indicates that kettles here have acted as accumulation basins, preserving a record of landscape stability and instability since deglaciation, via the sediments that are contained within them, particularly at their center-bottom areas (Walker and Ruhe, 1968). The purpose of this chapter is to explain the characteristics and likely origin(s) of these silty kettle bottom deposits, by describing their textural variability at various sites across the upland, as well as with depth at specific sites. The paleoenvironmental significance of such deposits, in the context of the regional landscape, will be discussed in Chapter 5.

Addressing Hypotheses- Slopewash vs. Aeolian Origin for the Kettle Bottom Silt

If slopewash were solely responsible for the accumulation of silt in kettle bottoms, then two conditions could be assumed to exist:

1. Silty kettle bottom deposits should have a diffuse lateral boundary, gradually transitioning up to the surrounding sandy kettle backslopes, and
2. Backslopes should contain significant amounts of silt that is of comparable particle size distribution (i.e., similar distribution of particle sizes within the silt [2-50 micron] fraction) to that in kettle bottoms, bearing in mind that the subtle sorting effect of downslope transport may skew the silt distributions slightly.

If these conditions do not hold, than it is reasonable to invoke an aeolian origin for the kettle bottom silt, because there are no other reasonable mechanisms by which such silty deposits could consistently occur in kettle bottoms in this landscape. The only other mechanisms to consider that could explain the origin of the silty sediments in kettle bottoms involve increased weathering of in situ sediments there, or deposition of silts in a subaqueous (i.e., a kettle lake), setting. However, both of these scenarios are unlikely because 1) the soils here are relatively young, and as such, have not weathered deeply, and 2) the soils in the sampled kettles are well drained, with deep water tables, and as such, have not likely ponded water in the past.

In this section, I will first discuss the nature of the outer boundary (edge) of kettle bottom deposits at two representative sites. Next, I will explain the textural characteristics of the kettle bottom deposits and their respective kettle backslope sediments. Finally, I will examine the textural difference between kettle bottom/backslope pairs at nine individual kettle sites, highlighting examples where the silty kettle bottom deposits exhibit the most, average, and least textural differences from their presumed upslope source (i.e. backslopes).

4.1 Extent of Silt in Kettle Bottoms

The outer boundary (edge) of the silty kettle bottom deposits was examined in detail at two kettles (site 17 and site 31). These sites represent the largest (site 31) and average (site 17) size kettles on the upland. I assumed that if the silt in kettle bottoms was winnowed out of the surrounding backslopes via slopewash, then the outer boundary of the silty kettle bottom deposits should be diffuse, extending up into the surrounding

backslopes. However, at both sites, the outer boundary of the kettle bottom deposits is marked by an abrupt transition (~1-2 m lateral distance along the ground) from silt-dominated sediments to sand-dominated sediments. The outer boundary was outlined in the field by placing stakes in the ground where the surface sediments became dry, sandy, and easily fell out of the push probe (see Methods). This outline of stakes crudely delineated the extent of the silty deposits at both sites, and confirmed that the silty deposits in both kettle bottoms are confined to (and concentrated in) the bottom-center portion of the depression, and have an abrupt lateral boundary (Figs 4.1 and 4.2).

In summary, by examining the outer boundary of the silty kettle bottom deposits at two representative sites, the following characteristics were confirmed:

1) The silty kettle bottom deposits are confined to, and concentrated in, the center-bottom portion of the basins.
2) The boundary between the silty kettle bottom deposits and the sandy backslope sediments is reasonably abrupt.
3) The silty deposits do not extend up the surrounding backslopes.

These combined characteristics suggest that the silty kettle bottom deposits lie unconformably within kettle bottoms, and as such, appear anomalous with respect to gradual downslope sorting of backslope sediments (i.e. slopewash). Furthermore, the silty deposits comprise very little of the area of the kettle bottom (Figs. 4.1 and 4.2). Therefore, condition 1 (listed above) does not hold true for the two representative sites examined in the field. The texture of backslopes and kettle bottom deposits will be explored next to examine condition 2.

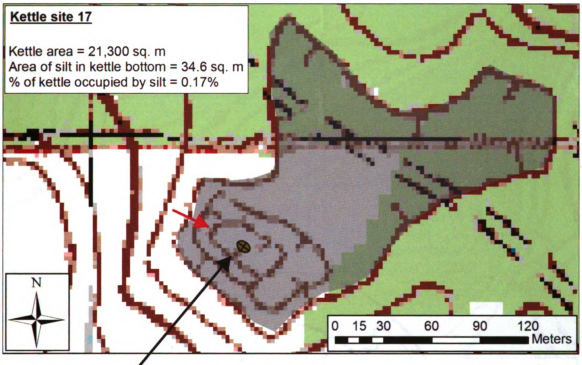

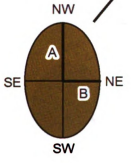

Area of silt in kettle bottom = ABπ

A = 4.04 m

B = 2.73 m

Area = (4.04)(2.73)π

Area = 34.6 sq. m

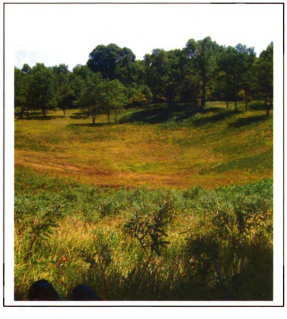

Figure 4.1- Aerial extent of silty sediments in the bottom of kettle site 17 (above). The kettle area is shaded gray. The extent of silt is shaded brown. The red arrow gives the perspective of the photograph at left.

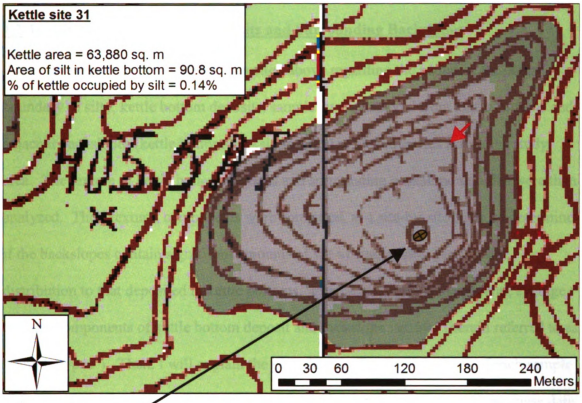

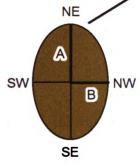

Area of silt in kettle bottom = ABπ

A = 6.25 m
B = 4.63 m

Area = (6.25)(4.63)π

Area = 90.8 sq. m

Figure 4.2- Aerial extent of silty sediments in kettle bottom at kettle site 31 (above). The area of the kettle is shaded gray. The extent of silt is shaded brown. The red arrow gives the perspective of the photograph at left.

4.2 Texture of Kettle Bottom Deposits and Surrounding Backslopes

In support of the evidence presented above regarding the nature of the outer boundary of silty, kettle bottom deposits, samples were gathered from kettle bottoms and adjacent backslopes (kettle bottom/backslope pairs) at 53 kettle sites across the study area. The texture of kettle bottom deposits and surrounding backslope samples were then analyzed. Their textural components were compared, at a site-by-site basis, to determine if the backslopes contain significant amounts of silt of comparable particle size distribution to that deposited in kettle bottoms. First, I will explain the general, average textural components of kettle bottom deposit and backslope samples (herein referred to as "sample types"). Then, I will explain the particle size distribution curves of each sample type at specific sites to compare their modal sand and silt components, and use these data to examine the feasibility of a slopewash origin for the silt in kettle bottoms.

4.2.1 General Texture

Results of the textural analyses revealed a number of important textural characteristics of both sample types (Table 4.1). The most important textural characteristic, with respect to the feasibility of a slopewash origin for the kettle bottom deposits is that, on average, kettle bottoms contain ~four times the amount of clayfree silt than do backslopes. The drastic textural contrast between the two sample types suggests that 1) kettle bottoms are greatly enriched with silt relative to backslopes, and thus, 2) backslopes do not contain enough silt to be the primary source of kettle bottom silt.

Table 4.1- Average textural components of backslope and kettle bottom deposit samples.

Sample Type	% Sand (σ)*	% Silt (σ)	% Clay (σ)	%Clayfree sand (σ)	% Clayfree silt (σ)
Backslopes	82.6 (7.8)	14.3 (6.1)	3.1 (2.0)	86.2 (6.7)	14.8 (6.7)
Kettle bottoms	36.1 (14.5)	48.6 (10.5)	15.3 (5.1)	41.9 (14.5)	58.1 (14.5)

* σ denotes standard deviation.

On average, both sample types are texturally much different from each other (Table 4.1). A paired t-test revealed significant differences ($\rho < 0.001$) between each sample type for all textural components listed in Table 4.1. Individual samples within each sample type exhibit significant textural variability. Figs. 4.3 and 4.4 show the particle size distribution curves of all 53 kettle bottom and backslope samples, respectively. These figures illustrate that kettle bottom deposit samples have greater textural variability than do backslope samples. Many kettle bottom deposits contain significant amounts of sand*, and some backslopes contain significant amounts of silt, thereby deviating from their average "silty" or "sandy" textures, as reported in Table 4.1. In effect, there are a number of backslope samples that texturally "overlap" with kettle bottom deposit samples (Fig. 4.5). Hence, some backslope sites may be a feasible source for silt accumulation in their respective kettle bottoms (via slopewash), other things being equal. However, the vast majority of other kettle sites exhibit a drastic textural contrast between the two landscape positions; the backslopes do not contain a comparable amount of silt to that deposited in kettle bottoms. Thus, at these sites, the backslopes could not be the source of kettle bottom silt.

* The potential sources of the sand in kettle bottom deposits will be discussed later in the chapter.

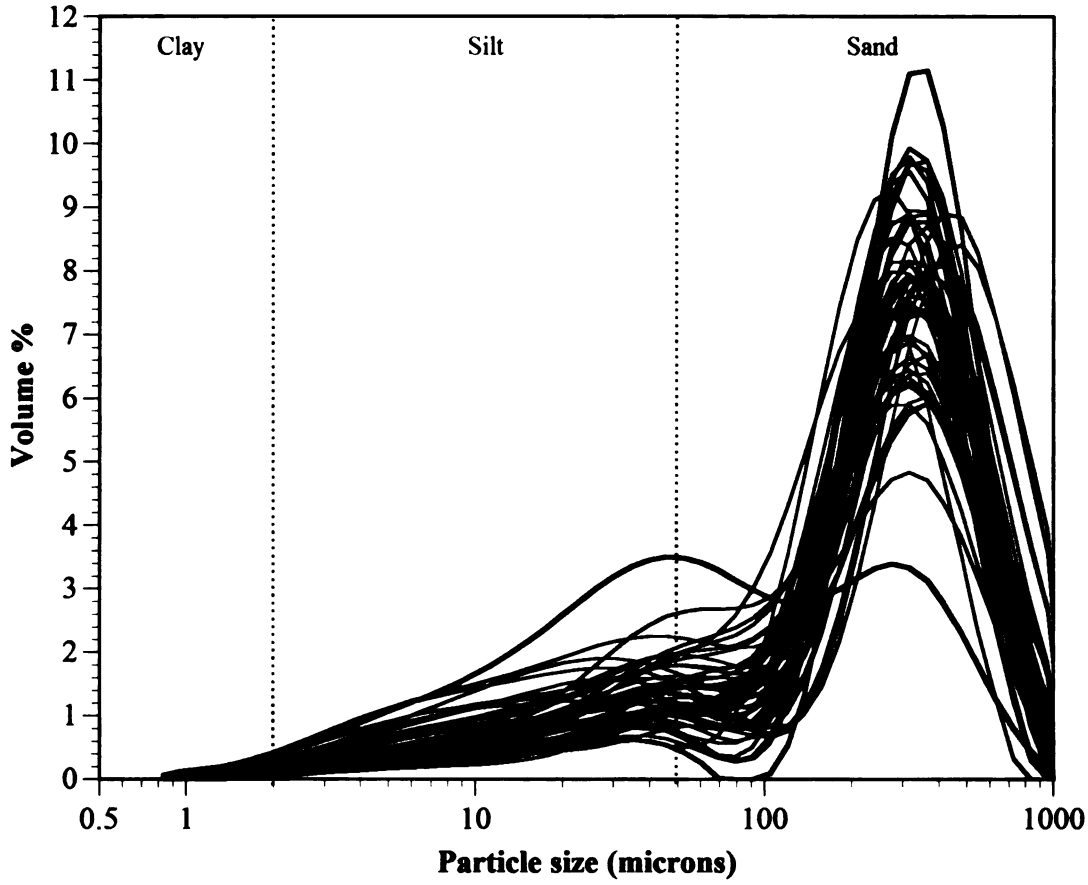

Figure 4.3- Particle size distribution curves of all 53 backslope samples. The average particle size distribution is highlighted red. Blue and green curves represent the coarsest and finest textured sample, respectively.

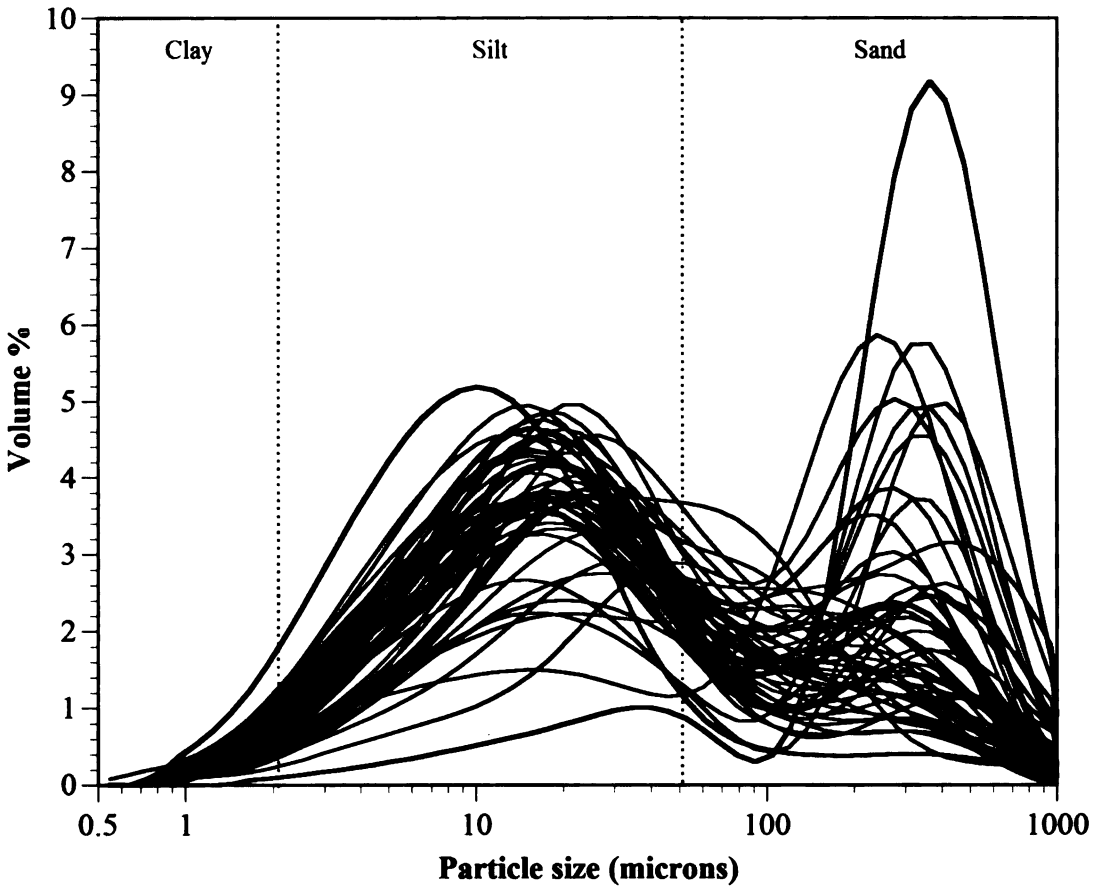

Figure 4.4- Particle size distribution curves of all 53 kettle bottom deposit samples. The average particle size distribution is highlighted red. Blue and green curves represent the coarsest and finest textured sample, respectively.

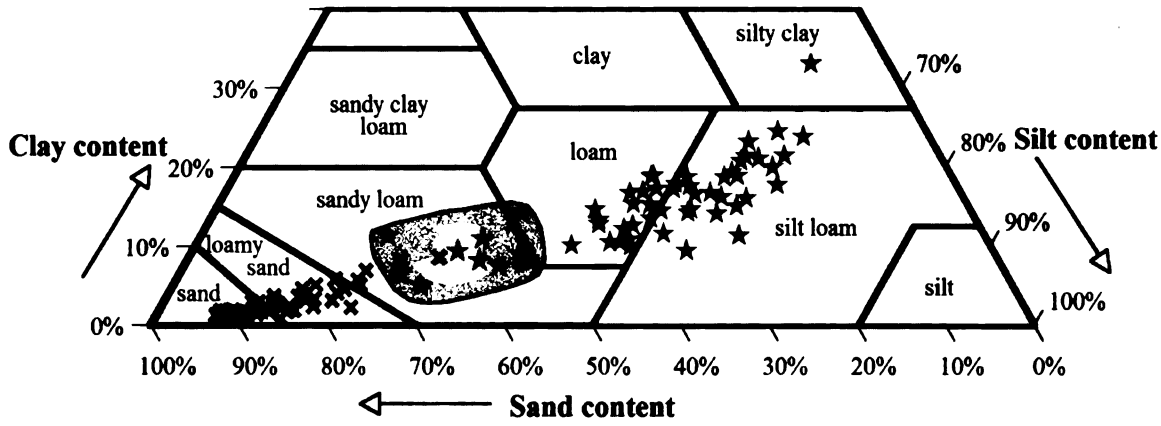

Figure 4.5- Lower half of the USDA textural triangle, showing the texture of kettle bottom samples (blue star) vs. kettle backslope samples (green x). Kettle bottom deposit samples generally have loam and silt loam textures. Kettle backslope samples are dominantly sand and loamy sand in texture. The main area of textural overlap of kettle bottoms and backslopes is circled and shaded gray.

To better clarify if slopewash is responsible for transporting silt to the kettle bottoms, the modal silt components of representative kettle bottom/backslope pairs was also compared, using more detailed particle size distribution data.

4.2.2 Particle Size Distribution Curves

Particle size distribution (PSD) curves (Figs. 4.3 and 4.4) show the distribution of grain sizes in a particular sample; particle size is represented on the x-axis, whereas the volume % of the sample within a given particle size range is represented on the y-axis. In actuality, the data for particle size distribution are composed of closely spaced (small x-axis binning value) x-y pairs, and the spacing of the binning value increases with increasing particle size. As a result, the particle size distribution data have a higher resolution in the smaller grain size ranges (i.e. clay and silt). Because the binning values are so closely spaced, the data are commonly plotted using a connecting line so that the result resembles a continuous curve (Beierle et al., 2002), which is somewhat misleading vis a vis the actual data. Traditionally, particle size distribution curves are plotted logarithmically, to highlight the details of smaller grain size ranges. The location of a curve peak, with respect to the x-axis, represents the most frequently occurring grain size (modal grain size) of the sample. If a sample contains significant amounts of multiple grain size components (such as sand *and* silt), it may contain a peak for each, and therefore, is considered bimodal. Many sample PSD curves in this research are bimodal, and as such, peaks will be herein referred to as "silt peaks" and "sand peaks" when and if they fall within the silt and sand fractions, respectively.

4.3 Comparing Silt Content in Kettle Bottom and Backslope Pairs

4.3.1 Average PSD Curves of All Kettle Bottoms and Backslope Samples

Fig. 4.6 shows the average particle size distribution (PSD) curves for kettle bottom and backslope deposits. The two curves are distinctly bimodal. The most prominent peak for kettle bottom deposits is the silt peak, centered at 18 μm, whereas the minor peak is in the sand range at 315 μm. In contrast, the prominent peak in kettle backslope samples is in the sand range at 315 μm, and the minor peak is in the silt range at 45 μm. These data show that the location of the sand peak (along the x-axis) is similar for both sampled populations, whereas the silt peak is drastically finer for kettle bottom deposits. The shared sand peak location in both curves suggests that the sandy component of kettle bottoms and backslopes is from the same population. In contrast, however, the difference in silt peak location for both curves suggests that the silty component of kettle bottoms and backslopes is from different populations.

The data in Fig. 4.6 suggest that slopewash may be responsible for contributing some *sand* to kettle bottoms, but it is not responsible for contributing finer modal silt (i.e. finer silt may have been transported into the kettle bottom from outside the basin). If this interpretation is correct, then backslopes may have contributed *some* silt to kettle bottoms via slopewash (albeit limited in quantity and coarser overall), but are not likely the source of the finer modal silt that dominates kettle bottom deposits. This interpretation will now be applied to data from a selection of kettle sites that contain the most, average, and least texturally different kettle bottom-backslope pairs.

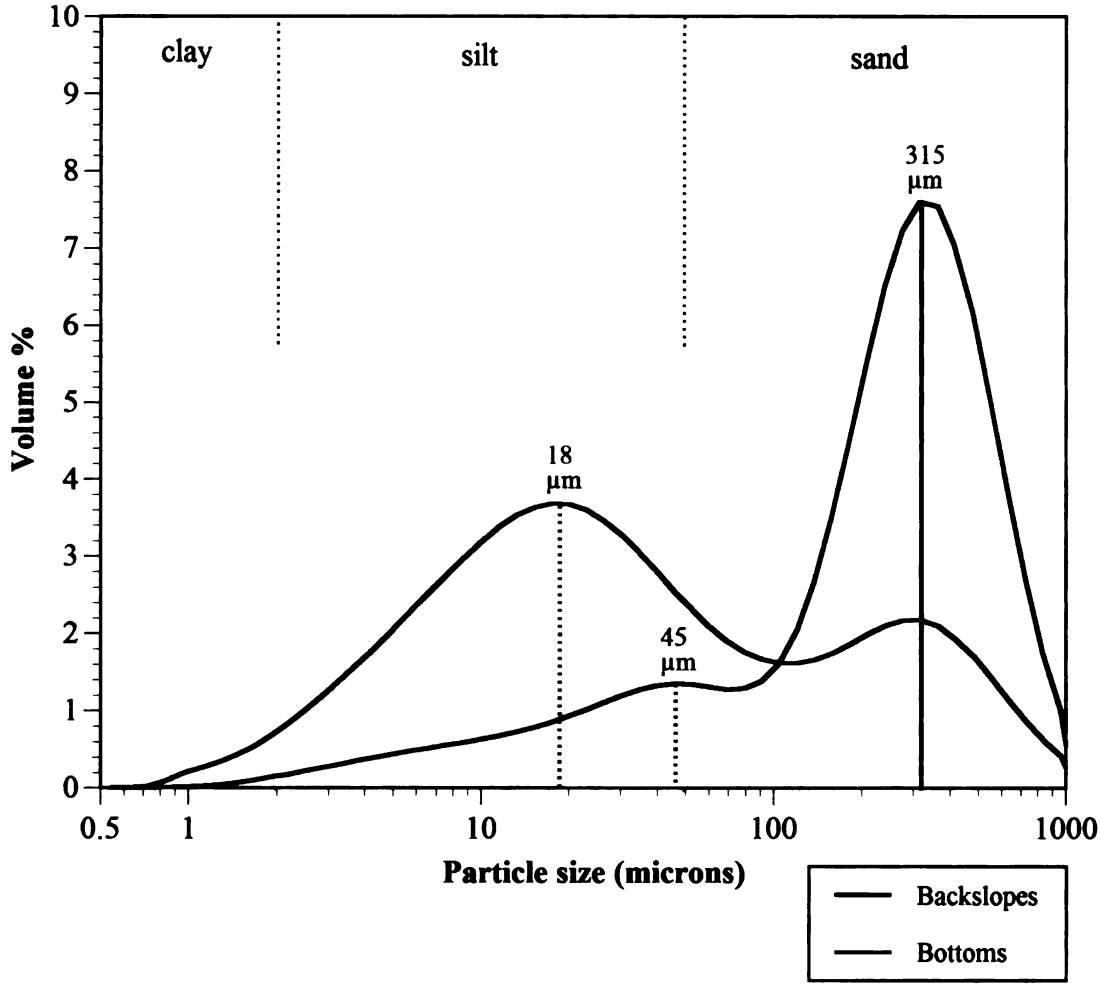

Figure 4.6- Average particle size distribution curves for all kettle bottom (red) and backslope (blue) samples. Both populations have a bimodal particle size distribution with peaks in the sand and silt range. The silt peak is different for each population (18 µm and 45 µm for bottoms and backslopes, respectively), while the sand peak is the same (315 µm).

4.3.2 Most Texturally Different Kettle Bottom/Backslope Pairs

Figure 4.7 shows three of the most texturally different kettle bottom/backslope pairs (i.e., the greatest difference in silt contents between both sample types). The three kettle bottom deposits average 51 % more silt than their respective backslope samples. Similar to the average PSD curves in Fig 4.6, the backslope samples have a minor peak in the silt range, but this peak is much coarser and less prominent than the corresponding silt peak in kettle bottom samples. The difference between the two silt peak locations (with respect to the x-axis) for adjacent sample types will be referred to herein as "silt peak spacing". The data in Fig. 4.7 support the notion that 1) kettle bottom deposits are enriched with silt relative to the backslopes, and 2) backslope deposits do not contain enough silt to be the primary source of kettle bottom silt. Perhaps most importantly, the data in Fig. 4.7 illustrate that the silt in these three kettle bottoms is much finer than the silt in backslopes, and therefore, probably not derived from the backslopes at all.

4.3.3 Average Textural Difference Between Kettle Bottom/Backslope Pairs

Figure 4.8 shows data from three kettle bottom/backslope pairs that represent the average difference in silt content between the two landscape positions. The PSD curves of backslope samples in this graph are very similar to those in Figure 4.7. The spacing of silt peaks in one of the kettle bottom/backslope pairs is slightly larger than in the previous example (23 μm→26 μm), whereas the other two are the same (35 μm and 45 μm). Therefore, the primary difference between these samples and the previous samples is that the kettle bottom deposit samples in this graph contain more sand. The data in Fig. 4.8 support the interpretation that slopewash processes may be responsible for

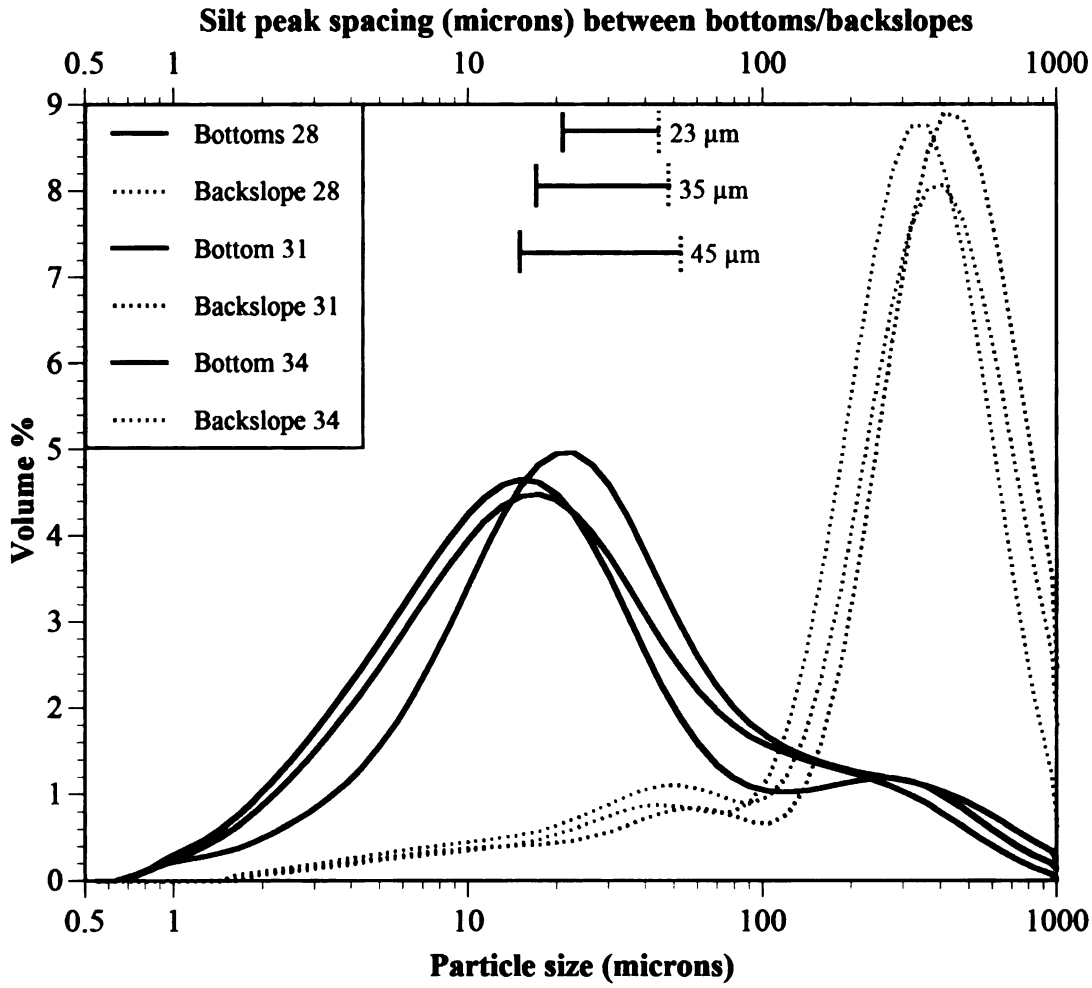

Figure 4.7- Particle size distribution curves for three kettle bottom/backslope pairs that have the greatest textural difference (i.e. have the greatest difference in silt content) of the population of sample pairs. The kettle bottom/backslope pairs are color-coded; solid lines represent kettle bottom samples, while the dashed lines represent corresponding backslope samples. The colored bars at the top of the graph indicate the difference in silt peak location between bottom/backslope pairs.

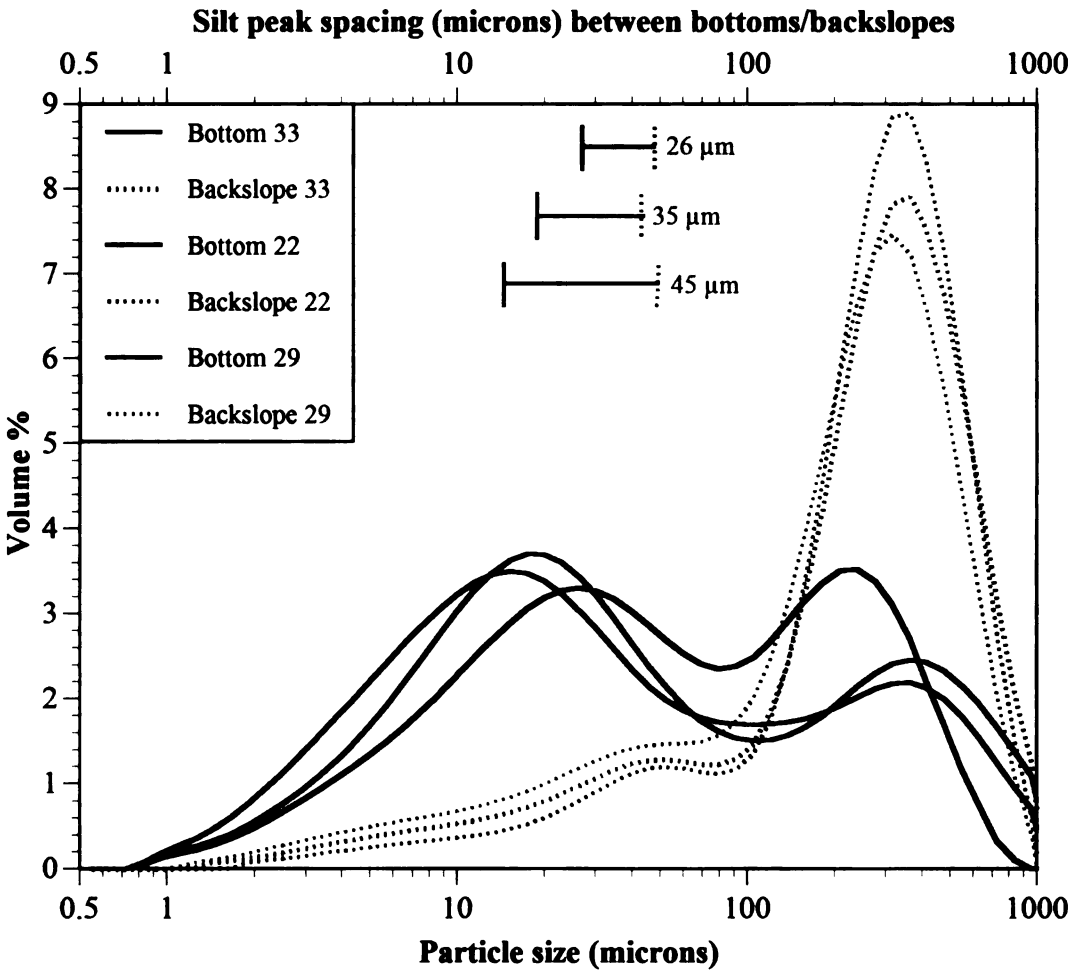

Figure 4.8- Particle size distribution curves for three kettle bottom/backslope pairs representative of the average difference in silt content among the whole population. The kettle bottom/backslope pairs are color-coded; solid lines represent kettle bottom samples, while the dashed lines represent corresponding backslope samples. The colored bars at the top of the graph indicate the difference in silt peak location between bottom/backslope pairs.

contributing some *sand* to kettle bottoms, but that the majority of the silty component is much finer, and therefore, probably not winnowed out of the backslopes via slopewash.

4.3.4 Most Texturally Similar Kettle Bottom/Backslope Pairs

Figure 4.9 shows data from the three kettle bottom/backslope pairs that exhibit the greatest similarity in texture. These samples have the least difference in silt content between the kettle bottom and adjacent backslopes. The kettle bottom samples in this graph contain more sand than any other kettle bottom samples. Interestingly, this subset of samples contains both the largest (kettle site 26) and smallest (kettle site 3) silt peak spacings between corresponding kettle bottom/backslope pairs, as compared to any of the previously shown samples (Fig. 4.9). The small silt peak spacing (and overall similarity of the PSD curves) for kettle site 3 may indicate that the two samples are from the same population (Fig. 4.9). Perhaps, the kettle bottom sample at site 3 was gathered from a depth interval dominated by an influx of sand from the surrounding slopes (i.e., a slopewash interval)*. The data in Fig 4.9 again suggest that slopewash is probably responsible for transporting some of the sandy sediment to the kettle bottom from the surrounding backslopes, but that slopewash is not likely responsible for the enrichment of finer modal silt in kettle bottom deposits. Such a conclusion is best expressed in the PSD curve data for site 26 (Fig. 4.9), where the large silt peak spacing indicates that, despite the preponderance of sand (possibly from the surrounding backslopes), silt of a different origin is nevertheless detectable in the kettle bottom deposit because the mode grain size of the silt peak is much finer.

---

* The depositional sequence of eight kettle bottom deposits will be explored later in the chapter to better understand their textural variation with depth.

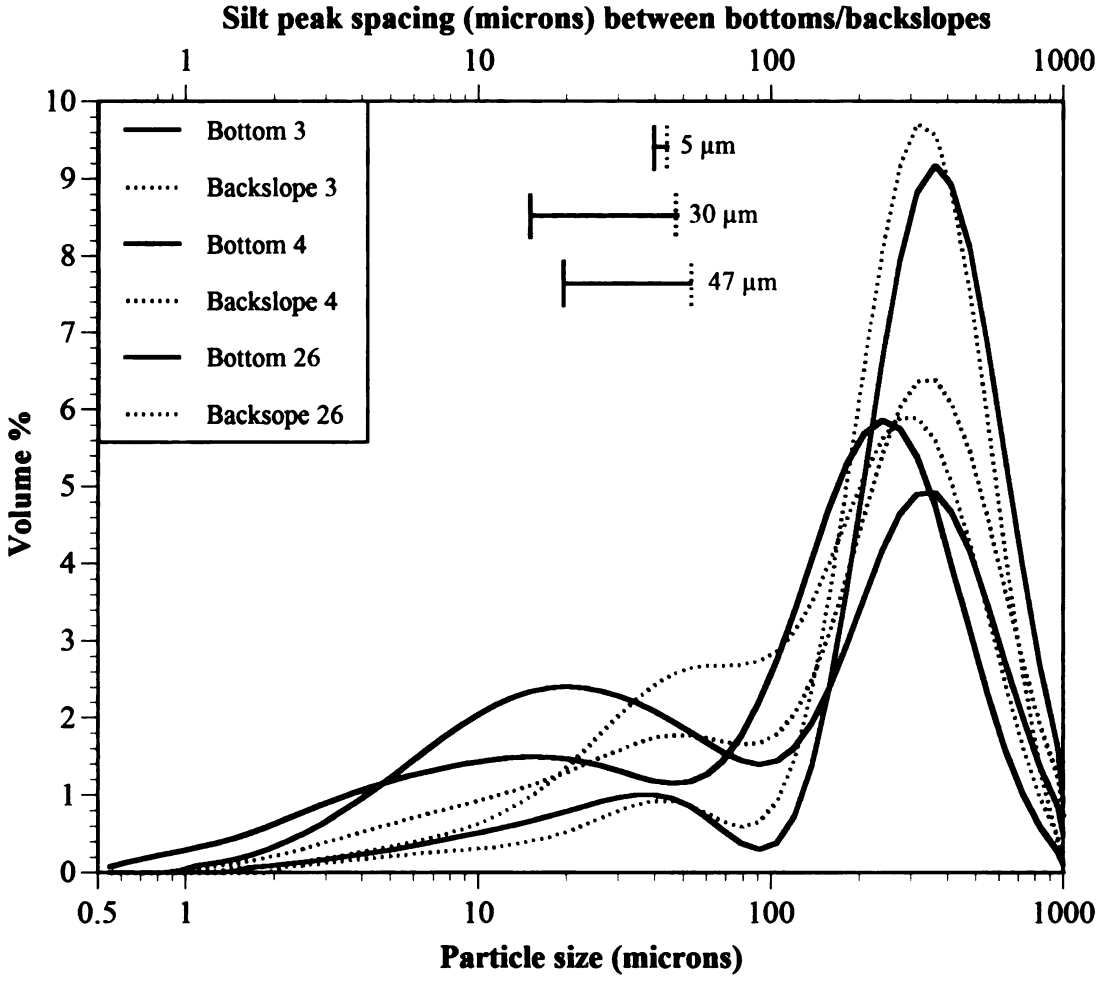

Figure 4.9- Particle size distribution curves for three kettle bottom/backslope pairs that are the most texturally similar. The kettle bottom/backslope pairs are color-coded; solid lines represent kettle bottom samples, while the dashed lines represent corresponding backslope samples. The colored bars at the top of the graph indicate the difference in silt peak location between bottom/backslope pair.

4.3.5 Summary of Textural Data

4.3.5a Silt contents

As shown above (Figs. 4.6-4.9), kettle bottom deposits contain more silt and finer modal silt contents than their corresponding backslope pairs. If slopewash alone were responsible for the silt in kettle bottoms, then the silt portion of the PSD curves for adjacent kettle bottom and backslope samples would have nearly similar silt peak locations, or perhaps slightly finer silt peaks in kettle bottom samples due to downslope sorting. The difference in silt peak locations suggests that the silt in kettle bottoms was not likely winnowed out of the surrounding backslopes via slopewash. Furthermore, in the context of slopewash processes, it is unlikely that fine silt would be transported in the absence of coarse silt, as the PSD data suggest (Figs. 4.6-4.9).

As stated earlier, another reasonable mechanism by which fine silt could be deposited in this landscape is if kettles here ponded water at some point in their evolution, offering a low energy environment for the deposition of silt. However, this scenario is not likely, given that the substrate sediments underlying the kettle bottom deposits are well drained with deep water tables. As such, condition 2 (listed above) does not hold true for these samples, and therefore, **it is likely that the majority of silt in kettle bottoms is aeolian.**

4.2.5b Sand contents

Significant variation with respect to sand content exists in the kettle bottom deposits. Some of the kettle bottom deposits contain very little sand, whereas others have bimodal PSD curves, containing a significant sand peak (Fig. 4.4). Because the modal sand components of backslopes and adjacent kettle bottom samples are similar (Figs. 4.6-4.9), it was previously suggested that slopewash might have been responsible for contributing sand to the kettle bottoms (but not finer modal silt). As it has been suggested that the majority of silt in kettle bottoms is aeolian, it must be acknowledged that perhaps *some* of the sand in kettle bottoms is also the result of aeolian deposition, rather than via slopewash. Furthermore, it is also possible that sand was brought up from the sandy substrate sediments that underlie the silty kettle bottom deposits via bioturbation. As such, sand in kettle bottom deposits may be attributed to three possible sources: 1) slopewash sand from the surrounding backslopes, 2) aeolian sand that was locally redistributed and deposited in the kettle bottoms, or 3) in-mixed sand from the underlying sandy substrate sediments, brought upward via bioturbation. The scenario favored herein is that the surrounding backslopes have contributed sand to kettle bottom deposits via slopewash deposition. Such a scenario seems most likely because it is the simplest explanation; nearly all of the sampled kettle bottoms have steep, sandy slopes surrounding them on all sides, which would have been susceptible to downslope transport during unstable periods. If so, then downslope sorting would likely result in a slightly finer mode sand grain size (sand peak) in kettle bottom deposit samples, as compared to backslope samples. To test this hypothesis, the modal sand components of adjacent samples at various kettle sites were compared.

Table 4.2 lists the sand peak locations for adjacent samples (backslope→kettle bottom), at a site-by-site basis, for all kettle bottom deposits that contain a recognizable sand peak in their PSD curve. In Table 4.2, sites are labeled "C", "F", or "-", to denote "coarser downslope", "finer downslope", or "no change" with respect to the sand peak in backslopes and adjacent kettle bottom deposits. To visually represent the data in Table 4.2, vectors showing the amount and direction of downslope changes in mode sand grain size were plotted (Fig. 4.10).

Overall, the sand peaks (mode sand grain size) in kettle bottom deposits nearly match the corresponding sand peaks in adjacent backslope samples, suggesting that the sand in kettle bottoms was derived from the surrounding backslopes, or similar sediment (Table 4.2). At 20 of the 32 sites examined, the sand peak in kettle bottoms is either the same or slightly finer than that in backslopes, as would be expected due to downslope sorting. In contrast, however, at 12 of the 32 sites, the modal sand grain size is coarser in kettle bottom deposits than in the backslope samples. It is difficult to interpret the "coarser downslope" data, other than they do not appear to fit with traditional notions of downslope particle size sorting along hillslopes (Malo et al., 1974; Chen et al., 2002). Furthermore, the data in Table 4.2 indicate that, at 8 of the12 "coarser downslope" sites, the sand peak location is only one x-axis bin size coarser (on the PSD curve), and therefore, may be insignificant. In summary, data from 20 of the 32 sites illustrate that slopewash is probably responsible for contributing some sand to kettle bottoms, but data from the remaining 12 sites do not support such a conclusion.

Table 4.2- Downslope, point-to-point comparisons of mode sand grain size.

For all kettle bottoms with a prominent sand peak (bimodal distribution)						
Sample site	Modal sand grain size in backslope (μm)	Volume % of sample at mode (peak height)	Modal sand grain size in kettle bottom deposit (μm)	Volume % of sample at mode (peak height)	C, F, or - ?	Amount of change (μm)
1	363	5.92	275	3.86	F	-88
3	315	5.89	363	4.92	C	48
4	363	6.38	239	5.86	F	-124
5	315	7.35	363	5.75	C	48
7	315	9.56	315	3.71	-	-
8	315	8.10	413	3.15	C	103
9	315	7.94	315	2.00	-	-
10	315	4.83	315	1.42	-	-
11	315	9.93	315	4.54	-	-
12	275	8.77	413	1.74	C	138
19	363	6.67	275	2.37	F	-88
20	315	6.25	315	0.40	-	-
22	363	8.89	239	3.51	F	-124
23	315	8.95	208	2.10	F	-107
24	315	7.90	158	2.11	F	-157
25	275	7.99	275	5.03	-	-
26	315	9.70	363	9.17	C	48
27	478	8.78	413	4.97	F	-65
29	315	7.46	363	2.45	C	48
30	315	7.91	363	2.57	C	48
31	413	8.91	275	1.18	F	-138
36	315	6.63	275	2.34	F	-40
38	315	6.18	275	0.86	F	-40
40	363	8.70	239	2.73	F	-124
41	315	7.90	275	2.38	F	-40
43	275	3.39	315	1.59	C	40
44	363	8.00	413	1.12	C	50
46	363	7.36	275	3.03	F	-88
47	315	9.79	275	2.29	F	-40
48	315	8.16	363	1.77	C	48
55	363	5.91	413	2.63	C	50
56	315	7.53	363	2.46	C	48
	Average = 331μm Mode = 315μm		Average = 315μm Mode = 276μm		F =14 C=12 (-) = 6	Average change = **-17 μm**

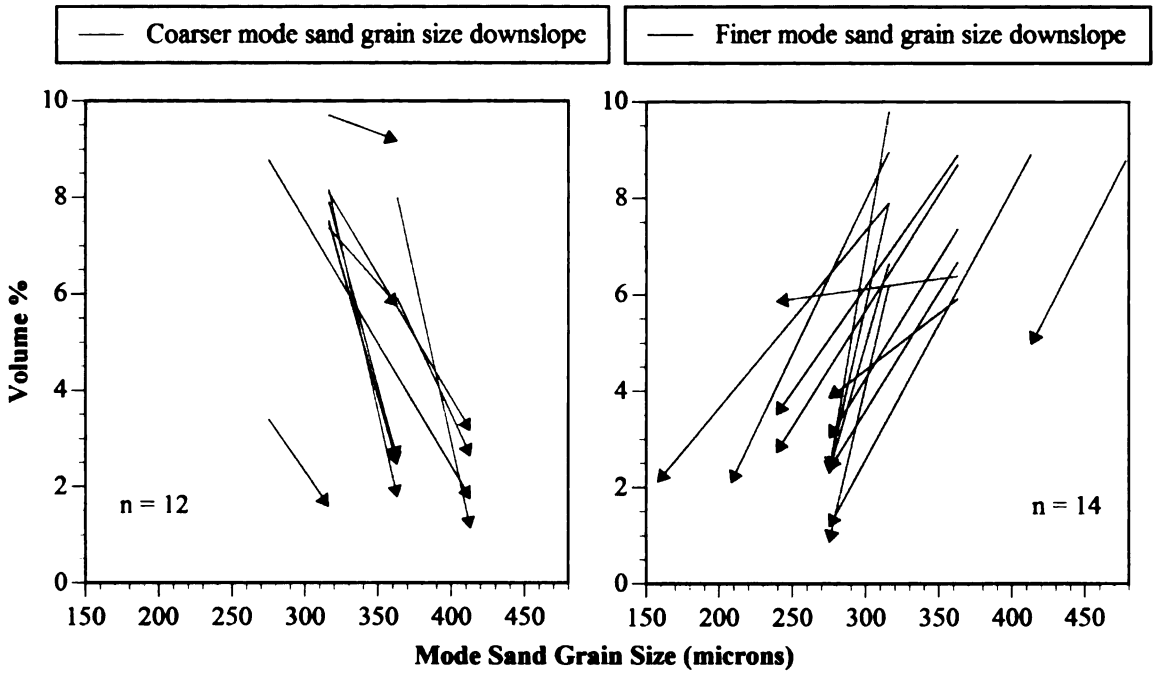

Figure 4.10- Vectors showing the amount of downslope coarsening (blue) and fining (red) with respect to mode sand grain size between backslopes and kettle bottoms. Each vector contains two sets of x-y coordinates. The starting position of the arrow is the sand peak in backslope samples. The end position of each arrow represents the sand peak in the adjacent kettle bottom. Large changes in the x-coordinate denote significant coarsening or fining downslope. Large changes in the y-coordinate denote significant differences with respect to the amount of sand between the two landscape positions.

A reconnaissance trip to the field revealed direct evidence for a recent slopewash event at kettle site 33 (Fig. 4.11). At this site, a gully has been eroded down the backslope, resulting in a fan-like deposit downslope in the kettle bottom. This erosional event is preserved in the kettle bottom deposit as a layer of sandy sediment overlying the uppermost buried soil (Fig. 4.12). The uppermost buried soil in Fig. 4.12 has abrupt lower and upper boundaries, and contains abundant charcoal, suggesting that this erosional event may have been triggered by, or directly followed, a fire. It has long been recognized that fire is responsible for causing temporary hydrophobicity in recently burned soils, thereby facilitating runoff in otherwise well drained sediments (Savage, 1974; DeBano et al., 1979). In that context, backslope deposits are probably the source of sand in kettle bottom deposits, especially where there has been direct disturbance due to fire*.

The textural evidence presented thus far suggests that the kettle bottoms have collected aeolian silt, as well as varying amounts of slopewash-derived sand, which have been redistributed to the bottom-center portions of the kettle basins. Because these two types of sediment are drastically different in the context of depositional processes, the aeolian silt may have been deposited in the kettles at different times than slopewash sand, leading to textural heterogeneity with depth in the kettle bottom deposits. Furthermore, it is possible that bioturbation has, to varying degrees, mixed slopewash-derived sand throughout the silty kettle bottom deposit profiles. Therefore, the textural variation in kettle bottom samples (Fig 4.4), particularly with respect to sand content, is probably

* The role of fire in destabilizing soils in the Evart Upland will be explored later in Chapter 5.

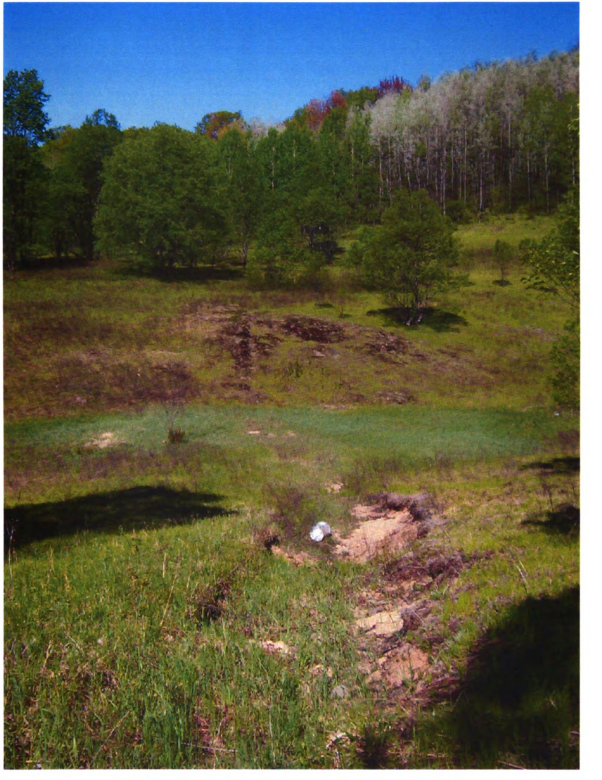

Figure 4.11- Photograph looking downslope from the rim of kettle site 33. A gully is visible in the foreground and leads to a fan-like deposit downslope in the kettle bottom. Photo by T. Hobbs.

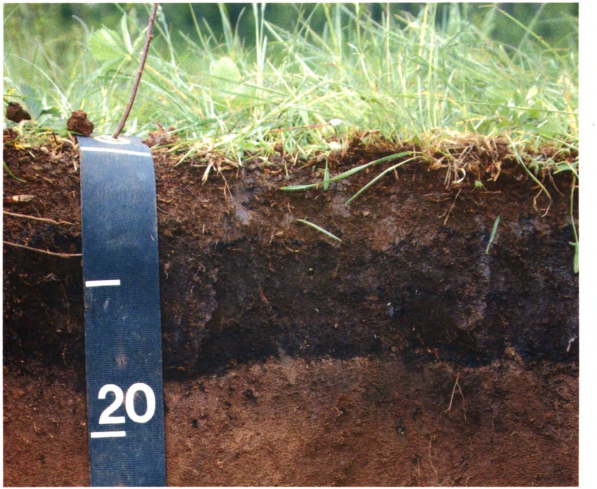

Figure 4.12- Photograph showing the top of the kettle bottom deposit profile at site 33. The fan deposit shown in Fig. 4.11 is preserved as a sandy layer from 0-5 cm in this photo. This erosional event buried the charcoal rich soil from 5-15 cm. Photo by R. Schaetzl.

related to the depth from which the sample was taken, given that there may be varying amounts of in-mixed sand due to slopewash and bioturbation at various depths throughout the kettle bottom deposits. To better understand the down profile textural variation in kettles, eight kettle bottoms were depth sampled and analyzed. Such data, explored later in this chapter, will also offer insight into the timing of silt deposition within kettles on the Evart Upland.

Supporting Evidence for an Aeolian Origin of the Kettle Bottom Silt

The textural evidence presented thus far suggests that the silt in kettle bottoms likely has an aeolian origin and was not winnowed out of the surrounding backslope soils. Because the Evart Upland is dominantly composed of sandy sediments, the spatially concentrated, silty kettle bottom deposits appear anomalous and unconformable. If the kettle bottom deposits are indeed deposits composed mostly of *aeolian* silt, then such a "patchy" pattern of deposition requires an important follow-up hypothesis: Kettle bottoms are not likely the only landscape positions that have collected silt. For example, perhaps flat, geomorphically stable surfaces should have also preserved some of the same aeolian silt that was preserved in kettle bottoms. In contrast, steeply sloping surfaces (i.e. backslopes) probably would not retain significant amounts of aeolian silt, because they are more prone to runoff. As a result, silt may have been retained on stable (flat) surfaces, while silt deposited on sloping surfaces eventually got spatially concentrated in kettle bottoms. To test whether or not this scenario applies to the Evart Upland, three geomorphically stable sites were depth sampled to determine their silt distribution with depth in the soil profile. The results of this additional sampling effort will offer supporting evidence for an aeolian origin for the kettle bottom silt.

4.4 Silt Contents with Depth - Geomorphically Stable Sites

The following figures (Figs. 4.13 - 4.18) show the distribution of four textural components with depth, at the three stable sites sampled in the field: total silt (2-50 μm), fine silt (12-25 μm), medium silt (25-35 μm), and coarse silt (35-50 μm). Each of these silt components was calculated on a clayfree basis to remove the influence of

pedogenically derived clay. Each depth figure is preceded by a figure containing a locator map and topographic map of the stable site, as well as a photograph of the understory vegetation.

4.4.1 Stable site-1

Stable site-1 is located on a relatively flat portion of a valley side that extends up the southern portion of the study area (Figs. 4.13), at 382 m elevation. The total clayfree silt content decreases from 17% to 9.5% at 75 cm depth (Fig. 4.14). The down-profile trend of medium and coarse clayfree silt is similar, decreasing from ~ 4% at the surface to ~2% at 75 cm depth. However, fine clayfree silt shows a greater decrease with depth (6% to 3% at 75 cm).

4.4.2 Stable site-2

Stable site-2 is located on a flat surface between kettles, just up-valley from stable- site 1 (Fig. 4.15), at 391 m elevation. The total clayfree silt content decreases from 26% to 12% at 105 cm depth (Fig. 4.16). The down-profile trend of medium and coarse clayfree silt is similar, decreasing from 5% at the surface to ~2% at 105 cm depth. However, fine clayfree silt shows a greater decrease down-profile than medium and coarse silt, from 10% to ~ 3.5% at 105 cm depth.

4.4.3 Stable site-3

Stable site-3 is located on a relatively flat surface surrounded by rolling ridges upslope (to the immediate east and north) (Fig 4.17), at 406 m elevation. The total clayfree silt content decreases from 10.5% to ~2.5% at 75 cm depth (Fig. 4.18). Similar to the previous two sites, the down profile trend in medium and coarse clayfree silt is

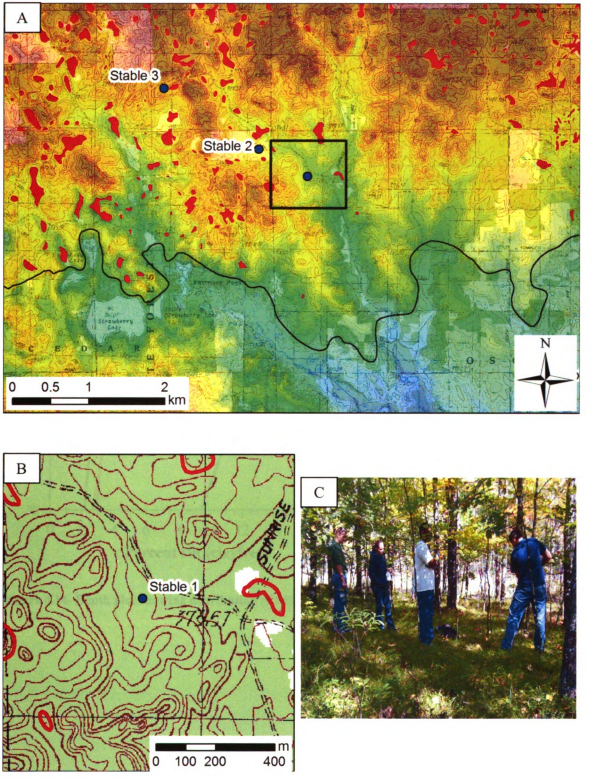

Figure 4.13- Location of stable site-1 relative to the other stable site locations. B) Topographic map showing surface characteristics of stable site-1. C) Photograph of surface vegetation at this site.

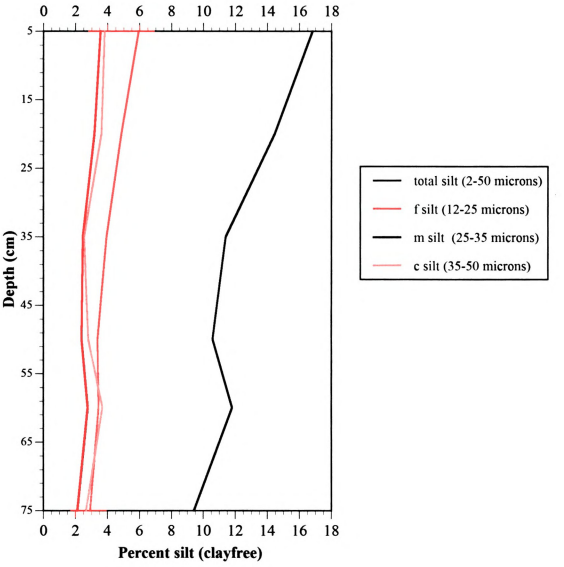

Figure 4.14- Depth plot showing distribution of four silt components with depth at stable site-1.

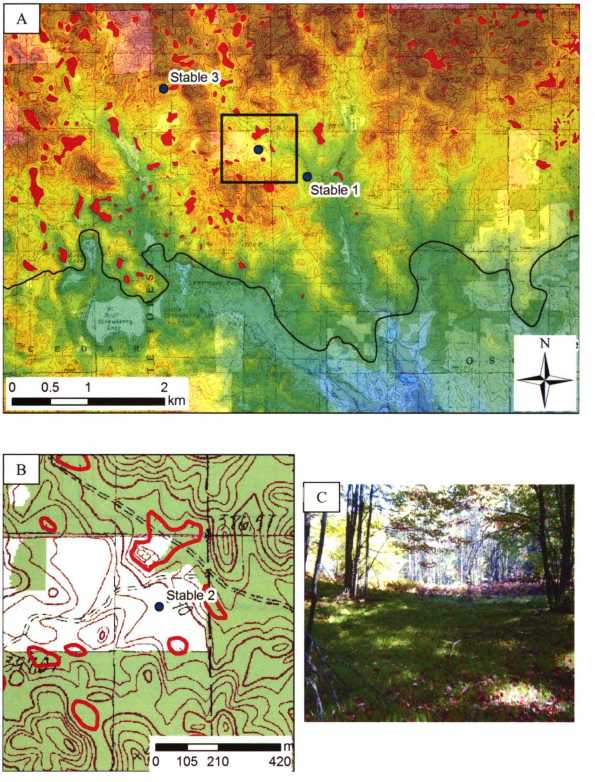

Figure 4.15- A) location of stable site-2 relative to the other stable site locations. B) Topographic map showing surface characteristics of stable site-2. C) Photograph of surface vegetation at this site.

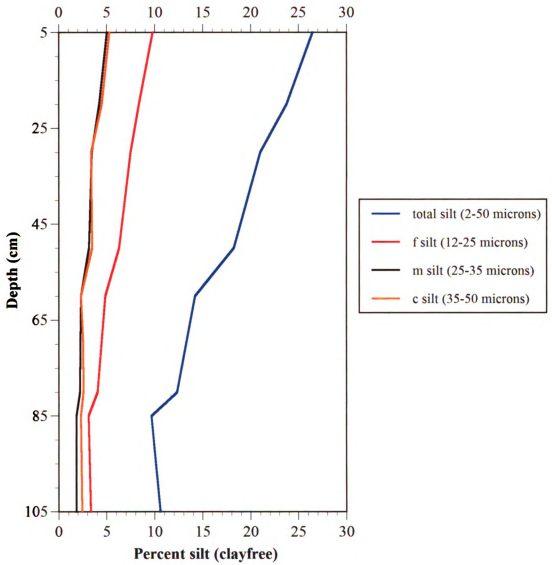

Figure 4.16- Depthplot showing distribution of four silt components with depth at stable site-2.

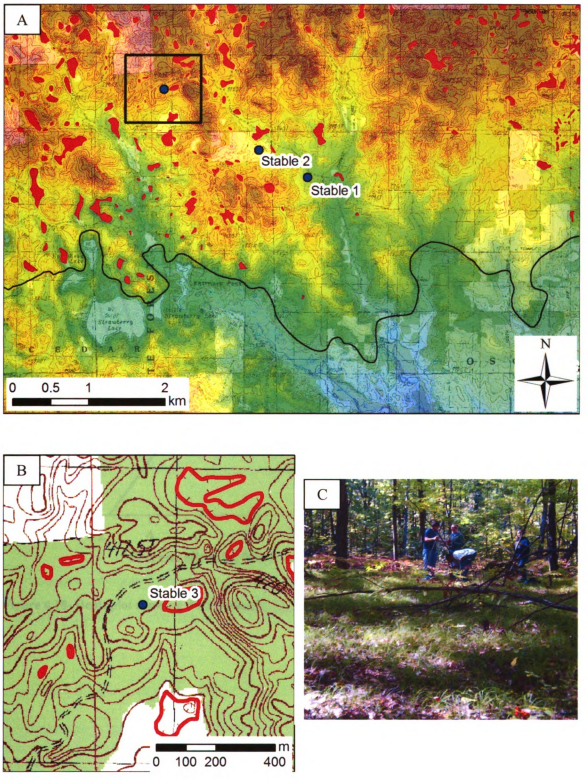

Figure 4.17 A) location of stable site-3 relative to the other stable site locations. B) Topographic map showing surface characteristics of stable site-3. C) Photograph of surface vegetation at this site.

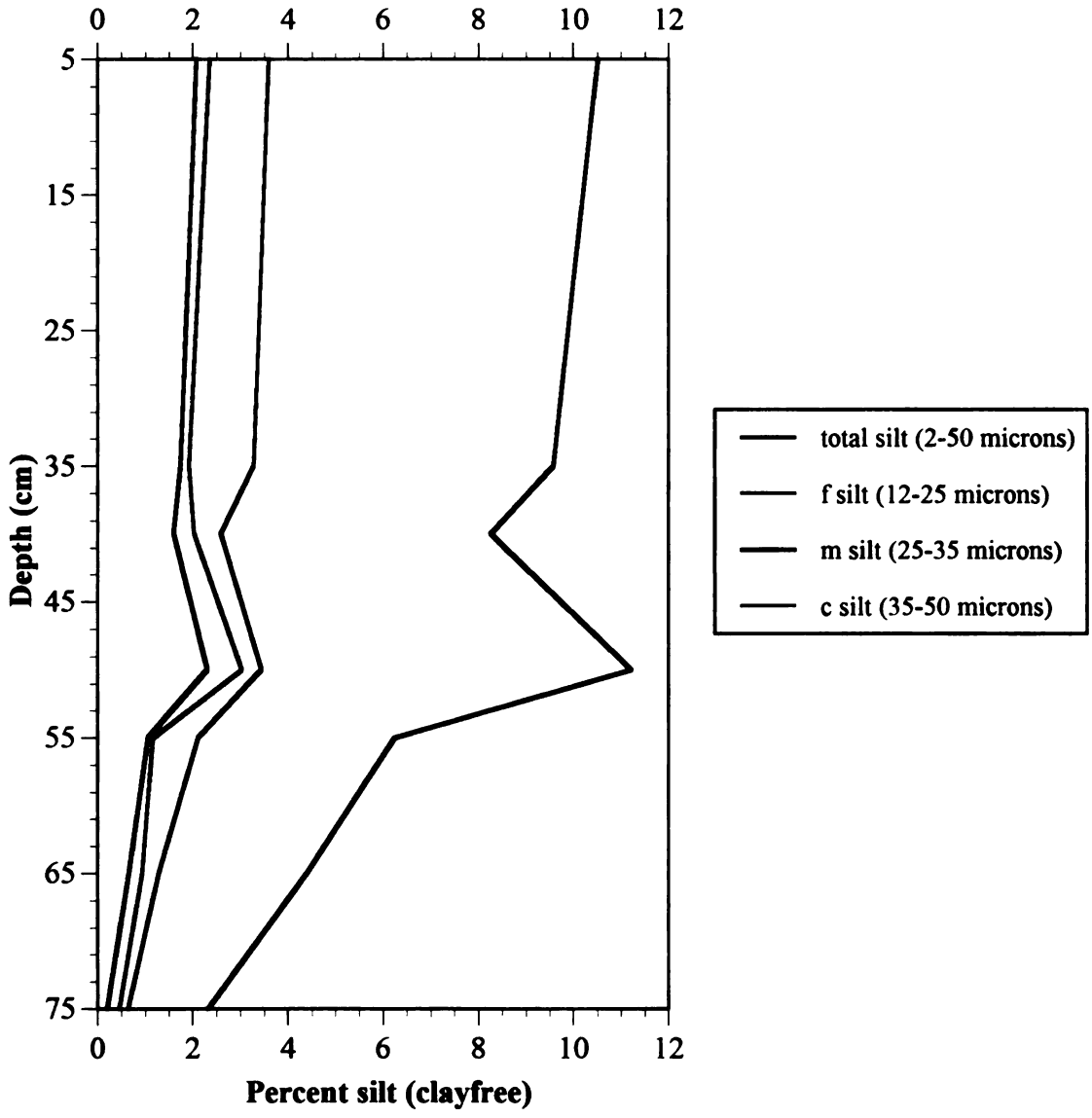

Figure 4.18- Depthplot showing distribution of four silt components with depth at stable site-3.

parallel, subtly decreasing from ~2 % to ~1% at 75 cm depth. Fine clayfree silt decreases more than medium or coarse silt down-profile, from ~ 4% to ~ 1% at 75 cm depth.

4.4.4 Summary of Depth Plot Data for Geomorphically Stable Sites

All three geomorphically stable sites show an increase in clayfree silt content in the upper profile. On average, the three profiles contain a ~10% up-profile increase in clayfree silt from the bottom to the top of the profiles (i.e. between from about 80 cm to the surface. Silt content ranges between 2-12% in the lower profiles (~80 cm) to 10.5-26% at the surface. Fine silt, which is more readily transported by wind, increases more than medium and coarse silt in the upper profiles of all three sites. Fine silt is also the dominant particle size in kettle bottom deposits (recall that the silt peak of all kettle bottom samples averaged 18 μm). These data suggest that aeolian silt has indeed been preserved on stable surfaces, and incorporated into the soil profiles.

At the three geomorphically stable sites sampled in the field, the understory vegetation is dominated by rice grass (*Oryzopsis asperifolia).* The presence of rice grass in the understory here may be associated with slightly higher water holding capacity near the surface, which may in turn be attributed to an increase in silt in the upper soil profile. Indeed, rice grass is commonly found growing on flat, sandy, upland soils, otherwise enriched with loess, in northern Wisconsin (R. Schaetzl, personal communication, 2008). As such, rice grass appears to be a good indicator of aeolian silt enrichment on upland, sandy landscapes of the upper Midwest.

In other landscapes, an up-profile increase in silt content could potentially be related to increased physical weathering, which can produce silt from sand. Mikesell et

al. (2004) studied the degree of hornblende etching (a mineral indicator of weathering) with depth in four sandy soils ~ 100-150 km north of the Evart Upland, to understand how different macroclimates influence weathering intensity in soils of similar age. Their results indicate that the intensity of up-profile hornblende etching somewhat parallels the degree of podzolization, which in their study area, is facilitated by heavy snowfall. Their data also show that the up-profile increase in hornblende etching is usually accompanied by an increase in silt content. They recognize that such silt may be due to increased weathering in the upper profile, but also acknowledge that it may be due to an aeolian influx. Barrett (2001) also documented silt increases in the upper profiles of sandy soils in northern Michigan and attributed such an increase to a slight aeolian influx. Given that soils in the Evart Upland are dry in summer and receive less snowfall than the study area of Mikesell et al. (2004), physical weathering is not likely a significant contributing factor to silt production in the Evart Upland. As such, the up-profile silt increase is likely due to aeolian influx, rather than via weathering.

Unlike sloping surfaces, geomorphically stable, flat surfaces are less apt to produce runoff. As such, flat surfaces are more likely to retain and pedogenically incorporate aeolian silt than sloping surfaces. Indeed, data from the Buckley Flats (a flat upland in northwest Lower Michigan) and the Grayling Fingers regions of Michigan demonstrate that aeolian silt is best preserved on flat, stable surfaces, and is commonly absent on surfaces with even the slightest slope or presence of erosion (Schaetzl and Weisenborn, 2004; Schaetzl, 2008; Schaetzl and Hook, 2008).

At the stable sites sampled, the silt increase in the upper profile is gradual and subtly expressed within a textural background heavily dominated by sand. It is unclear

whether additions of aeolian silt at these sites were intermittent, or added during a single depositional event, because pedogenic processes have since mixed the silt into the profile and blurred any definitive depositional characteristics or lithologic contacts. Regardless of the gradual nature of the up-profile silt increase, these data considered in combination with the particle size distribution data from kettle bottoms (which illustrate that both are composed of very similar modal silt), strongly suggests that: **1) aeolian silt has indeed been deposited across the Evart Upland after the landscape stabilized, and 2) the degree to which silt has been preserved and incorporated into the soil may be influenced by the slope/long-term stability of the surface**, or perhaps, the paleo-vegetation on site at the time of deposition.

Finally, the mechanism by which silt has been spatially concentrated in kettle bottoms is unclear, but the scenario favored herein is that perhaps, over millennia, late-lying snowpack (which would have lasted the longest in kettle bottoms), acted as a trap for aeolian silt, subsequently focusing it in the center-bottom portions of the kettle upon meltout of the snow.

4.5 Spatial Patterns of Silt Content - Backslopes vs. Kettle Bottoms

The spatial pattern of silt content within backslope and kettle bottom samples across the upland offers further evidence that the silty kettle bottom deposits are likely the result of aeolian deposition. If the silt in kettle bottom deposits were winnowed out of the surrounding backslopes via slopewash, then the spatial variation in kettle-bottom silt content across the upland should be very similar for both sample types. For example, where there is more fine silt in backslopes, there too should be more fine silt in kettle

bottom deposits (if slopewash were the mechanism of silt deposition in kettle bottoms). To compare the spatial variation of silt content between both sample types, the textural data were linked with the sample locations in ArcMap, and grids of three ranges of silt content (coarse silt (35-50 μm), medium silt (25-35 μm), and fine silt (12-25 μm)) were created using an ordinary kriging interpolation method in Geostatistical Analyst (ArcMap, Redlands, CA).

The results of the kriging operation revealed an increasing discordance between the two sample types with decreasing silt particle size (Fig. 4.19). For example, backslopes exhibit similar spatial patterns for all three silt components, having greater concentrations of all three silt ranges in the east and north (represented by darker brown) (Fig 4.19). Because the sediments comprising backslope samples were deposited in a glaciofluvial setting, the spatial variation in coarse, medium, and fine silt content should be (and indeed, are) very similar because, in the context of transport and deposition, flowing water did not crisply discriminate between coarse and fine silt. In contrast, kettle bottoms exhibit different spatial patterns for all three silt components, having greater concentrations of fine silt in the southeast and central portions of the study area than the rest of the study area (Fig. 4.19). The discordance between the two sample types would be expected if fine silt has been deposited across the upland by a process that is landscape-scale, like wind, rather than a small scale, slope-based process like slopewash. The different spatial distribution of fine silt between kettle bottoms and backslopes further supports the conclusion that the majority of silt in kettle bottoms is the result of aeolian deposition.

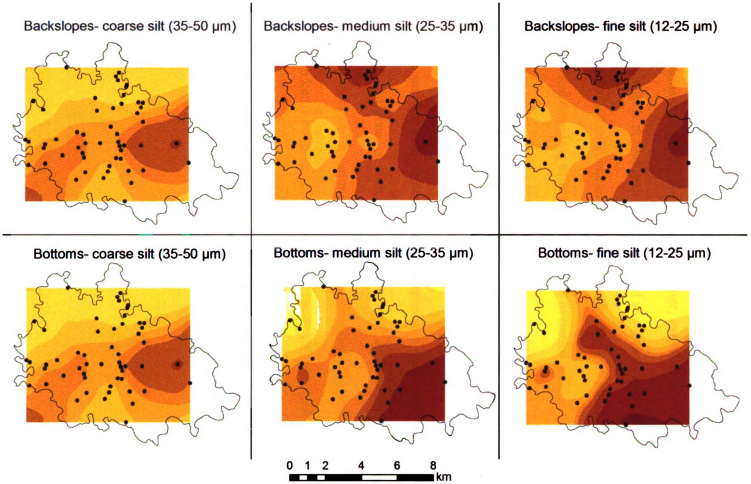

Figure 4.19- Ordinary kriged grids of three silt components: coarse silt (left), medium silt (middle), and fine silt (right) between backslope samples (top row) and kettle bottom samples (bottom row). North is up in all of the grids. Black dots represent sample locations across the study area. Greater silt content is represented by increasingly darker color in both sample types. However, the values of percent silt are different for each sample type because kettle bottoms have far more silt than backslopes.

4.6 Depth Characteristics of Kettle Bottom Deposits

Analysis of the kettle bottom deposits revealed significant textural variation, particularly with respect to sand content (Fig. 4.4), suggesting that they may be texturally heterogeneous with depth. As suggested earlier, variation in sand content in kettle bottom deposits is probably due to influxes of slopewash sand. Eight of the sampled kettle bottoms had evidence of buried soils within the kettle bottom silt deposits, during the initial field sampling effort. The presence of buried soils in the kettle bottom deposits, coupled with the varying amounts of sand with depth, indicates that surfaces in this landscape have experienced periods of stability and instability in the past. Surface instability could potentially lead to different kinds of sediment deposition (aeolian silt or slopewash sand) in kettle bottoms, further explaining why kettle bottom deposits are texturally heterogeneous with depth. Therefore, the eight kettle bottoms containing buried soils were depth sampling to 1) better understand the depositional history of silt and sand in kettle bottoms, and 2) determine the degree to which the kettle bottoms are texturally heterogeneous with depth. Such evidence will be used to confirm or deny that the textural variation among kettle bottom deposit samples (as revealed in Fig 4.4) is related to the depth from which the sample was taken.

4.6.1 Explanation of depth-plot method and depth-plot figures

4.6.1a Depth-plot method

The method used in this thesis to display down profile changes in soil texture in this section is based on a method developed by Beierle et al. (2002), originally applied to lake sediment cores. Their method is used here because it visually enhances subtle down-profile changes in particle size distribution, and therefore, highlights depositional processes that may otherwise remain unseen in standard depth-plots of simple statistical measurements, such as mean particle size. By incorporating the entire particle size distribution at every sampled interval into a continuous grid surface, subtle depositional events in the kettle bottom deposits are made more evident.

The graphs use three axes of data (x, y, z) for each depth-sampled interval. The x-axis corresponds to the particle size, y-axis to the depth of sample, and z-axis to the volume percent of the sample (obtained from the near-continuous particle size distribution curve data from the Malvern Mastersizer; see Methods chapter). Essentially, the graphs display the particle size distribution curve at each depth-sampled interval, and interpolate z-axis values (volume percent) between sampled intervals. The result is a continuous grid surface of particle size distribution characteristics throughout the entire soil profile.

4.6.1b Explanation of depth plot figures

The following figures (Figs. 4.20 - 4.35) display data from eight depth-sampled kettle bottom deposits. Each of the figures are accompanied by a facing page that

contains a locator map and a topographic map, which show the location of the eight sample sites relative to each other, and a close up of the surrounding topography and kettle shape, respectively. In addition to the geography of the depth sampled kettles, some basic morphometric characteristics of the kettles themselves and the surrounding area are also provided. These characteristics include: elevation, kettle area, drainage basin area, aspect of backslope sample, and backslope gradient. Kettle area and drainage basin area were previously calculated in ArcMap (Redlands, CA). Aspect and gradient data were determined in the field.

Each kettle that was depth sampled contains at least one buried soil. In each of the depth plot figures that follow, a solid black line marks the depth of the top of a buried soil. Coarse, sandy substrate sediments lie beneath the kettle bottom deposits in all of the kettle bottoms that were depth-sampled. A dashed line on the depth plot figures marks the boundary (lithologic discontinuity) between the coarse sandy substrate sediments and the overlying silty sediments.

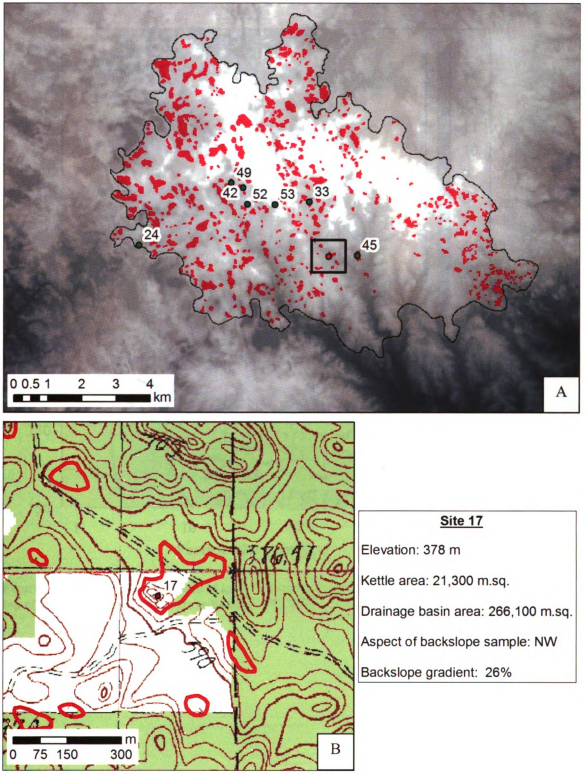

Figure 4.20- A) Location of site 17 in relation to other depth sampled kettles on the Evart Upland. B) Topographic map showing kettle site 17 with additional basin characteristics (right).

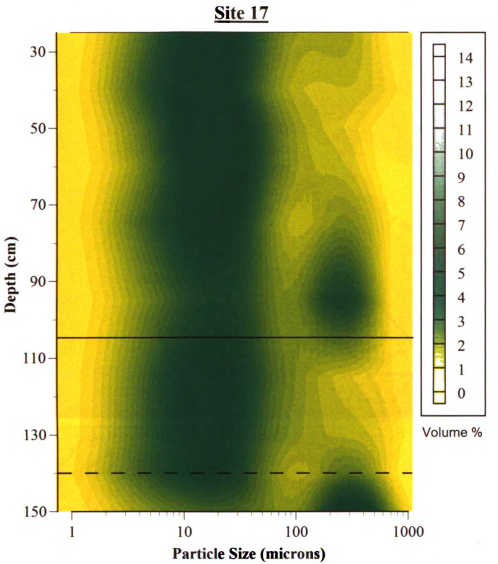

Figure 4.21- Depositional sequence of kettle bottom sediments at site 17. The dashed line marks the top of the coarse, sandy substrate sediments. The solid line marks the top of a buried soil.

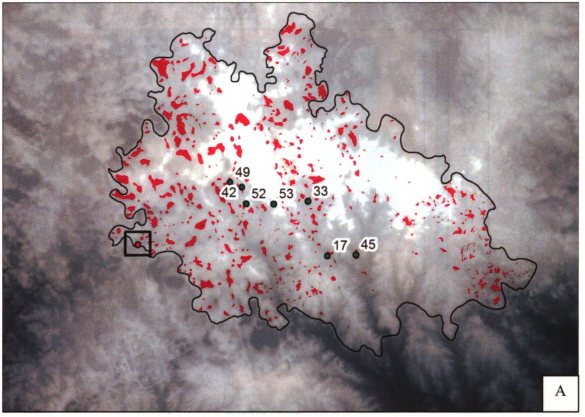

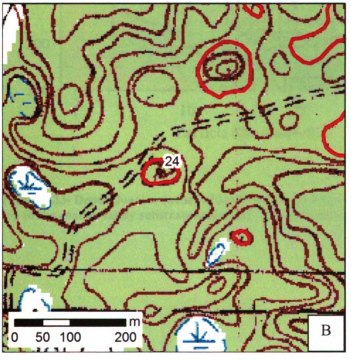

Site 24

Elevation: 372 m

Kettle area: 175 m.sq.

Drainage basin area: 84,457 m.sq.

Aspect of backslope sample: E

Backslope gradient: 45%

Figure 4.22- A) Location of site 24 in relation to other depth sampled kettles on the Evart Upland. B) Topographic map showing kettle site 24 with additional basin characteristics (right).

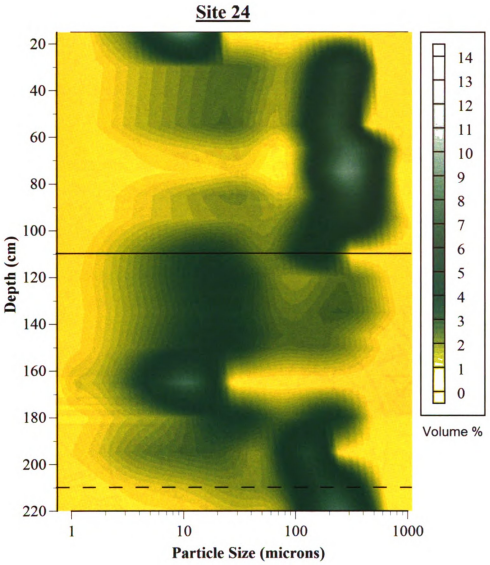

Figure 4.23- Depositional sequence of kettle bottom sediments at site 24. The dashed line marks the top of the coarse, sandy substrate sediments. The solid line marks the top of a buried soil.

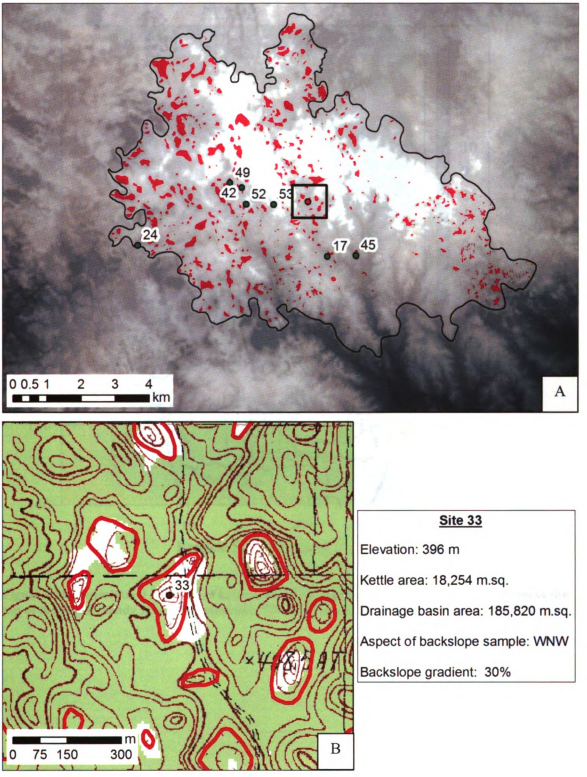

Figure 4.24- A) Location of site 33 with in relation to other depth sampled kettles on the Evart Upland. B) Topographic map showing kettle site 33 with additional basin characteristics (right).

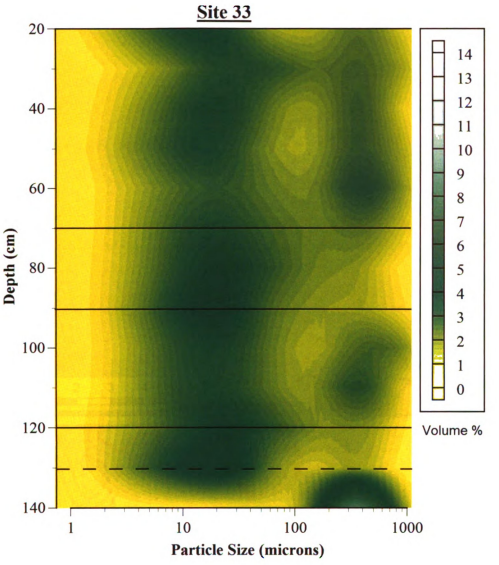

Figure 4.25- Depositional sequence of kettle bottom sediments at site 33. The dashed line marks the top of the coarse, sandy substrate sediments. The solid lines mark the top of buried soils.

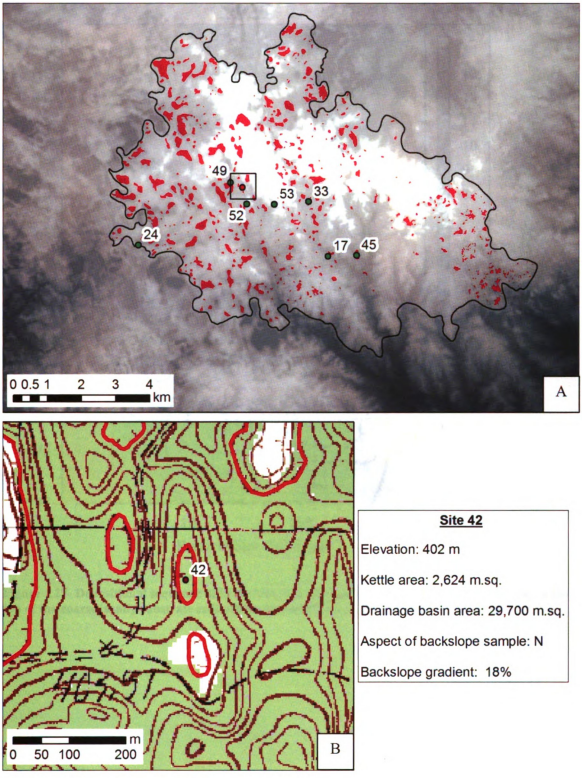

Figure 4.26- A) Location of site 42 with in relation to other depth sampled kettles on the Evart Upland. B) Topographic map showing kettle site 42 with additional basin characteristics (right).

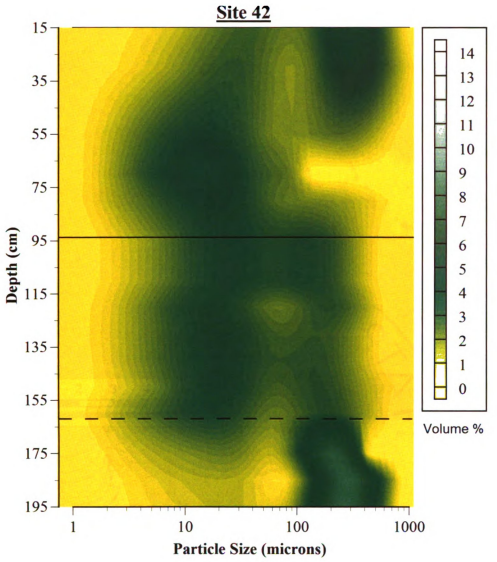

Figure 4.27- Depositional sequence of kettle bottom sediments at site 42. The dashed line marks the top of the coarse, sandy substrate sediments. The solid line marks the top of a buried soil.

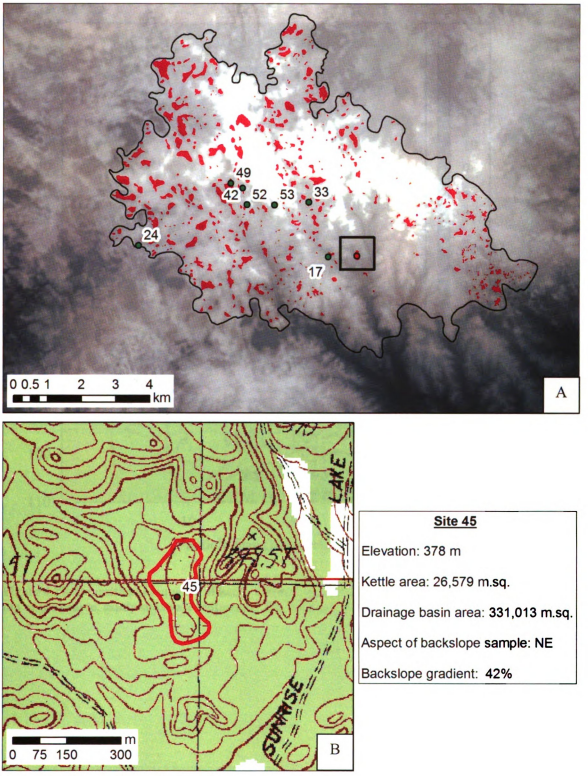

Figure 4.28- A) Location of site 45 with in relation to other depth sampled kettles on the Evart Upland. B) Topographic map showing kettle site 45 with additional basin characteristics (right).

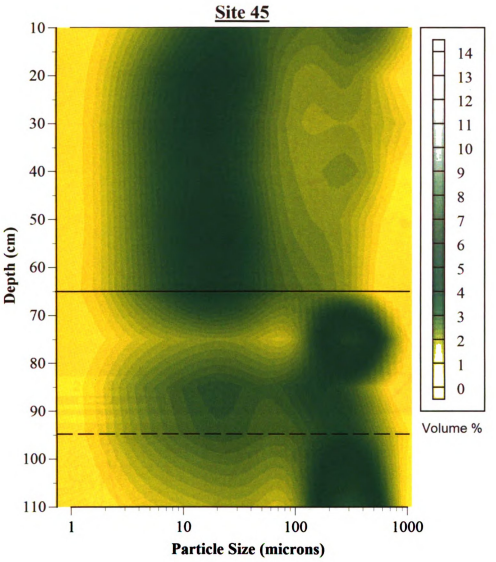

Figure 4.29- Depositional sequence of kettle bottom sediments at site 45. The dashed line marks the top of the coarse, sandy substrate sediments. The solid line marks the top of a buried soil.

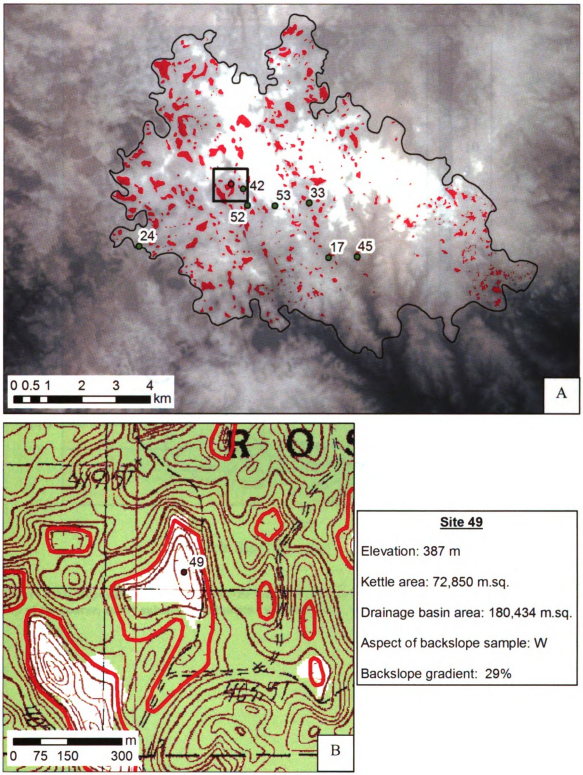

Figure 4.30- A) Location of site 49 with in relation to other depth sampled kettles on the Evart Upland. B) Topographic map showing kettle site 49 with additional basin characteristics (right).

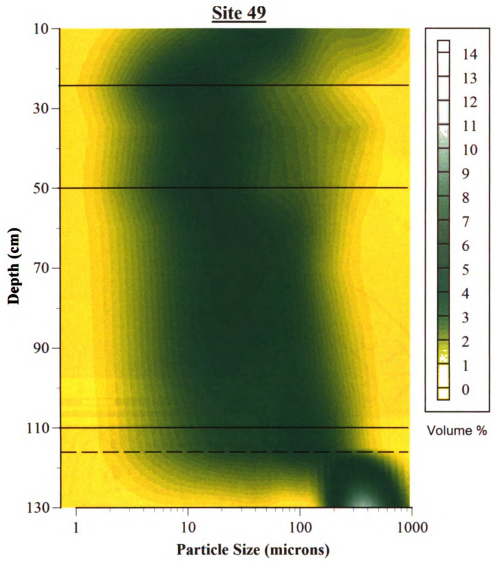

Figure 4.31- Depositional sequence of kettle bottom sediments at site 49. The dashed line marks the top of the coarse, sandy substrate sediments. The solid lines mark the top of buried soils.

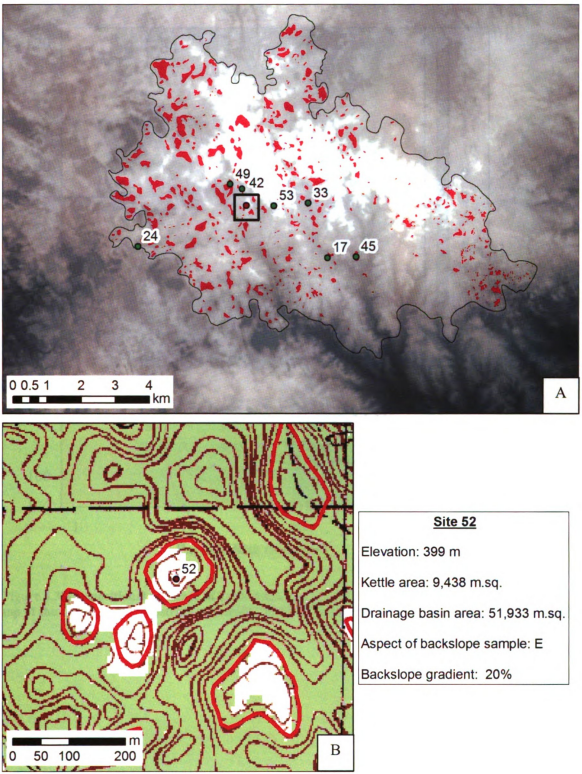

Figure 4.32- A) Location of site 52 with in relation to other depth sampled kettles on the Evart Upland. B) Topographic map showing kettle site 52 with additional basin characteristics (right).

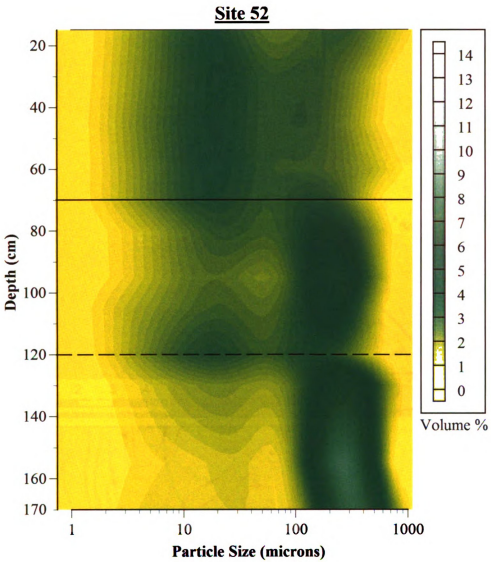

Figure 4.33- Depositional sequence of kettle bottom sediments at site 52. The dashed line marks the top of the coarse, sandy substrate sediments. The solid line marks the top of a buried soil.

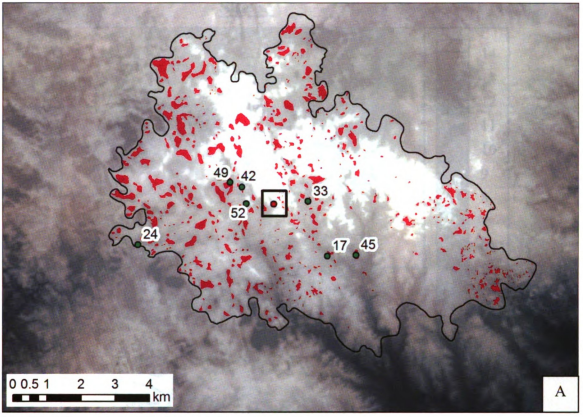

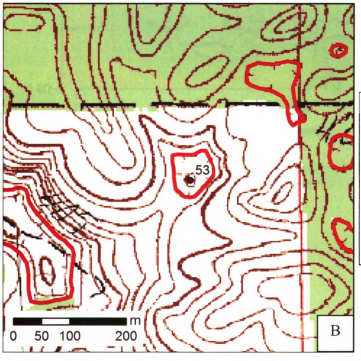

Site 53

Elevation: 411 m

Kettle area: 4,505 m.sq.

Drainage basin area: 418,007 m.sq.

Aspect of backslope sample: N

Backslope gradient: 52%

Figure 4.34- A) Location of site 53 with in relation to other depth sampled kettles on the Evart Upland. B) Topographic map showing kettle site 53 with additional basin characteristics (right).

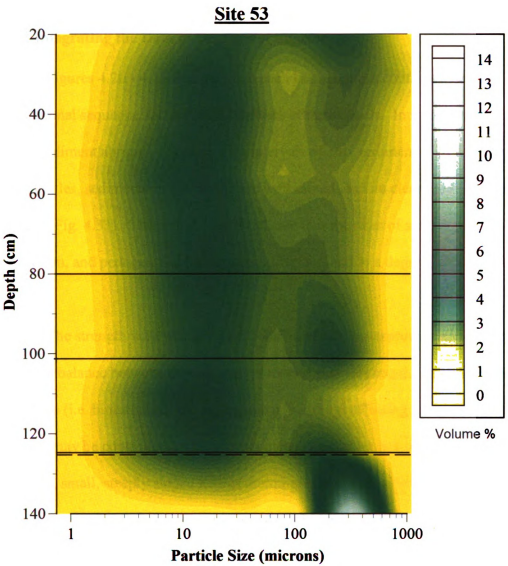

Figure 4.35- Depositional sequence of kettle bottom sediments at site 53. The dashed line marks the top of the coarse, sandy substrate sediments. The solid lines mark the top of buried soils.

4.6.2 Integrating the Data in Depth-Plot Figures

Figures 4.20 - 4.35 illustrate that each kettle bottom contains a unique depositional sequence and different numbers of buried soils. In some kettles, intervals of sandy sediment abruptly alternate with intervals of silty sediment (Fig. 4.23), while in other kettles, sediments in the profile are well mixed, and no clear mode of deposition is evident (Fig. 4.31). These differences indicate that the rates of sand deposition, silt deposition, and pedogenic upbuilding are different, and to a degree, site-specific, for each kettle.

The strength with which depositional intervals are expressed may be dependent upon the balance between depositional processes (i.e. slopewash) and pedogenic processes (i.e. bioturbation and pedogenic upbuilding) affecting the kettle bottom. This balance may be controlled by the morphometric characteristics of the kettle basin. For example, small, steeply sloped kettles draining a large area may be more influenced by slopewash processes than pedogenic processes because 1) as backslope gradient increases, runoff and erosion are more likely, and 2) small kettles that drain a large area can potentially integrate and "focus" more overland flow than large kettles that drain a small area. Therefore, the depositional sequence in small, steep kettles may have more clearly preserved sandy intervals in the kettle bottom than large, shallow kettles, because sediment deposition would be more frequent, and perhaps overwhelm the rate of pedogenic upbuilding in the former.

To determine if this interpretation applies to the eight depth-sampled kettles, simplified, integrated versions of the depth plot figures were created and compared relative to each other (Fig. 4.36). Each kettle site was ranked in order from steepest to

shallowest backslope, then again by kettle area-to-drainage basin ratio. The depth-plots are grayscale shaded based on particle size distribution, and range between two end member depositional processes: aeolian silt or sandy influx. Aeolian silt intervals are indicated by a unimodal particle size distribution with the modal grain size in the fine-medium silt range (~10-35 μm). Sandy influx intervals are indicated by a unimodal particle size distribution with the modal grain size in the sand range (generally coarser than 100 μm). Mixed intervals, which fall between the two end members on the scale, are indicated by a bimodal particle size distribution with no clear dominance by either silty or sandy sediments. These units likely represent periods of pedogenic upbuilding when neither depositional process (aeolian silt deposition or slopewash sand) dominated, or perhaps are the result of post-depositional mixing (bioturbation). Mixed intervals can be further subdivided into coarsening upward or fining upward sequences depending on the up-profile trajectory of the PSD curves in the depth plots.

In effect, if the above assumptions are true regarding the role of basin characteristics in controlling the balance between slopewash processes and pedogenic processes, then the profiles should become more texturally homogenous from left to right in Figure 4.36, reflecting a decreasing influence by slopewash processes, and increasing capacity to pedogenically incorporate sediments. Qualitatively, the depth plots in Fig. 4.36 do appear to be slightly more homogenous from left to right. For example, site 42 (far right) contains a mixed profile and fewer distinct depositional intervals than site 33 (middle left). Furthermore, site 53 (far left) has three buried soils, whereas site 42 has one buried soil, suggesting that slopewash processes are more common in the former. Such comparisons between sites suggest that the above assumptions regarding the role of

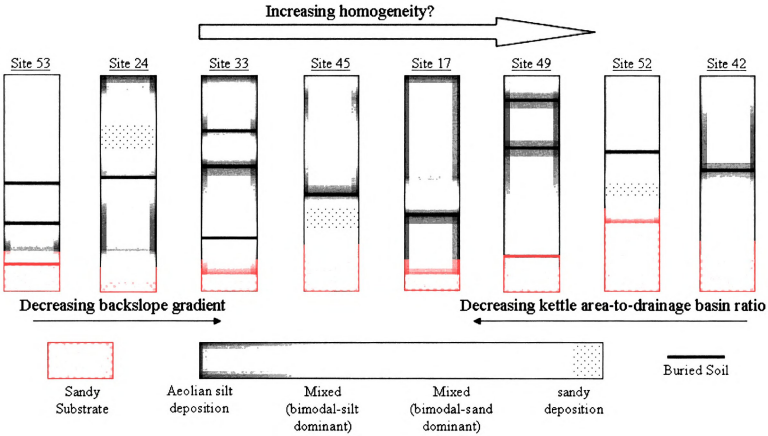

Figure 4.36- Simplified versions of the depthplots in figures 4.20 - 4.35, ranked in order of increasing susceptibility to slopewash deposition from the surrounding backslopes: steepest backslopes and smallest area-to-drainage basin ratio (left) to shallowest backslopes and largest area-to-drainage basin ratio (right). These profile representations are not drawn to scale relative to each other.

basin characteristics in controlling the strength with which depositional intervals are expressed may have a slight influence on the depositional sequence in kettle bottoms.

Other factors have probably influenced the depositional sequence in kettle bottoms in this landscape, such as paleo-vegetation changes (Almendinger and Hobbie, 1992) and historical precipitation (Lamoureux, 2000). As of yet, the influences of these factors remain ambiguous in the context of this landscape, and are not evident in the data presented herein. However, what *can* be said of the data in Figs. 4.20 - 4.35 is that depositional events cannot be correlated between the eight sampled kettle basins. Therefore, the deposition of silt and sand has probably occurred differently in each kettle, suggesting that surface instability and subsequent redistribution of sediments into depressions has been episodic and localized. Overall, the depth plot data suggest that this landscape is highly sensitive to disturbance, which is reflected in the sequence of sediments within kettle bottoms.

4.6.3 Summary of Depth-Plot Figures

The depth plots in Figs. 4-20 - 4.35 clearly show that the texture of kettle bottom deposits fluctuates with depth. Each kettle bottom deposit has a unique depositional sequence that fluctuates between two end members of deposition, silt (aeolian deposition) and sand (slopewash deposition). In many cases, intervals in the kettle bottom sediments are mixed with respect to particle size distribution, suggesting no clear dominance by either depositional process. Fining upward and coarsening upward mixed sequences may indicate pedogenic upbuilding in response to ever increasing aeolian deposition, or increasing sand deposition, respectively. Mixed intervals may be the result of varying

degrees of bioturbation. Furthermore, each kettle bottom contains a unique sequence of buried soils, reflecting former periods of landscape stability and instability. The different number of buried soils in each kettle implies that disturbances leading to the deposition of sediments were localized, rather than affecting the entire study area. Furthermore, the preservation of such disturbance intervals in the kettle bottom deposits may be related to the balance between depositional processes and pedogenic processes, which are ultimately influenced by the morphometry of the kettle basins. In general, the data in Figs. 4.20 - 4.35 indicate that **this landscape is highly sensitive to disturbances,** as reflected in the sequence of sediments in the kettle bottoms.

As suggested earlier, fire may be the disturbance mechanism responsible for facilitating the redistribution of sediments in this highly sensitive landscape. Indeed, charcoal was found in many of the buried soils that were revealed during the depth sampling effort. The charcoal found in these soils provided an opportunity to radiocarbon date the timing of such disturbances. The following section will explore evidence from buried soils in the study area, which revealed details about the timing of aeolian silt deposition across the Evart Upland.

4.7 Timing of Silt Deposition

4.7.1 Evidence from Site 53

During the depth sampling effort, a buried soil was discovered at site 53, which had developed within the sandy, substrate sediments that underlie the sequence of silt deposition (Fig. 4.37). Though such evidence offers no absolute date on the timing of silt deposition, the presence of a strongly developed, relatively thick (~15 cm), buried A-horizon within the sandy substrate sediments at this site suggests that there was a significant period of landscape stability (and plant growth) in the post-glacial period that pre-dated silt deposition in the study area.

4.7.2 Evidence from Site 33

Charcoal is abundant within buried A horizons in the kettle bottom profile at site 33 (Fig. 4.38). Approximately 0.2 grams of charcoal fragments (<0.5 cm in size) were gathered from the lowermost buried A horizon (~120 cm depth) and radiocarbon dated together as one sample, using AMS to determine the minimum limiting age of silt deposition in this kettle (Fig. 4.39) (see Methods). In addition to the charcoal fragments, many small twig-like fragments and seeds were extracted from the buried soil. These fragments could not be identified to species, due to their small size. Furthermore, amorphous black-colored silica fragments were found in the sandy matrix after sieving (Fig. 4.40). These fragments are interpreted to be sand grains that were partially melted and re-crystallized due to fire. The charcoal fragments yielded an age of **6,840 ± 30 (1 σ)** years BP. The very small error range, despite the many fragments used to obtain the date, strongly suggests that the charcoal fragments are the result of only one fire event.

Figure 4.37- This photograph shows a trough containing the sequence of kettle bottom sediments at site 53. The pale tan sediments at the bottom of the photo are the sandy substrate sediments (lowermost C-horizon). Overlying the buried soil is the first interval of silty, aeolian sediment (brown colored). Photo by R. Schaetzl.

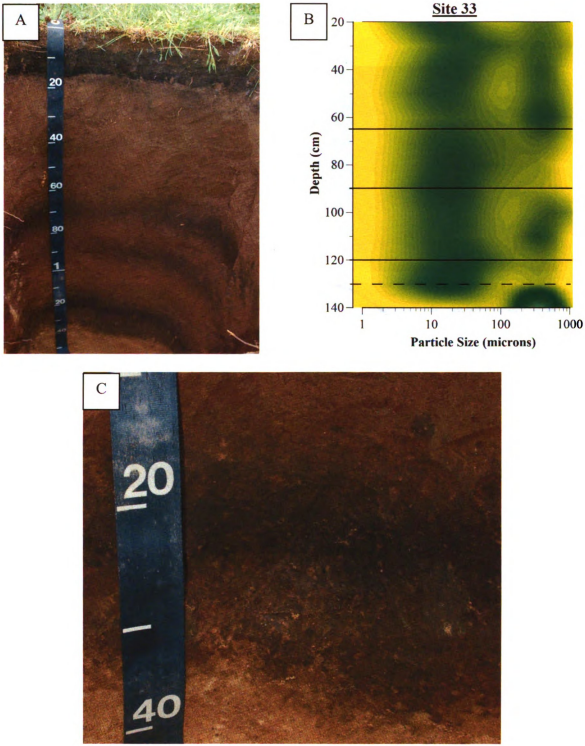

Figure 4.38- A) Photo and data from the soil profile excavated at site 33. This site contains four buried soils, with charcoal randomly spread throughout the profile, but mostly concentrated within the soils. B) Depth plot showing the down profile textural variation at site 33. Black lines indicate the top of buried soils. C) Close up of the lowermost buried soil from which charcoal was extracted at ~ 120 cm. Note: the one-meter mark on the tape measure is above the extent of the picture, therefore, the 20 cm mark in this frame is actually 120 cm. Photos by R. Schaetzl.

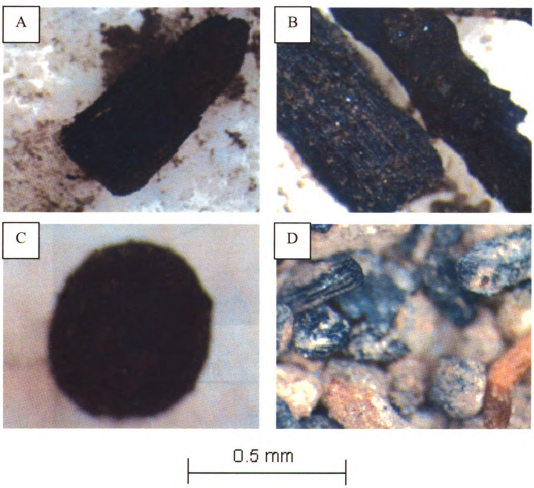

Figure 4.39- A) and B) Woody charcoal pieces commonly found in buried soil at site 33. C) Seeds were also found in the buried soil. D) Many small fragments of charcoal sticks (~0.25-0.5 mm) within the matrix of sand grains.

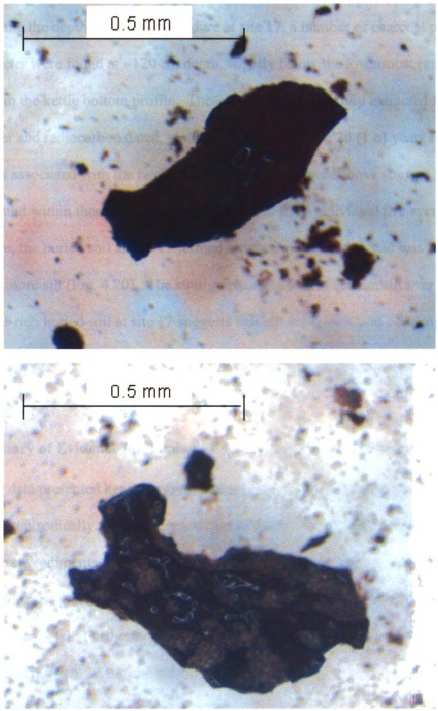

Figure 4.40- Pieces of amorphous, black-colored silica found interspersed within the lowermost buried soil at Site 33.

4.7.3 Evidence from Site 17

During the depth-sampling procedure at site 17, a number of charcoal pieces > 0.5 cm in diameter were found at ~120 cm depth, slightly below the lowermost (and only) buried soil in the kettle bottom profile. These pieces were carefully extracted from the bucket auger and radiocarbon dated, yielding and age of **920 ± 20 (1 σ)** years BP. The small errors associated with the two radiocarbon dates reported above suggest that the charcoal found within these buried soils each resulted from individual fire events. Furthermore, the buried soil at site 17 formed within a silty interval, and was later covered by more silt (Fig. 4.20). The stratigraphic position of aeolian silt *over* and *under* the charcoal-rich buried soil at site 17 suggests that silt deposition was contemporaneous with, or at least bracketed in time, a fire event or events.

4.7.4 Summary of Evidence for Timing of Silt Deposition on the Evart Upland

The data presented herein suggest that aeolian silt deposition on the Evart Upland has occurred episodically. The lowermost buried soil at site 53, which formed in the sandy substrate sediments, indicates that the Evart Upland experienced a period of stability in the post-glacial period that pre-dates at least some of the aeolian silt depositional period(s). Furthermore, the two radiocarbon dates from site 33 and site 17 yielded ages of 6,840 ± 30 BP and 920 ± 20 years BP, respectively, indicating that fires occurred in this landscape in the middle and late Holocene. The charcoal fragments used to obtain these dates were gathered at or below soils that are buried by sediments indicative of drastic changes in depositional process. As such, the charcoal fragments record distinct fire events that may have caused localized surface instability, thereby

facilitating sedimentation (either aeolian silt or slopewash sand) in kettles. Overall, these data suggest that the Evart Upland is an unstable, geomorphically sensitive landscape that has experienced various periods of stability and disturbance throughout the Holocene. To summarize, three important conclusions can be made regarding silt deposition on the Evart Upland:

1. **Aeolian silt deposition was episodic, and spatially discontinuous (i.e. not all kettles were collecting silt at the same time)**
2. **Some silt deposition events did not begin until well after the landscape had stabilized, and**
3. **Episodic silt deposition continued to occur well into the middle and late Holocene.**

The evidence presented thus far indicates that the majority of the silt in kettle bottoms is loess that was deposited episodically during the Holocene, and is associated with local fire disturbances. Furthermore, this loess is unequally distributed across the upland, being more concentrated in lower, stable landscape positions (i.e. kettle bottoms and flat sites) than higher unstable landscape positions. The uneven and patchy distribution of loess across the upland suggests that perhaps it is *locally* redistributed silt that was winnowed out of surfaces disturbed by fire. To test this interpretation, silt within kettle bottom deposits and adjacent backslopes samples were extracted and compared using X-ray diffraction techniques (see Methods). The result of this analysis follows.

4.8 Source of Kettle Bottom Silt - Local vs. Extra Regional?

To better understand the possible source(s) of loess comprising kettle bottom deposits, the silt mineralogy of a selection of kettle bottom/backslope pairs was determined using X-ray diffraction. Kuffman (2003) used a similar approach in comparing mineralogical differences between presumed aeolian silt and local silt, in an investigation into the origin of high mountain loess deposits in the German Alps. If significant mineralogical differences occur between backslope silt and kettle bottom deposit silt, then it is reasonable to suggest that the kettle bottom silt is from outside the region (allochthonous dust). On the other hand, if no (or minimal) significant mineralogical differences are apparent between the two sample types, it is reasonable to assume that 1) the silt in kettle bottoms is more local in origin, or 2) the source region has the same mineralogical composition.

4.8.1 Evidence from Texturally Different Kettle Bottom/Backslope Pairs

Four pairs of samples were chosen for the silt mineralogy comparison. The kettle bottom deposit samples in each pair have as much as ~51% more clayfree silt than their adjacent backslopes (Figs 4.41 and 4.42). Therefore, mineralogical differences (if evident) would most likely be present in *these* kettle bottom-backslope pairs than others (if the silt were allochthonous) because these kettle bottom samples would have had the least influx of sediment from the surrounding backslopes.

The first two of these pairs were obtained from kettle sites that exhibit the greatest difference in silt content (of all kettles sampled) between the kettle bottom deposit

sample and kettle backslope sample (sites 28 and 31) (Fig. 4.41). The most common mineral found in these two kettle bottom-backslope pairs is quartz. Two other minerals of lesser intensity are also found: K-feldspar, and plagioclase feldspar (Fig. 4.43). The diffraction patterns in Fig. 4.43 suggest that the silt in backslope samples and kettle bottom samples are mineralogically similar (i.e. there are no mineral peaks that are unmatched among kettle bottom and backslope pairs), and are from the same population, or source sediment. As mentioned previously, it is possible that the source sediment is extra-regional, but has the same mineralogical composition as the silt deposited on the upland. However, given that the silt in kettle bottoms was deposited contemporaneously with macroscopic charcoal (i.e. locally derived charcoal), it is unlikely that the silt is extra-regional. As such, the kettle bottom silt in these samples is likely locally redistributed loess.

4.8.2 Evidence from Intervals of Aeolian Deposition in Depth-Plots

The second pair of kettle bottom/backslope samples that was chosen for mineralogical comparison contains discrete intervals of aeolian silt deposition in the kettle bottom profile, based on textural evidence from the depth plots (Fig. 4.42). These sample pairs are from sites 24 and 42. The two aeolian intervals are indicated in the depth plot by a unimodal particle size distribution with the modal grain size in the silt range (~10-25 μm). For consistency with regard to the previous samples, the 20-53 μm range of silt from these extracted and compared to the same silt range in the adjacent backslopes. The aeolian intervals within the kettle bottom deposits at sites 24 and 42 appear to be mineralogically similar to their adjacent backslope samples (Fig.4.44).

Again, there are no mineral peaks that are unmatched among aeolian intervals in the kettle bottom and backslope pairs. As such, the intervals of aeolian silt deposition are most likely comprised of local silt.

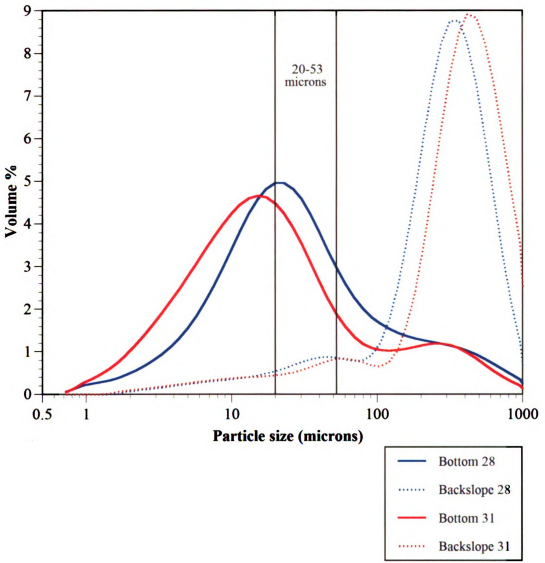

Figure 4.41- Particle size distribution curves for two of the most texturally different kettle bottom-backslope pairs. The range of silt-sized particles extracted from both is outlined (20-53 microns).

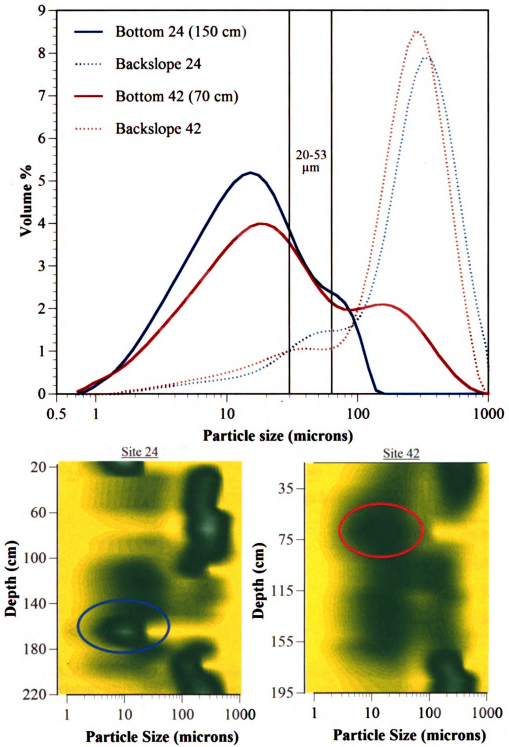

Figure 4.42- Bottom: sites 24 and 42 both have distinct intervals of aeolian deposition in the kettle bottom as indicated in the depthplots (intervals circled). Above: Particle size distribution curves of the two aeolian intervals and their adjacent backslopes. The 20-53 µm fraction of these samples and their adjacent kettle backslope samples were extracted for X-ray diffraction analysis.

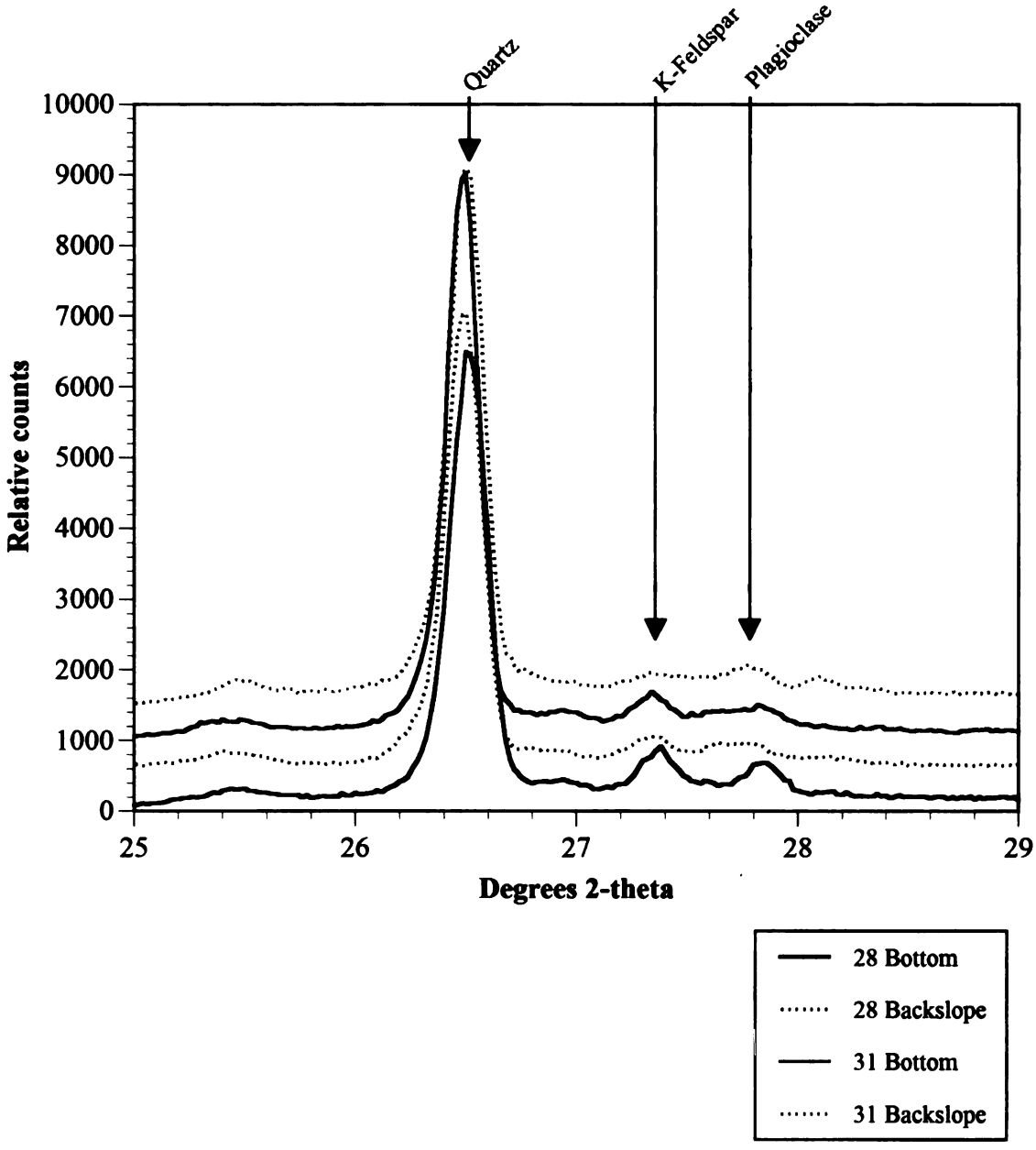

Figure 4.43- Results of the X-ray diffraction analysis for the two most texturally different kettle bottom-backslope pairs. Each kettle bottom-backslope pair is color-coded. Dashed lines represent backslope samples, while solid lines represent kettle bottom samples. Each diffraction pattern is offset 500 counts above the underlying pattern for ease of visual comparison. As such, the Y-axis should not be read as an absolute count. Three significant minerals are present in the samples: Quartz, K-feldspar, and plagioclase feldspar.

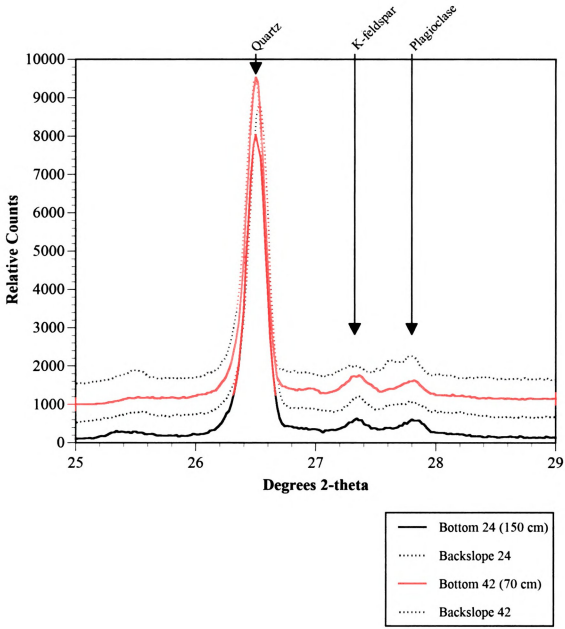

Figure 4.44- Results of the X-ray diffraction analysis for the two kettle bottoms containing distinct aeolian units. Each kettle bottom-backslope pair is color-coded. Dashed lines represent backslope samples, while solid lines represent kettle bottom samples. Each diffraction pattern is offset 500 counts above the underlying pattern for ease of visual comparison. As such, the Y-axis should not be read as an absolute count. Three significant minerals are present in the samples: Quartz, K-feldspar, and plagioclase feldspar.

4.8.3 Summary of X-ray Diffraction Analysis

The silt in kettle bottom deposits was most likely locally derived. The diffraction patterns of silt in the two selected kettle bottom/backslope pairs appear to be mineralogically similar. Quartz is by far the most abundant mineral in the eight samples analyzed, and indeed probably the most abundant mineral found within soils of the surrounding regions, which, in this part of northern Lower Michigan, are dominantly comprised of outwash sands (Schaetzl and Forman, 2008).

The intensity of quartz in the diffraction patterns may have "drowned out" the presence of other less significant minerals that could potentially show differences between kettle bottoms and backslopes. As such, it may have been helpful to combine data from X-ray diffraction analysis with data on heavy minerals within the two sample types (Kufmann, 2003). However, the diffraction patterns nonetheless illustrate that there are no significant mineral peaks present in one sample that are not present in another. Therefore, it is likely that the silt in kettle bottoms is locally redistributed loess that was winnowed out of nearby exposed surfaces and deposited across the Evart Upland, rather than being derived from some extra-regional source area.

4.9 Origin of Kettle Bottom Deposits - Summary of Evidence

Table 4.3 summarizes the evidence regarding the characteristics and origin of the silty kettle bottom deposits in the Evart Upland. The kettle bottom deposits are dominated by aeolian silt. This silt was probably winnowed out of nearby disturbed surfaces either contemporaneously or immediately following fire. The charcoal used to date the fire events that are responsible for the destabilization of surfaces in and around the Evart Upland indicate that such events occurred during the Holocene. Fires in this landscape were probably not spatially extensive, given that the upland is topographically complex, and hence, fires probably did not spread easily. Perhaps kettles nearest a surface disturbed by fire collected more silt than kettles further from the source. Such an interpretation is supported by the fact that 1) each kettle has collected a different amount of silt, and 2) the sequence of sediments and buried soils within each of the depth sampled kettle bottom deposits are not correlative across the upland (Figs. 4.20 - 4.35).

Table 4.3- Summary of evidence regarding the origin of kettle bottom deposits.

The silt comprising kettle bottom deposits...

Characteristic	*Evidence*
has an **aeolian origin**	*The kettle bottom deposits...*
	a) lie unconformably over the underlying sandy substrate sediments.
	b) have abrupt lateral boundary with the surrounding backslope sediments (i.e. were not winnowed out of the surrounding slopes via slopewash).
	c) contain 44% more clayfree silt than backslopes.
	d) have a modal silt grain size of 18 μm (as compared to 45 μm in the backslopes).
	Other evidence
	a) Nearby flat, stable surfaces have a 10% up profile increase in clayfree silt suggesting subaerial deposition via eolian processes.
	b) The spatial distribution of fine silt in kettle bottoms is different than that in backslopes, suggesting significant sorting via wind (rather than slopewash)
was deposited **episodically** throughout the **Holocene**	a) Charcoal found in buried soils provided radiocarbon ages of ~ 6840 and 920 years BP
	b) Charcoal is commonly found in other buried soils in kettle bottoms (not yet radiocarbon dated)
was winnowed from **local** sediments	The diffraction patterns of silt in representative kettle bottom and backslope samples are qualitatively the same
was deposited contemporaneously with **fire**	Depthplots (Figs. 4-17 - 4.25) show that aeolian silt often buries and/or contains charcoal fragments

CHAPTER 5 - Paleoenvironmental Significance

5.1 Soil Charcoal as an Indicator of Fire

The charcoal in the kettle bottom deposits has utility as dating tool, as shown above; it also can be used as a proxy for reconstructing local historic fire regimes (Berli et al., 1994; Gavin et al., 2003). However, using soil charcoal as an indicator of former fire regimes can be problematic due to the variability in processes related to transport, burial, and pedogenic mixing, as well as the methods used to assess the age of the charcoal. As such, many factors must be considered before making confident interpretations regarding the intensity and periodicity of former fires.

In the context of transport and deposition, there are two main types of charcoal: *primary* and *secondary*. Primary charcoal is deposited directly from a fire, or shortly thereafter, whereas secondary charcoal is deposited much later, sometimes transported great distances by wind or water before it reaches its final resting place (such as a soil or nearby lake basin) (Whitlock and Larsen, 2001). In general, the size of charcoal pieces usually decreases with distance from the source of the fire; much of it is carried aloft by convective air currents (Pisaric, 2002), or fragmented if traveled a great distance over land via runoff or slopewash. After it has been deposited and buried, various aspects of pedogenesis, such as bioturbation and freeze-thaw processes, may translocate and mix the charcoal within the soil profile. In general, Gavin (2003) has found that, because deposition of charcoal occurs at the surface, charcoal within lower mineral horizons tends to be much older than charcoal found in organic horizons, as would be expected due to soil mixing processes. In cases when the soil charcoal is not *in situ* (or in other words, eroded and re-deposited), it no longer provides an accurate age estimate for the horizon in

which it is found. Such was the case described by Arbogast and Packman (2004) for a ~ 39 ka radiocarbon age estimate on charcoal found at a depth of ~1.5 m in a Holocene inland dune field in northern Lower Michigan.

The radiocarbon-dated charcoal from the kettle bottom deposits in the Evart Upland likely resulted from local fires. A number of charcoal pieces found immediately below the buried soil at site 17 were >0.5 cm. As such, they are most likely primary charcoal, indicating that they have not been transported a great distance, and are, therefore, byproducts of a local fire. On the other hand, the charcoal pieces found in the lowermost buried soil at site 33 were <0.5 mm. It is unclear whether the size of these charcoal pieces is related to long distance transport prior to burial, or continual post-depositional fragmentation in the >6000 years since they were buried. However, both radiocarbon dates have small errors (20-30 years) despite the fact that multiple small pieces of charcoal were used to obtain each radiocarbon date. As such, these charcoal pieces likely resulted from single fire events, and therefore, the sediments deposited within kettle bottoms thereafter are probably associated with the individual fire events.

Despite the number of problems associated with using charcoal as a fire proxy, the presence of charcoal in a soil horizon nonetheless clearly documents the former occurrence of fire in the area. The two radiocarbon dates of charcoal associated with buried soils in the study area have very different dates (6820 ± 30 and 920 ± 20 years BP). When viewed in conjunction with the presence of other charcoal-rich buried soils found in kettle bottoms (that are yet undated), the data suggest that fire disturbances occurred episodically in this region from at least the middle through the late Holocene, and perhaps at all times since final landscape stabilization ca 13-15 ka.

5.2 Fire on Sandy Substrates

Many workers have demonstrated that dry, sandy outwash or ice-contact landforms in Michigan primarily supported fire-prone species prior to European settlement (Brubaker, 1975; Whitney, 1986; Leahy and Pregitzer, 2003). Perhaps the most fire-prone of these landform/vegetation associations are the various sandy outwash plains in northern Michigan that now support Jack pine forest (*Pinus banksiana)* (Simard and Blank, 1982). Host and Pregitzer's (1992) analysis of current species distributions on the sand-dominated glaciofluvial landforms of northwestern Lower Michigan suggested that variation with respect to landform has greatly influenced the successional pathways of forest development, which in turn influences the likelihood of fire. For example, in the Upper Peninsula of Michigan, Brubaker (1975) found that Holocene vegetation succession varied significantly with respect to substrate type. The flat, dry, sandy outwash deposits of the Yellow Dog Plains facilitated the development of jack pine forest throughout the Holocene and into pre-settlement times, while more mesic, finer textured till deposits in the surrounding areas tended to support eastern white pine. Essentially, fire was the discriminating agent in preventing white pine from competing on the infertile, dry substrates of the Yellow Dog Plains. These studies have demonstrated that there are inextricable links between geomorphology, soil texture (an indirect proxy of soil moisture), and forest succession, which result in a given fire regime for a particular landscape.

There is no shortage of evidence that fire was common before European settlement in the sandy regions surrounding the Evart Upland. In an analysis of GLO reports for Roscommon and Crawford Counties, Whitney (1986) found that ~ 7.3% of the

total area of sections surveyed made reference to burned patches, the majority of which were in pine-dominated stands. In the Grayling outwash plains region, GLO surveyors noted that 3% of the land area was recently burned, and several fires covered thousands of acres (Albert, 1995). These findings suggest that fires were indeed frequent and episodic on sandy substrates in the region surrounding, and within, the Evart Upland. The intensity and spatial patterns of fire likely varied with respect to landform, but as suggested by Whitney (1986), fire occurrence in the region was probably more related to vegetation type than natural firebreaks. This notion is particularly important in the context of this study because the Evart Upland is topographically very undulating, a trait that is considered detrimental to the efficient spread of fire. However, soils in the upland are also excessively drained and supported white pine-mixed hardwood forest prior to European settlement, a combination that probably promoted episodic fire (Comer et al., 1998) (see Fig. 2.15, study area chapter). As such, if fires were indeed episodic in the study area (as the wide range of radiocarbon dates suggests), they may have also been patchy and localized, since the highly undulating topography of the Evart Upland probably constrained fires to small areas.

5.3 A Warmer and Dryer Climate During the Mid-Holocene

It is well documented that climate has fluctuated significantly in the Great Lakes region during the Holocene (the past 10,000 years) (Davis et al., 2000). Many paleoenvironmental proxies have been used to demonstrate such variability, e.g., pollen analysis (Delcourt et al., 2002), lake sediment cores (Dean, 1997), paleohydrologic records (Booth and Jackson, 2003), and geomorphic studies of increased dune

mobilization (Arbogast and Packman, 2004) and fluvial incision (Arbogast et al., 2008), to name a few. Of particular interest to this discussion are other studies that have documented time intervals of dry climate or aeolian activity that closely match the two radiocarbon dates obtained from buried soils in the Evart Upland.

In order to make reasonable comparisons between the radiocarbon dates in this study and other climatic events cited in the literature, it must first be recognized that such comparisons can only be made within a regional context. Booth et al. (2006) found a significant correspondence between paleohydrologic records from two bogs in the Midwest, separated by ~1000 km: Minden bog in Salinac County, MI, and Hole bog in Cass County, MN. As such, it is herein considered reasonable to reference proxy data of Holocene climatic variability obtained within ~1000 km of the Evart Upland, but most emphasis will be placed on those within 500 km of the upland. The following discussion will highlight some examples of what others working in the region have found with respect to Holocene climate, particularly during the time intervals that correspond to the two radiocarbon dates found in this study. To reiterate, the two radiocarbon dates obtained in this study yielded ages of 6840 ± 30 and 920 ± 20 cal yrs ago.

5.4 Evidence for Climate Fluctuation from Nearby Studies

In a study of lake sediments from Elk Lake, MN, Dean (1997) used concentrations of silt-sized quartz and Na in lake cores as indicators of increased aeolian activity. Since Elk Lake is a closed system (as are kettles), Dean attributed the abundance of well-sorted, silt-sized quartz to aeolian deposition, presumably deflated and deposited in Elk Lake during drier climatic intervals. Fluctuations in % Na content in the

lake sediments (the primary source of which is liberated from plagioclase feldspar via hydrolysis) were used to track periods of former moisture availability (Fig. 5.1). Therefore, drier periods are indicated in core samples by increased levels of Na relative to the total detrital fraction, since less plagioclase is decomposed during periods of low available moisture. Among the many cycles of decreased moisture availability during the Holocene, a distinct dry interval is recorded by an increase in Na at ~6900 (varve years before present) (Fig. 4.34). The results of Dean's analysis (1997) confirm that the mid-Holocene in Minnesota (8,000-5,500 years ago) was much winder and probably drier/dustier than it is today (Dean, 1997).

A likelihood of drier and warmer climate during the mid-Holocene may also be evident in the nearby landforms of the Muskegon River (Arbogast et al., 2008). Using radiocarbon dates obtained from basal peats in paleomeanders of the Muskegon River, Arbogast et al. (2008) reconstructed the geometry and chronology of terraces in the valley. Evidence from the sequence of terraces in the valley suggested that a significant period of incision occurred in the Muskegon River sometime after 8,000 cal. years BP, which the authors assumed was in response to a warmer and drier climate, and subsequent decreases in discharge. Indeed, as new seismic profile and lake core evidence from Lewis et al. (2007) shows that Lakes Huron and Michigan experienced a hydrologically closed lake low-stands at about this time (~7,900 years BP), presumably driven largely driven by a warm, dry Holocene climate.

Further north, in the Baraga dune field in Baraga County, in Michigan's western upper peninsula, Arbogast and Packman (2004) obtained OSL (optically stimulated luminescence) dates from vegetated dunes to reconstruct the history of their formation.

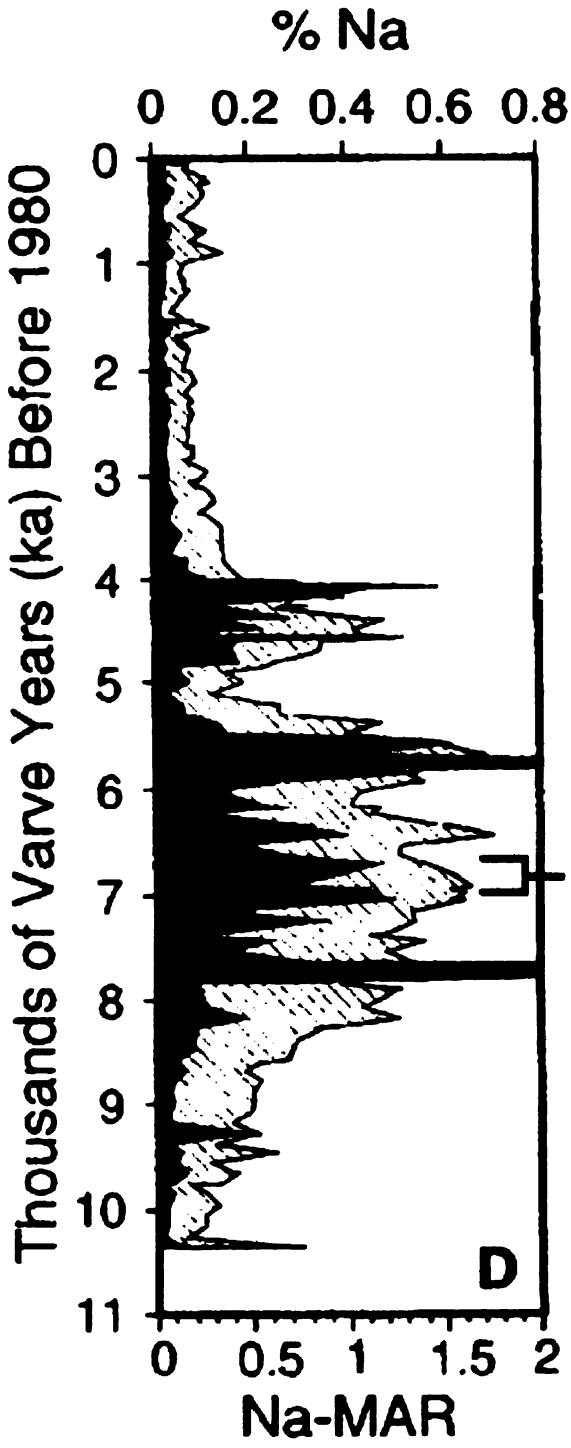

Figure 5.1- A Holocene record of aeolian activity from Elk Lake, MN. Black shading represents % Na (higher values indicate increased dryness). Line pattern shading indicates mass accumulation rate. The red bracket highlights a cycle of increased aeolian activity that corresponds with the oldest radiocarbon date obtained in this study. Diagram after Dean (1997).

Their OSL dates indicated that aeolian activity in the Baraga dune field occurred in the middle Holocene, from 7.0 to 6.0 ka (thousands of years before present). They cited two possible mechanisms for the onset of dune formation: 1) increased westerly winds associated with the 8.2 ka dry/cold climate event, as verified by evidence from lake sediments in Elk Lake, MN (Dean et al., 2002), and/or 2) destabilization of surfaces due to increased fire activity associated with Jack pine on sandy, flat, substrates.

In a similar study, Arbogast et al (2002) obtained samples for OSL dating from dunes in the Newberry dune field, in the eastern upper peninsula of Michigan. The OSL dates in their study indicated that aeolian activity occurred between 7.0 and 5.5 ka. Fluctuating climatic conditions alone (i.e. warmer and dryer) were revoked as the sole mechanism responsible for the onset of dune formation. Instead, they suggested that isostatically driven regressions in the Lake Superior and Lake Michigan basins caused a drastic drop in watertables in the region surrounding the Newberry dune field. Because the dune field formed in a relatively thick sequence of sandy glacial sediments, they suggested that even a small increase in temperature and dryness could combine with the drop in groundwater to destabilize surface sediments and trigger the onset of aeolian activity (Arbogast et al., 2002).

In a study comparing two sediment cores obtained from bogs in Michigan and Minnesota, Booth et al. (2006) used testate amoeba analysis to reconstruct the paleohydrology at each site. Among other episodes of widespread drought indicated in the analysis, their findings document the presence of a large drought interval between 900 and 1000 cal. years BP (Fig 4.35). They associated this drought interval with widespread changes in vegetation and fire regime in southeastern Michigan.

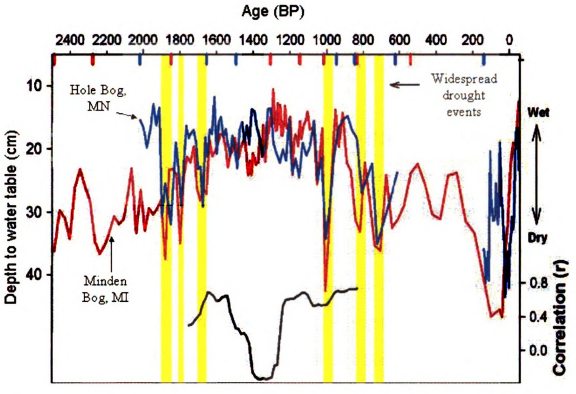

Figure 5.2- Diagram showing the comparison of hydroclimate histories reconstructed from Hole Bog, MN (Blue) and Minden Bog, MI (red) for the past 2500 yrs after (Booth et al., 2006). Both records show a prominent dry interval around 1000 cal. years BP (highlighted yellow). This time period corresponds to the radiocarbon date of 920 cal. years BP obtained in this research.

Other studies (Booth and Jackson, 2003; Davis et al., 2000; Dean et al., 2002) also confirm periods of dry/warm climate and episodic drought throughout the Holocene in the Great Lakes region; however, it is not the purpose of this discussion to provide a comprehensive comparison to other published dates, because only two were obtained during this research. The main point, in the context of this study, is that sandy upland areas, such as the Evart Upland, would have been susceptible to climatic fluctuations throughout the Holocene. Indeed, the radiocarbon dates obtained in this study (6840 ± 30 and 920 ± 20 years BP) overlap with periods of increased dryness during the Holocene. As the highest and driest parts of the regional landscape, sandy uplands like the Evart

Upland are closer to t he threshold of disturbance from destabilizing agents such as fire and wind than are adjoining regions/areas.

5.5 The Possible Role of Climate and Fire in Destabilizing Sandy Surfaces

There is unequivocal evidence in the literature suggesting that, historically, sandy substrates in Michigan promoted vegetation types susceptible to fire (Brubaker, 1975; Whitney, 1986; Leahy and Pregitzer, 2003; Arbogast and Packman, 2004). However, as noted by Arbogast et al. (2004), the role of fire as a destabilizing mechanism for surface soils is contested. The root of this debate centers on the question of how quickly stabilizing surface vegetation re-grows, and stabilizes the surface, after fire. The efficiency of re-growth depends on the type of vegetation and general climate of the region. For example, fire-adapted species may rapidly re-establish ground cover and quickly stabilize soils after fire, but not if such a fire is associated with cold-climates when rapid regrowth is not possible.

It has long been recognized that recently burned surfaces are temporarily hydrophobic because of the addition of water repellent organic compounds released from plant materials during fire (Savage, 1974; DeBano et al., 1979). Fire-induced soil hydrophobicity increases the potential for runoff and soil erosion by water (Dragovich and Morris, 2002; Gabet, 2003). Newer evidence suggests that the same compounds responsible for fire-induced soil-hydrophobicity also increase the potential for wind erosion (Ravi et al., 2006). Ravi et al (2006) carried out experiments on well-sorted, clean sandy sediments in a wind tunnel that were artificially coated with a fatty acid commonly found in plants (palmitic acid), which is released upon burning. Their results

indicated that fire-induced water repellency results in a decrease of threshold velocity for wind transport, thereby enhancing the efficacy of wind erosion on sandy soil. In a wind erosion study of semi-arid ponderosa pine forests of the western U.S., Whicker et al. (2008) measured the amount of wind-eroded dust emanating from both burned and thinned areas, as opposed to non-burned areas. Their results indicated that thinned areas of the pine forest were just as susceptible to wind erosion as burned areas, and that both emitted more wind-eroded dust than non-burned areas.

Although recent studies of the relationship between fire, wind-erosion, and dust deflation are primarily focused on the arid and semi-arid portions of the U.S., it is possible that similar processes were operating during the Holocene in the Great Lakes region, especially on dry sandy upland areas, such as the Evart Upland, which would have been more susceptible to the destabilizing mechanisms of drought, fire, and subsequent wind-erosion.

5.6 Paleoenvironmental Significance - Summary

Fire was probably frequent on dry, sandy landforms, such as the Evart Upland, throughout the Holocene because dry, sandy substrates allow for occasional fire, which tends promote fire-prone species, and subsequent feedbacks. The presence of charcoal in buried soils on the Evart Upland confirms that this landscape indeed has experienced fire throughout the Holocene, and probably also throughout the Late Pleistocene. Indeed, GLO reports of other sandy regions of Lower Michigan surrounding the Evart Upland confirm that expansive areas of recently burned forest were common at the time of the surveys (~1850's) (Simard and Blank, 1982; Whitney, 1986). These reports confirm that

fire was a natural (and probably frequent) occurrence on sandy substrates in Lower Michigan. Given the preponderance of sandy substrates and undulating topography in the Evart Upland, fires may have been frequent, but localized and patchy.

In the context of the Evart Upland, linking the occurrence of fire to Holocene climate proxies is simplistic. However, given that there are many lines of evidence indicating that the Great Lakes region experienced significantly warmer and drier climate during the Holocene, such a link is also realistic. Being the highest and driest parts of the regional landscape, sandy uplands like the Evart Upland are close to the threshold of disturbance from destabilizing agents such as fire. As such, even the smallest fluctuations in Holocene climate would have impacted sandy, dry uplands more than other sites in this part of Michigan.

As the data in this thesis suggest, silt deposition on the Evart Upland has occurred episodically throughout the Holocene, and contemporaneously with fire. It is unclear whether fire or a warm/dry Holocene climate was the actual causal mechanism triggering destabilization of surfaces in and around the Evart Upland. In either case, deposits of aeolian silt and charcoal in kettle bottoms on the Evart Upland record a history of landscape evolution, greatly impacted by disturbance mechanisms such as wind and fire.

CHAPTER 6 - Conclusions

6.1 Geomorphology of the Evart Upland

The Evart Upland, a ~68 km^2 dome-like upland of rolling hills in north-central Lower Michigan, contains an abundance of topographically closed basins (kettles). These kettles likely formed as a complex arrangement of stagnant ice, leftover after the Lake Michigan and Saginaw ice lobes retreated from the region, was surrounded and variously buried by thick deposits of outwash. Subsequent meltout of the buried ice resulted in a ubiquitous assemblage of kettles, many of them dry, set within a landscape dominated by sand. These kettles have subsequently acted as accumulation basins, preserving records of landscape stability and instability via the sediments that are contained within their center-bottom portions.

The majority of kettles (53/59) sampled on the Evart Upland contain lenticularly-shaped, silty deposits in the center-bottom portion (i.e., the deepest part) of the depression. Silty deposits in kettle bottoms here are anomalous. Therefore, the purpose of this research was to determine the most likely geomorphic origin(s) of these silty deposits, and assess their paleoenvironmental importance.

6.2 Characteristics and Origin of Silty Kettle Bottom Deposits

6.2.1 Aeolian Silt

Kettles in the Evart Upland have variously accumulated sediments since final landscape stabilization. Indeed, nearly all of the kettles (53/59) investigated in the Evart Upland contain small (< 1 % of the kettle area) silty deposits in the bottom center of the

depression; these sediments may extend to ~1 m depth. Overall, these silty deposits are texturally much finer than the surrounding backslope soils, which are sandy. On average, kettle bottoms contain 44 % more clayfree silt than the surrounding backslopes. Furthermore, the silt in kettle bottoms has a modal grain size of 18 μm, whereas the silt in backslopes has a modal grain size of 45 μm. Finally, these silty deposits do not extend up the surrounding backslopes, as would be expected if downslope sorting processes were responsible for the silt. Because these silty deposits are anomalous with respect to the surrounding backslope soils, as well as the preponderance of sand in the region, I conclude that their origin is most likely aeolian.

Soils on three flat, geomorphically stable surfaces on the Evart Upland show an increase in silt content in the upper (~0-50 cm) profile. These sites exhibit a 10% silt increase in the upper profile, and in each case, fine silt (2-20 μm) increases more than medium (20-35 μm) or coarse silt (35 μm). Furthermore, fine silt is also the modal grain size in kettle bottom deposit samples. I interpret this evidence to indicate that silt was added to flat stable sites from above, via aeolian deposition, and later, pedogenically assimilated into the profile, this process diminishing with depth. Similar scenarios were proposed for the preservation of aeolian silt in other flat landscape positions in northern Lower Michigan (i.e. the Buckley flats (Schaetzl and Hook, 2008) and the Grayling Fingers region (Schaetzl, 2008). Such an increase in silt in the upper profiles of flat, stable sites offers supporting evidence that the silty kettle bottom deposits have an aeolian origin, and confirms that aeolian processes have impacted soils in this landscape. This evidence also suggests that the degree to which aeolian silt has been preserved and incorporated into soils here may have been influenced by the slope (susceptibility to

runoff) or long-term stability of the surface. Surfaces with even the slightest slope may not have preserved aeolian silt because it would have been easily washed downslope, and spatially concentrated in the nearest basin.

6.2.2 Slopewash Sand

Kettle bottoms have also accumulated various amounts of sand within the otherwise silty deposits; this sand presumably originated from the surrounding backslopes during periods of increased slopewash deposition. Recent evidence (Fig 4.11) and the depthplot diagrams (Figs. 4.20 - 4.35) indicate that kettle backslopes have been subject to erosion at different times, and to different intensities, in the past. Each kettle investigated with depth preserved a unique record of depositional events in the kettle, ranging from intervals of pure silt (loess) deposition to sandy (slopewash) deposition from the surrounding slopes, attesting to the variation in processes that were operative on this landscape in the past.

6.2.3 Buried Soils

Various numbers of buried soils exist in each of several kettles investigated. The soils are indicative of episodes of former landscape stability and instability. In some kettle bottoms, a soil formed within a silty interval of sediment and was subsequently buried by slopewash, whereas in other kettles, such a soil was buried again by loess. At one site in particular (site 53), the lowermost buried soil (which formed in the underlying sandy substrate sediment), was buried by loess (Figs. 4.35 and 4.37), indicating that a period of stability pre-dated at least some of the aeolian silt depositional periods on the Evart Upland. The variation in depositional sequence among kettles suggests that the

buried soils in kettle bottoms cannot be correlated among basins, and that some kettles were experiencing significant erosion, while others were stable. Similarly, some kettles were collecting loess while others were not, as indicated by the different amounts of silt preserved within each kettle bottom deposit. As such, loess deposition in the study area was probably both spatially and temporally discontinuous.

6.3 Silt Deposition Contemporaneous with Holocene Fires

The silt comprising the majority of kettle bottom deposits was probably deposited contemporaneously with, or shortly after, fire events. Evidence for this includes fragments of charcoal found within buried soils and throughout the profiles of silty kettle bottom deposits. Samples of charcoal from two sites were radiocarbon dated. These two dates span the middle to late Holocene (6840 ± 30 and 920 ± 20 cal. years BP). Furthermore, these fires may have been intense, as indicated by the presence of scorched, amorphous silica grains found in the kettle bottom deposits (Fig. 4.40). Such fires may have liberated surficial sediments, thereby facilitating the aeolian redistribution of silt into local kettle bottoms.

6.4 Kettle Bottom Silt is Local

The silt mineralogy of kettle bottom deposits was compared to the autochthonous silt found in backslope soils. The similarity of the X-ray diffraction patterns between the two types of sediments suggests that the silt deposited in kettle bottoms is locally redistributed silt, perhaps winnowed out of surfaces disturbed by fire.

6.5 Paleoenvironmental Significance

It is well known that fire is a significant factor that regulates forest succession. For example, some researchers in northern Lower Michigan have outlined significant differences in forest succession pathways among different geomorphic landforms, which are influenced largely by topography, soil type (an indirect proxy of soil moisture), and ultimately, fire history (Host et al., 1987; Host and Pregitzer, 1992). An important conclusion of their work is that landform types in Michigan control species composition at the site level, as well as long-term disturbance patterns such as fire, the understanding of which is traditionally obtained from quantitative analysis of original land survey records (Whitney, 1986; Leahy and Pregitzer, 2003).

Sandy upland areas, like the Evart Upland, would have been susceptible to periods of drought, increased warmth, and fire during the Holocene. Consequently, the Evart Upland has preserved long-term records of fire disturbance via the aeolain, silty sediments that are contained in kettle bottoms. Such records may be useful in developing an understanding of long-term disturbance histories in regions with sandy upland landforms susceptible to fire, where traditionally, an understanding of such histories is primarily restricted to analyses of GLO reports (i.e., short term records) (Leahy and Pregitzer, 2003; Whitney, 1986). Finally, this research demonstrates that, on sandy upland landforms of Lower Michigan, fire may have been a significant geomorphic agent capable of liberating surficial sediments and facilitating silt deflation.

APPENDIX

Table A.1- Textural data for backslope samples. Numbers expressed as percent of sample. MWPS = mean weighted particle size.

Raw Data- Backslope Samples

	MWPS	Clay	Silt	Sand	VC Sand	C Clay	VF Silt	F Silt	M Silt	C Silt
Sample	um	<2 um	2 - 50 um	50 - 2000 um	1000-2000 um	0.2 - 2 um	2 - 12 um	12 - 25 um	25 - 35 um	35 - 50 um
1	237.5	6.3	25.1	68.6	0.5	6.2	6.6	9.4	4.6	4.5
2	234.1	8.3	24.1	67.6	0.4	8.2	7.0	8.8	4.2	4.1
3	206.6	2.3	21.5	76.2	0.1	2.3	3.0	6.8	5.2	6.6
4	249.3	4.6	19.6	75.8	0.4	4.6	4.5	6.7	3.9	4.6
5	249.4	5.9	18.0	76.1	0.1	5.9	5.4	6.4	3.1	3.1
6	389.6	1.8	9.8	88.4	1.8	1.8	2.1	3.1	2.0	2.7
7	274.9	0.9	7.2	91.9	0.0	0.9	1.1	2.2	1.8	2.2
8	268.9	1.0	10.4	88.6	0.1	1.0	1.3	2.8	2.6	3.8
9	262.4	3.7	12.1	84.2	0.1	3.7	2.8	3.9	2.4	2.9
10	185.5	8.6	28.3	63.0	0.2	8.5	7.3	9.9	5.3	5.8
11	297.5	1.3	8.2	90.5	0.0	1.3	1.4	2.7	2.0	2.1
12	242.4	2.8	13.1	84.1	0.0	2.8	2.4	4.4	3.0	3.3
16	343.5	2.2	13.6	84.2	1.1	2.2	2.5	4.6	3.0	3.5
17	231.8	2.4	17.2	80.4	0.2	2.4	2.8	5.4	3.9	5.1
18	233.7	1.9	15.3	82.8	0.1	1.9	2.1	4.6	3.7	4.9
19	277.0	3.3	16.8	79.8	0.7	3.3	3.5	5.7	3.5	4.2
20	235.7	3.2	18.9	77.9	0.3	3.2	3.4	6.3	4.2	5.0
21	261.0	2.4	14.5	83.1	0.4	2.4	2.5	4.9	3.3	3.9
22	286.8	1.7	10.2	88.2	0.1	1.7	1.8	3.1	2.3	3.0
23	304.1	1.1	8.9	90.0	0.3	1.1	1.4	2.8	2.1	2.5
24	283.5	1.5	11.2	87.3	0.3	1.5	1.7	3.3	2.7	3.6
25	226.8	1.8	14.5	83.7	0.0	1.8	2.0	4.4	3.6	4.6
26	292.0	1.3	8.6	90.1	0.0	1.3	1.5	2.7	2.0	2.4
27	393.6	1.6	9.8	88.6	1.7	1.6	2.0	3.1	2.0	2.6

Table A.1- continued

Sample	MWPS	Clay	Silt	Sand	VC Sand	C Clay	VF Silt	F Silt	M Silt	C Silt
28	308.0	1.5	8.6	89.9	0.4	1.5	1.7	2.8	1.9	2.2
29	240.5	3.8	15.3	80.9	0.0	3.8	3.3	5.1	3.2	3.7
30	284.1	1.7	9.9	88.5	0.3	1.7	1.9	3.1	2.1	2.8
31	392.2	1.8	7.6	90.6	1.5	1.8	1.8	2.3	1.4	2.0
32	265.1	1.4	8.9	89.7	0.0	1.4	1.4	2.7	2.1	2.7
33	287.8	2.7	12.6	84.8	0.4	2.7	2.6	4.1	2.7	3.3
34	344.3	2.2	10.5	87.3	1.1	2.2	2.2	3.3	2.2	2.8
35	192.8	1.9	14.6	83.5	0.0	1.9	1.8	4.4	3.6	4.8
36	216.8	7.0	20.9	72.2	0.0	6.9	5.7	7.3	3.8	4.1
37	273.1	5.2	16.1	78.7	0.4	5.2	4.2	5.4	3.0	3.4
38	232.0	4.1	19.0	76.8	0.3	4.1	4.1	6.3	3.9	4.7
39	250.8	3.0	10.7	86.3	0.0	3.0	2.4	3.5	2.2	2.6
40	328.1	1.6	9.0	89.5	0.7	1.6	1.7	2.8	2.0	2.5
41	286.5	2.1	11.3	86.7	0.4	2.1	1.8	3.2	2.7	3.6
42	238.5	2.0	11.7	86.3	0.0	2.0	2.4	4.1	2.5	2.7
43	128.0	8.0	38.0	54.0	0.0	7.8	7.9	13.2	7.9	9.0
44	298.7	4.7	14.8	80.5	0.6	4.6	3.9	5.1	2.8	3.1
45	235.7	5.8	20.5	73.7	0.4	5.7	5.4	7.7	3.8	3.6
46	268.8	5.8	17.9	76.3	0.4	5.7	5.3	6.8	3.0	2.8
47	281.1	1.7	8.8	89.4	0.0	1.7	1.8	3.1	2.0	1.9
48	269.1	3.7	14.8	81.5	0.2	3.7	3.7	5.4	2.9	2.8
49	247.8	1.4	6.7	92.0	0.0	1.4	1.3	2.5	1.5	1.4
51	315.7	1.9	6.9	91.1	0.0	1.9	1.8	2.4	1.4	1.4
52	311.7	2.0	8.3	89.7	0.1	2.0	2.1	2.9	1.6	1.6
53	253.4	3.2	15.9	80.9	0.4	3.2	3.4	5.4	3.3	3.9
54	298.4	3.0	9.9	87.1	0.3	3.0	2.6	3.5	1.9	2.0
55	255.6	5.2	21.1	73.7	0.7	5.1	4.7	7.1	4.3	5.0
56	246.2	3.6	15.6	80.8	0.1	3.6	3.4	5.4	3.2	3.6
57	266.0	3.2	12.4	84.4	0.2	3.2	2.9	4.4	2.5	2.7

Table A.2- Textural data for kettle bottom deposit samples. Numbers expressed as percent of sample. MWPS = mean weighted particle size.

Raw Data- Kettle bottom deposit samples

	MWPS	Clay	Silt	Sand	VC Sand	C Clay	VF Silt	F Silt	M Silt	C Silt
Sample	um	<2 um	2 - 50 um	50 - 2000 um	1000-2000 um	0.2 - 2 um	2 - 12 um	12 - 25 um	25 - 35 um	35 - 50 um
1	137.3	9.0	37.0	54.0	0.0	8.8	9.8	13.9	6.7	6.7
2	61.4	16.1	59.0	24.8	0.1	15.8	18.5	23.7	9.2	7.6
3	192.4	8.3	32.8	58.9	0.3	8.2	9.7	12.6	5.5	5.1
4	173.7	11.4	20.9	67.7	0.1	10.4	7.0	7.8	3.1	3.0
5	206.2	9.4	29.7	60.8	0.2	9.3	9.8	11.6	4.6	3.8
6	74.3	20.8	56.1	23.1	0.2	20.4	19.6	22.3	8.0	6.2
7	134.7	14.7	42.7	42.6	0.1	14.4	14.0	16.9	6.5	5.3
8	192.0	11.0	31.8	57.2	0.9	10.8	9.3	11.7	5.3	5.5
9	96.5	11.6	52.0	36.4	0.1	11.3	13.6	20.5	9.3	8.5
10	76.5	15.1	58.5	26.4	0.1	14.8	17.0	24.0	9.8	7.7
11	179.5	7.5	35.3	57.1	0.2	7.3	8.0	13.4	7.0	6.9
12	99.4	16.8	54.7	28.6	0.3	16.3	17.0	21.9	8.7	7.0
16	53.6	21.5	56.3	22.2	0.0	20.9	19.2	22.3	8.3	6.6
17	58.2	17.8	61.8	20.4	0.1	17.3	19.2	25.2	9.7	7.6
18	82.2	17.0	46.9	36.0	0.0	16.6	14.6	17.9	7.5	7.0
19	105.0	15.4	46.7	37.9	0.2	15.0	14.9	18.3	7.2	6.2
20	32.2	33.2	57.9	8.9	0.1	32.4	25.5	22.5	6.1	3.8
21	69.2	18.0	50.1	31.9	0.1	17.6	16.8	19.2	7.5	6.6
22	107.5	10.1	42.3	47.5	0.0	9.9	10.7	16.3	7.8	7.4
23	86.7	14.6	50.2	35.2	0.1	14.2	15.1	19.8	8.1	7.1
24	77.8	17.3	50.3	32.4	0.1	16.7	15.7	19.8	8.0	6.8
25	177.3	5.0	27.8	67.2	0.1	4.9	4.9	9.2	6.3	7.4
26	328.0	2.0	11.3	86.7	0.6	2.0	2.4	4.0	2.4	2.5
27	205.4	14.2	34.6	51.2	0.5	13.9	12.2	13.6	5.0	3.8
28	73.9	11.4	60.6	28.0	0.2	11.0	15.6	25.3	10.8	8.9

Table A.2- continued

Sample	MWPS	Clay	Silt	Sand	VC Sand	C Clay	VF Silt	F Silt	M Silt	C Silt
29	137.7	12.3	47.1	40.6	0.5	12.0	14.1	19.2	7.6	6.2
30	128.7	11.0	48.4	40.6	0.3	10.7	12.5	19.4	8.8	7.7
31	59.7	21.1	58.0	20.9	0.1	20.6	20.2	23.6	8.2	6.0
32	83.1	9.5	55.6	34.8	0.2	9.1	12.7	22.3	10.8	10.0
33	115.8	16.8	45.6	37.6	0.3	16.4	15.5	17.9	6.6	5.6
34	46.1	20.0	60.2	19.8	0.0	19.6	20.1	23.9	9.0	7.2
35	72.7	17.6	51.9	30.4	0.1	17.2	16.2	19.9	8.3	7.5
36	95.7	17.3	48.3	34.3	0.1	16.9	16.2	19.1	7.2	5.8
37	86.4	16.7	53.0	30.3	0.2	16.4	17.6	20.9	7.9	6.6
38	49.6	21.5	60.7	17.8	0.1	20.8	20.3	24.5	9.0	6.9
39	69.2	18.8	51.1	30.1	0.1	18.3	16.7	19.6	7.8	7.1
40	114.5	10.6	46.4	43.0	0.2	10.3	12.0	18.7	8.4	7.4
41	98.2	10.1	49.0	40.9	0.0	9.8	11.6	19.0	9.4	9.0
42	86.2	12.8	47.9	39.3	0.1	12.3	13.8	19.2	8.0	7.0
43	76.2	14.2	56.7	29.1	0.0	13.9	16.0	22.4	9.7	8.6
44	77.2	23.3	55.7	21.0	0.3	22.7	19.4	22.0	8.1	6.3
45	57.2	18.8	55.3	25.9	0.0	18.5	17.6	21.6	8.7	7.4
46	102.7	10.6	47.6	41.9	0.0	10.3	12.4	18.9	8.6	7.6
47	91.1	19.0	47.1	33.9	0.0	18.7	16.3	18.6	6.8	5.4
48	90.9	16.3	56.2	27.5	0.2	15.8	18.3	23.2	8.4	6.3
49	51.8	14.7	53.5	31.8	0.0	14.4	15.0	20.0	9.2	9.3
50	41.6	23.9	61.7	14.5	0.0	23.3	22.2	24.9	8.5	6.1
51	68.5	19.4	55.8	24.8	0.2	19.0	19.1	22.3	8.1	6.4
52	81.7	13.4	43.7	42.8	0.0	13.2	13.5	16.7	6.9	6.6
53	96.3	12.9	44.0	43.1	0.0	12.8	14.0	17.0	6.8	6.1
54	59.3	19.0	56.7	24.4	0.1	18.6	18.3	22.0	8.7	7.6
55	131.7	13.6	49.5	36.9	0.4	13.3	15.3	19.9	7.8	6.4
56	119.3	18.9	46.9	34.2	0.3	18.3	16.0	18.5	6.9	5.5
57	64.1	14.4	53.3	32.3	0.1	13.9	15.3	20.6	8.9	8.5

BIBLIOGRAPHY

Albert, D. A. 1995. *Regional landscape ecosystems of Michigan, Minnesota, and Wisconsin: a working map and classification.* St. Paul, Minn.: U.S. Dept. of Agriculture, Forest Service, North Central Forest Experiment Station.

Almendinger, J. E. & S. Hobbie (1992) Influence of terrestrial vegetation on sediment-forming processes in kettle lakes of west-central Minnesota. *Quaternary Research,* 38, 103-116.

Arriaga, F. J., B. Lowery & M. D. Mays (2006) A fast method for determining soil particle size distribution using a laser instrument. *Soil Science,* 171, 663-674.

Barrett, L. (2001) A strand plain soil development sequence in Northern Michigan, USA. *Catena,* 44, 163-186.

Beierle, B. D., S. F. Lamoureux, J. M. H. Cockburn & I. Spooner (2002) A new method for visualizing sediment particle size distributions. *Journal of Paleolimnology,* 27, 279-283.

Bennett, M. & N. F. Glasser. 1996. *Glacial geology: ice sheets and landforms.* Chichester; New York: Wiley.

Beuselinck, L., G. Govers, J. Poesen, G. Degraer & L. Froyen (1998) Grain-size analysis by laser diffractometry: comparison with the sieve-pipette method. *Catena,* 32, 193-208.

Booth, R. K. & S. T. Jackson (2003) A high-resolution record of late-Holocene moisture variability from a Michigan raised bog, USA. *Holocene,* 13, 863-876.

Booth, R. K., M. Notaro, J. E. Kutzbach & S. T. Jackson (2006) Widespread drought episodes in the western Great Lakes region during the past 2000 years: Geographic extent and potential mechanisms. *Earth and Planetary Science Letters,* 242, 415-427.

Buurman, P., T. Pape & C. C. Muggler (1997) Laser grain-size determination in soil genetic studies 1. Practical problems. *Soil Science,* 162, 211-218.

Chen, Y., M. Song & M. Dong (2002) Soil properties along a hillslope modified by wind erosion in the Ordos Plateau (semi-arid China). *Geoderma,* 106, 331-340.

Davis, M., C. Douglas, R. Calcote, K. L. Cole, M. G. Winkler & R. Flakne (2000) Holocene climate in the western Great Lakes National Parks and Lakeshores: Implications for future climate change. *Conservation Biology,* 14, 968-983.

Dean, W. E., R. M. Forester & J. P. Bradbury (2002) Early Holocene change in atmospheric circulation in the Northern great plains: An upstream view of the 8.2 ka cold event. *Quaternary Science Reviews,* 21, 1763-1775.

DeBano, L. F., R. M. Rice & C. E. Conrad (1979) Soil heating in chaparral fires: effects on soil properties, plant nutrients, erosion, and runoff. *USDA Forest Service Research Paper*, PSW-145.

Folsom, M. M. 1971. Glacial geomorphology of the Hastings quadrangle, Michigan. 5, v, 166 leaves. Michigan State University. Dept. of Geography, 1971.

Ham, N. R. & J. W. Attig (1996) Ice wastage and landscape evolution along the southern margin of the Laurentide Ice Sheet, north-central Wisconsin. *Boreas,* 25, 171-186.

Host, G. E. & K. S. Pregitzer (1992) Geomorphic influences on ground-flora and overstory composition in upland forests of northwestern lower Michigan. *Canadian Journal of Forest Research,* 22, 1547-1555.

Host, G. E., K. S. Pregitzer, C. W. Ramm, J. B. Hart & D. T. Cleland (1987) Landform-mediated differences in successional pathways among upland forest ecosystems in northwestern Lower Michigan. *Forest Science,* 33, 445-457.

Jenny, H. 1941. *Factors of soil formation; a system of quantitative pedology*. New York, London: McGraw-Hill.

Johnson, M. D., D. M. Mickelson, L. Clayton & J. W. Attig (1995) Composition and genesis of glacial hummocks, western Wisconsin, USA. *Boreas,* 24, 97-116.

Kleiss, H. J. (1970) Hillslope sedimentation and soil formation in northeastern Iowa. *Soil Sci. Soc. Am. Proc.,* 34, 287-290.

Konert, M. & J. Vandenberghe (1997) Comparison of laser grain size analysis with pipette and sieve analysis: a solution for the underestimation of the clay fraction. *Sedimentology,* 44, 523-535.

Kufmann, C. (2003) Soil types and eolian dust in high-mountainous karst of the Northern Calcareous Alps (Zugspitzplatt, Wetterstein Mountains, Germany). *Catena,* 53, 211-227.

Lamoureux, S. (2000) Five centuries of interannual sediment yield and rainfall-induced erosion in the Canadian High Arctic recorded in lacustrine varves. *Water Resources Research,* 36, 309-318.

Leahy, M. J. & K. S. Pregitzer (2003) A comparison of presettlement and present-day forests in northeastern lower Michigan. *American Midland Naturalist,* 149, 71-89.

Lewis, C. F. M., C. W. Heil Jr, J. B. Hubeny, J. W. King, T. C. Moore Jr & D. K. Rea (2007) The Stanley unconformity in Lake Huron basin: Evidence for a climate-driven closed lowstand about 7900 p14 sC BP, with similar implications for the Chippewa lowstand in Lake Michigan basin. *Journal of Paleolimnology,* 37, 435-452.

Loizeau, J. L., D. Arbouille, S. Santiago & J. P. Vernet (1994) Evaluation of a wide range laser diffraction grain size analyser for use with sediments. *Sedimentology,* 41, 353-361.

Malo, D. D., B. K. Worcester, D. K. Cassel & e. al. (1974) Soil-landscape relationships in a closed drainage system. *Soil Sci. Soc. Am. J.,* 38, 813-818.

Michigan Department of Information Technology, Center For Geographic Information. Online Content. Available online at http://www.michigan.gov/cgi accessed February 26, 2007

Mikesell, L., R. J. Schaetzl & M. A. Velbel (2004) Hornblende etching and quartz/feldspar ratios as weathering and soil development indicators in some Michigan soils. *Quaternary Research,* 62, 162-171.

Milne, G. (1936) Normal erosion as a factor in soil profile development. *Nature,* 138, 548.

NOAA, Data from NOAA Midwestern Regional Climate Center. Illinois State Water Survey at the University of Illinois at Urbana-Champaign under the Institute of Natural Resource Sustainability. Available online at http://mrcc.isws.illinois.edu. accessed 11/6/08

NRCS, Plant fact sheet: Sweetfern, *Comptonia peregrina.* United States Department of Agriculture, Natural Resources Conservation Service. Available online at http://plant-materials.nrcs.usda.gov/ accessed 12/2/2008

Paton, T. R., G. S. Humphreys & P. B. Mitchell. 1995. *Soils: a new global view.* New Haven: Yale University Press.

Pennock, D. J. & E. De Jong (1987) The influence of slope curvature on soil erosion and deposition in hummocky terrain. *Soil Science,* 144, 209-217.

Rieck, R. L. 1976. The glacial geomorphology of an interlobate area in southeast Michigan: relationships between landforms, sediments, and bedrock. [4], xci, [218] leaves. Michigan State University. Dept. of Geography, 1976.

--- (1979) Ice stagnation and paleodrainage in and near an interlobate area. *Papers Mich. Acad. Sci., Arts, Letters,* 11, 219-235.

Rieck, R. L. & H. A. Winters (1993) Drift volume in the Southern Peninsula of Michigan - a prodigious Pleistocene endowment. *Physical Geography,* 14, 478-493.

Savage, S. M. (1974) Mechanism of Fire-Induced Water Repellency in Soil. *Soil Sci. Soc. Am. J,* 38, 652-657.

Schaetzl, R. J. (1996) Spodosol-Alfisol intergrades: bisequel soils in NE Michigan, USA. *Geoderma,* 74, 23-47.

--- (2008) The distribution of silty soils in the Grayling Fingers region of Michigan: Evidence for loess deposition onto frozen ground. *Geomorphology: in press.*

Schaetzl, R. J. & S. L. Forman (2008) OSL ages on glaciofluvial sediment in northern Lower Michigan constrain expansion of the Laurentide ice sheet. *Quaternary Research: in press.*

Schaetzl, R. J. & J. Hook (2008) Characterizing the silty mantle on the Buckley Flats outwash plain: Evidence for loess in NW Lower Michigan. *Physical Geography: in press.*

Schaetzl, R. J., B. D. Knapp & S. A. Isard (2005) Modeling soil temperatures and the mesic-frigid boundary in the central Great Lakes region, 1951-2000. *Soil Science Society of America Journal,* 69, 2033-2040.

Schaetzl, R. J. & B. N. Weisenborn (2004) The Grayling Fingers region of Michigan: Soils, sedimentology, stratigraphy and geomorphic development. *Geomorphology,* 61, 251-274.

Simard, A. J. & R. W. Blank (1982) Fire history of a Michigan jack pine forest. *Mich. Academ.,* 15, 59-71.

Soil Survey Staff, Natural Resources Conservation Service, United States Department of Agriculture. Soil Survey Geographic (SSURGO) Database for Osceola County, MI. Available online at http://soildatamart.nrcs.usda.gov accessed 02/17/2007

Sperazza, M., J. N. Moore & M. S. Hendrix (2004) High-resolution particle size analysis of naturally occurring very fine-grained sediment through laser diffractometry. *Journal of Sedimentary Research,* 74, 736-743.

Walker, P. H. & R. V. Ruhe (1968) Hillslope models and soil formation. II. Closed systems. *Trans. 9th Intl Congr. Soil Sci.,* 58, 561-568.

Whitney, G. G. (1986) Relation of Michigan's presettlement pine forests to substrate and disturbance history. *Ecology,* 67, 1548-1559.

Zhang, G., J. Germaine, R. Martin & A. Whittle (2003) A simple-sample mounting method for random powder x-ray diffraction. *clays and clay minerals,* 51, 218-225.